NTNU
Det skapende universitet

Experimental Set-up for partial discharge detection

Ingrid Roen Velo

Master i energi og miljø
Innlevert: januar 2015
Hovedveileder: Frank Mauseth, ELKRAFT
Medveileder: Pål Keim Olsen, ELKRAFT

Norges teknisk-naturvitenskapelige universitet
Institutt for elkraftteknikk

Problem Description

Production of electric power from floating wind turbines will be a big oncoming challenge. Numerous Norwegian companies are working on different aspects of floating wind power generation.

Power electronics used for HVDC converters will stress the cable with a DC voltage with overlaid transients. The effect of these transients on the performance of the polymeric cable insulation is yet not known and the main purpose of the project is to investigate how transients can influence the life time of the cable insulation.

The work will mainly be experimental. In the first stage, a noise reduced test circuit for AC voltage at higher frequencies must be designed and built. Further work will be to measure partial discharges for AC voltage at different frequencies. Ultimately, the test objects should be tested with a DC voltage with an overlaying AC to simulate the voltage stress a HVDC cable will be subjected to close to the HVDC converters.

Preface

This report is a result of work with the master thesis conducted at the Norwegian University of Science and Technology, NTNU, at the Department of Electrical Power Engineering.

There are so many people I am grateful to for all the help during the work on this master thesis. Most of all I would like to thank my co-supervisor and labparter; Pål Keim Olsen. Without your previous work on the subject and your great spirit, none of this would be possible in such a short amount of time. Further I would like to thank my supervisor Frank Mauseth for the help with interpreting the results and giving answers to the difficult questions that emerged throughout the thesis work.

I would like to thank the guys in the service lab, Aksel Andreas Reitan Hanssen and Vladimir Klubicka for the help with the experimental set-up in the lab. Most of all Bård Aalmaas, you have been a huge help with the security measures and the finalizing of the experimental set-up. You always know what do, even when I do not really know what I am asking.

To everyone in the workshop, thank you for the help with finding equipment and the neccessary parts. A special thanks to Morten Flå, always quick on the fix and Dominik Häger for the help with making artificial cavities in the test samples.

Last but not least, thank you to all my fellow students, friends and family, especially the guys at room G-220. Thank you for the great working environment, great experiences and many laughs. Without you, being at shcool every day would not be the same, and neither would the great memories of writing this master thesis.

Abstract

There are many technological challenges related to the production of electrical power from offshore wind farms. In offshore HVDC transmission systems converter stations are installed between the AC and DC power grid. The resulting DC voltage from the converter stations will contain transients originating from the switching of the power electronic components. The AC ripple voltage on the DC side of the HVDC stations can be in the range of 1-10% of the nominal DC voltage, depending on the size of the engaged filter. Harmonic content of the ripple can range up to 30-100 times the switching frequency, with the dominant components close to the switching frequency which can be around 1-2 kHz.

The effect of the DC component and the overlaid transient on the ageing of polymeric insulation is not yet known. An operational insulation system is one of the most important prerequisite for functional high voltage system and partial discharge are one of the main ageing mechanisms in a dielectric.

The main purpose of this master thesis has been to develop and build a low interference experimental set-up for partial discharge detection that can simulate the conditions in offshore cable insulation close to the converter stations. The experimental set-up should be able to apply a combined DC voltage and high frequency AC voltage across a test sample.

This master thesis is mainly experimental and have been performed in three sections; sub-system test, system test and main test. The sub-system test was an analysis of the AC voltage source and transformers to find a combination able to deliver a 2 kV_{rms} sinusoidal voltage with little distortion across the frequency range 1-5 kHz. The Behlman signal generator and Messwandler Bau transformer gave a THD below 1% at all frequencies and is the AC voltage supply system used in the further tests.

The experimental set-up, based on a partial discharge straight detection circuit, is built inside a faraday cage. During the system testing the noise and intereference from the surrounding and circuit was tested and the nessesary alterations were done. Resulting in a noise band of approximately 0.6 pC, allowing a detection limit of 1 pC. The system test also included a benchmark test on the layered PET samples compared to solid ones. The results indicaticated partial discharges in the interfaces between the layers and the pressure was increased.

The results from the main test on the layered samples was very inconsistent when applying the same voltage. The variation reduced the quality and credability of the test making it difficult to interpret the results. The problem with the OMICRON

measuring system with interpreting the correct polarisation of the detected discharges further complicate the intrepretation with reducing the ability to distinct the signal from noise at unipolar applied fields.

The combined DC and AC voltage test show a clear distinction between the samples with and without a cavity. The repetition rate during the cavity tests at 50 Hz AC and DC voltage had a high initial value, decreasing down to a stable level. This is consistent with the expectations that repetition rate is dependent of the conductivity of the dielectric and the cavity. The 1 kHz AC and DC tests had a significantly lower repetition rate, both initially and at the stable level, but a similar shape as the repetition rate during the 50 Hz test. The pure DC voltage test is too inconsistent and unreliable results to make any comparison to the results from the combined AC and DC voltage tests.

The results indicate that more tests and further improvements must be done in the experimental set-up to increase the reliability of the results.

Sammendrag

Offshore HVDC overføringssystemer bruker omformerstasjoner mellom AC- og DC-kraftnettet. Likespenning fra omformerstasjonene vil inneholde transienter. Disse ligger i området 1 til 10 % av den nominelle likespenningen, avhengig av filteringen. Det harmonisk innholdet i AC rippelen kan være opptil 30-100 ganger bryterfrekvensen, som kan være rundt 1-2 kHz. Effekten av DC spenning overlagt en høyfrekvent AC transient på aldring av polymer isolasjoner er ennå ikke kjent. Et velfungerende isolasjonssystem er en av de viktigste forutsetningene for et driftssikkert høyspentanlegg, og partielle utladninger er en av de mest krevende aldringsmekansismene man må ta hensyn til i et isolasjonsmateriale.

Hovedformålet med denne masteroppgaven har vært å utvikle og bygge et eksperimentelt oppsett for måling av partielle utlandninger som kan simulere forholdene i offshore kabelisolasjon nært omformerstasjoner. Det eksperimentelle oppsettet skal være i stand til å påtrykke en kombinasjon av DC-spenning og høyfrekvent vekselspenning over et testobjekt.

Denne masteroppgaven er i hovedsak en eksperimentell oppgave og ble gjennomført i tre seksjoner; sub-systemtest , systemtest og hovedtest. I sub-system testen ble en analyse av en Behlman signalgenerator og ulike transformatorer gjennomført for å finne en kombinasjon som var i stand til å levere en 2 kV_{rms} sinusformet spenning med liten forvrengning over hele frekvensområdet 1-5 kHz. Behlman signalgeneratoren og Messwandler Bau transformatoren ga en THD under 1% på alle frekvenser og ble valgt for videre testing.

Det eksperimentelle oppsettet ble bygget inne i et faradaybur. Systemtesten ble gjennomført ved å støyteste omgivelsene, oppsettet og komponentene. Det endelige støybåndet ligger på omtrent 0.6 pC, og en deteksjonsgrense på 1 pC ble satt. Systemtesten inkluderte en test på de lagdelte prøvene sammenlignet med en solid prøve for å utelukke partielle utladninger i grensesjiktene. Resultatene indikerte at det forekommer partielle utladninger i grenseflatene mellom lagene og trykket på prøveobjektene ble økt.

Resultatene fra hovedtesten på de lagdelte prøvene var meget inkonsistente ved samme påtrykte spenning. Variasjonene reduserer kvaliteten og validiteten til resultatene som gjør det vanskelig å tolke resultatene. Problemet med OMICRON målesystemet i tolkningen av korrekt polaritet i små utladninger gjør tolkningen av resultatene enda vanskeligere.

Testresultatene fra den kombinerte AC- og DC-spenningen viser et klart skille mellom

prøvene med og uten hulrom. Repetisjonsraten i prøvene med hulrom og påtrykt både 50 Hz AC- og DC-spenning, hadde en høy initiell verdi som reduseres gradvis til et stabilt nivå. Dette er i overensstemmelse med forventningene om at repetisjonsfrekvens er avhengig av isolasjonens og hulrommets ledningsevnen. Testene med kombinert 1 kHz AC-og DC-spenning hadde et forløp lignende 50 Hz testen, men med en merkbar lavere repetisjonsfrekvens, både i initiell verdi og stabilt nivå. Den rene DC-spenningstesten har for inkonsistente og upålitelige resultater til å gjennomføre en sammenligning av resultatene fra de kombinerte AC-og DC-testene.

Resultatene tyder på at ytterligere forbedringer må gjøres i det eksperimentelle oppsettet for å øke påliteligheten av resultatene.

Contents

1. Introduction

1.1 Background

The market for HVDC transmission systems has increased substantially over the last years, driven by intercountry connections, technological developments and new renewable energy sources. The application of wind energy and especially offshore wind energy is a keystone in the policy of several European countries due to the higher wind speeds and hence a greater production. However, the further out to sea and the higher the power capacity, the greater is the challenge of transmission of the energy to the mainland. [1]

1.1.1 Transmission

From the offshore wind turbine collection point, the transmission link to the shore may be High Voltage Alternating Current (HVAC) or High Voltage Direct Current (HVDC). Today the majority of power transmission from offshore wind farms are conducted using HVAC, but as the offshore wind farms get a higher installed power capacity and are located further from the onshore grid connection point, HVDC has proven to have several advantages compared to HVAC. [1]

The submarine AC cables generate reactive current due to its capacitance characteristics. This reduces the power carrying capability of the cable and reactive shunt compensation may be needed. [1] The capacitive charging current limits the possible lenght of the AC cable to a maximum practical length of about 50 to 100 km and may cause system instability. Also the compensation alternatives are expensive and hard to implement offshore. [2] In addition, the AC grid of wind turbines and the onshore grid is synchronously coupled; all fault is propagated from one to the other. However the AC solution is a well-etablished system with low investment costs compared to HVDC. [1]

In DC no reactive power is generated and all of the line capacity is used for transmitting active power. The main advantages with choosing DC is the low losses and no charging current in the cable. There is virtually no limit on connection distance beyond practical constraints of the manufacturers and the laying of the cable. [1]

1.1.1.1 Converter Technology

An HVDC system takes electrical power from an AC network via a transformer, converts it to DC at a converter station and transmits it to the receiving point, where it

is converted back to AC and connected to the existing grid.

The HVDC connection using thyristor based line-commutated converters (LCC) is an established and well documented technology that can transfer large amount of energy over a large distance with low losses. In spite of its excellent results onshore it has proven to not be very suitable in offshore application. The converter stations and auxiliary equipment have demanding space requirements, resulting in big offshore converter platforms. Furthermore, the LCC technology is highly susceptible to AC network disturbances, resulting in converter commutation failures which can temporarily shut down the entire HVDC system. The main limitations of the classical HVDC are the need for large converter stations onshore and offshore and a strong AC network in both ends to control the thyristors, making the LCC technology an unfavourable choice for radial connections such as offshore wind energy. [2] [3]

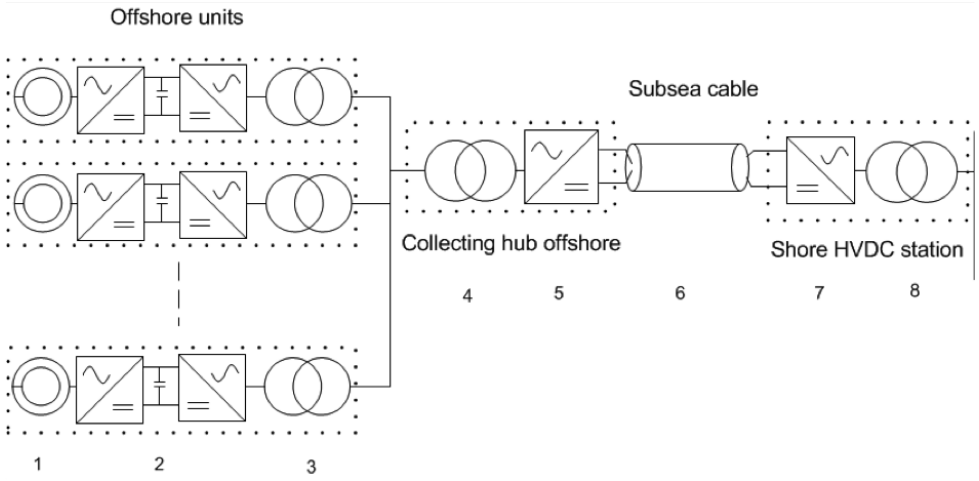

Figure 1.1: HVDC transmission scheme

The voltage source converter (VSC) HVDC system uses Insulated-Gate Bipolar Transistors (IGBT). A self-commutating VSC based HVDC technology with pulse width modulation (PWM). A technique where the commutations do not require an AC voltage source and are practically instanteneous. VSCs are able to independently control both active and reactive power exchange with the AC grid and may help with voltage regulation and are able to operate in weak or even dead AC networks. Power reversal can be accomplished by keeping the same voltage polarity. The major drawbacks of the VSC technology is the high converter loss caused mainly by switching losses in the converters and the high investment cost for the converter stations. Nevertheless the VSC HVDC is considered more suitable for offshore application due to its increased controllability and compact architecture. [4]

1.1.1.2 Harmonics

The resulting DC voltage from the converter stations will contain transients originating from the switching of the power electronics components. The AC ripple voltage on

the DC side of the HVDC stations can be in the range of 1-10 % of the nominal DC voltage, depending on the size of the filter employed. Harmonic content of the ripple can range up to 30-100 times the switching frequency, with the dominant components close to the switching frequency, which can be around 1-2 kHz. [6]

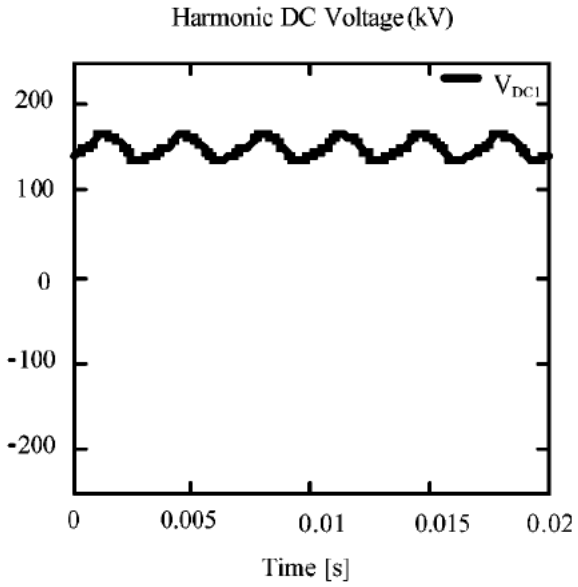

Figure 1.2: Harmonic DC voltage [5]

The high voltage transients will experience dampening along the cable due to the capacitative properties. The insulation closest to the power electronic converters will experience the most severe harmonics. [7]

1.1.1.3 Cable insulation

Oil-impregnated cables have been the leading techology for HVDC power transmission since its introduction. Recently however, much research and development has been devoted to the development of extruded HVDC cables due to their advantages. Such as the low material and production costs, as well as their dielectric strength, electrical resistivity and their physical properties such as resistance to cracking and moisture penetration. The main reason that prevents the use of polymer cables for HVDC transmission lies in the degradation of polymers under high electric stress. This phenomenon is associated with the formation of space charges. Space charge accumulation in polymeric material poses major scientific and technological problems. The continued development of the polymer material and the converter technology increase the possibility of making extruded cables a feasible choice for HVDC transmission. [8]

1.2 Aim of work

Polymers is vulnerble to partial discharges, one of the most important ageing mechanisms. Repetition rate during pure DC voltage is very low, several order less that at applied AC voltage at 50 Hz. However introducing a AC ripple will increase the repetition rate and may affect the ageing of the polymeric insulation. The goal of this assigment is to develop an experimental set-up for detecting and measuring partial discharge at a combined DC and high frequency AC voltage. This is done to simulate a stress similar to the one the cable insulation is subjected to close to the converter stations in an offshore HVDC transmission system. This is to determine the partial discharge characteristics during combined DC and high frequency AC voltage to further ascertain its influence on ageing of polymeric material.

The work is mainly experimental and is divided into several different sections before the circuit is built and the testing on partial discharge in a test object with a cavity can begin. One part is to test the Behlman signal generator together with transformers to generate a low distortion sinusoidal voltage across a frequency range, 1-5 kHz at 1 kV_{rms} and 2 kV_{rms}. As the hardware analysis is done, noise elimination/attenuation tests should be preformed on the components of the circuit, and the set-up as a whole to increase the sensitivity. When the sensitivity is at an acceptable level partial discharge tests are preformed on test objects. The test objects may either be solid or with a artificially manufactured cavity. Both AC, DC and Cobined DC and AC voltage is applied across the sample to investigate the partial discharge activity to further ascertain the capability of the experimental set-up.

2. Theory

2.1 Partial discharges

Partial discharges (PD) are one of the main fault and ageing mecanisms in an insulation system. Partial discharges are small sparklike short circuits across parts of the insulation, an electrical discharge that does not completely bridge the electrodes. Partial discharges will gradually lead to degradation and ageing of the insulation. How fast depends on the type of insulation system, the material as well as the repetition rate and magnitude of the discharges. Consequently the occurrence of PDs give a good indication of the state of the insulation system and have an impact on its lifespan. [9]

Partial discharges include internal discharges, surface discharges and corona discharges. This report concentrates on partial discharges in cavities. Cavities occur during the manufacturing and ageing of the dielectric. Due to the generally lower permittivity and breakdown strength in the cavity, compared to the surrounding dielectric, a local field enhancement is developed and partial discharges can occur. Partial discharges result in a release of energy and cause degradation of the surrounding insualtion through a combination of chemical, mechanical, thermal and radiative processes. Especially the cavity surface is affected and by-products may form on the surface. This causes local field enhancements within the cavity which leads to a concentration of the partial discharges. This may cause inception of electrical trees and could eventually lead to a breakdown of the insulation system. [10]

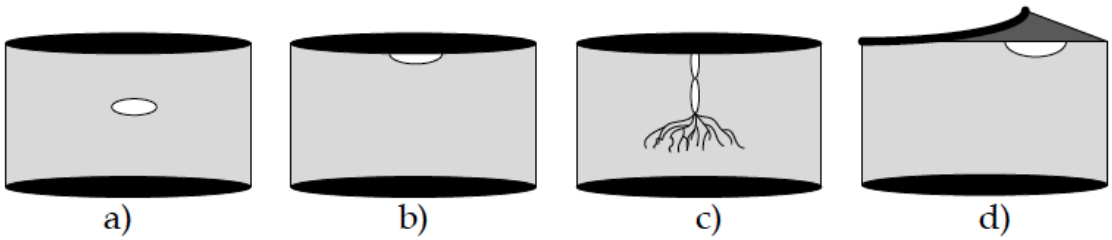

Figure 2.1: Different types of internal discharges, a) isolated cavity, b) cavity with electrode contact, c) cavity developed to an electrical tree, d) cavity in interface between different dielectric materials. [11]

Two criteria must be fulfilled in order for partial discharge to occur in cavities within a dielectric; there must be free electrons to initiate an electron avalanche and a suffieciently high electric field to start an avalanche and create a breakdown path. These critera are both stochastical phenomenons explaining why partial discharges are a very complicated phenomenon that often display chaotic behaviour. [6]

Free electrons can originate from volume or surface generation of electrons, such as ionization by energetic photons from radiation, electron release by ion impact, detrapping of electrons from traps at insulation surfaces or thermal ionization. The critical field value is assumed to follow Paschens law, that is dependent of the type of gas, its pressure and the size of the cavity. In a small cavity there will only rarely get an exited atom/molecule, even though the field is of sufficient size. Partial discharge is therefor a stochastical phenomenon, that will vary in both size and frequency from time to time. [12] [13]

The actual field distribution which initiates the discharge is dependent of the shape and amplitude of the applied voltage, the characteristics of the involved materials, and the geometry of the cavity. The DC stationary field distribution is governed by geometry and conductivity of the materials. The conductivity of the materials is significantly influenced by temperature, amplitude of the electrical field and the present ions. The AC field distribution is determined by geometry and permittivity of the involved materials. The permittivity will vary with the frequency of the field, due to different polarization mechanisms in the dielectric materials. Permittivity will also vary with temperature, but not to the same extent as the conductivity. [14]

2.2 Breakdown voltage of cavities

2.2.1 Pachens curve for breakdown in air

The electrical resilience of a cavity, or its breakdown strength, is dependent of the type and the pressure of the gas as well as the cavity dimensions. The breakdown voltage in a homogeneous field is a function of the product of the gas pressure and size of the cavity at a given temperature. This is Paschens law. [15]

$$U = \phi(pd) \tag{2.1}$$

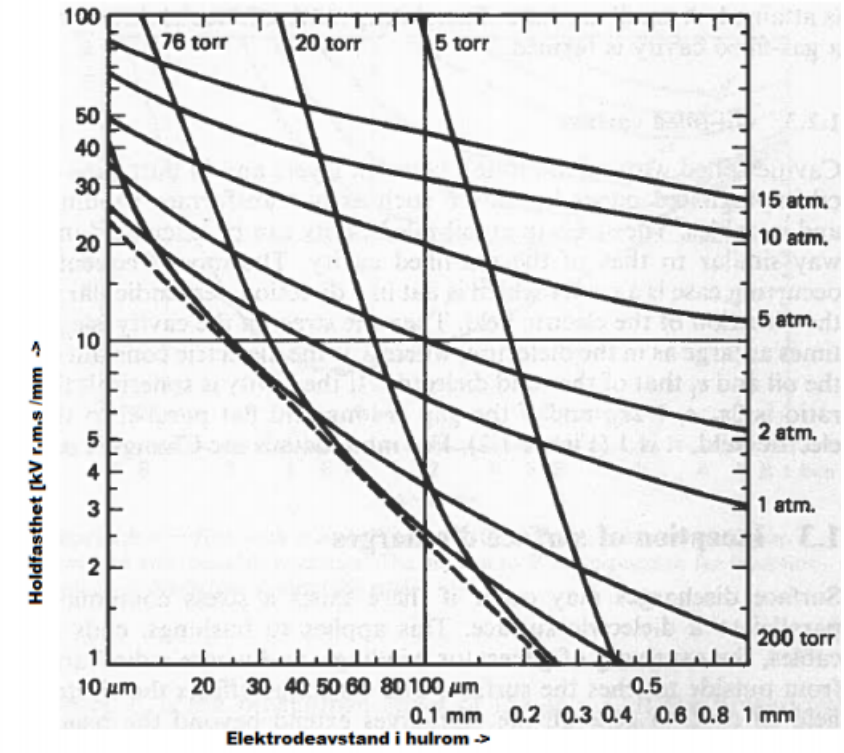

Figure 2.2: Paschens curve for air at T=20°C [16]

A breakdown in a cavity bound by a dielectric occurs at approximately the same voltage as between equally spaced electrodes. This voltage can be found in Paschens curve. Considering a gap of a given size, as the pressure decreases so will the gas density and the electron free path increases. Resulting in a reduced number of collisions and a increase of the breakdown strength. Several factors may cause the breakdown voltage to be lower than predicted. The walls of the cavity may be covered by static charges produced when the cavity was formed or left after previous partial discharges. Semiconducting layers may also occur on the cavity walls, more or less short circuiting the cavity. This may cause a significant increase of the breakdown stress. [9]

The discharges will start at some critical field, E_p, given by Pachen's law. As long as height$\ll$radius of the amplitude, the amplitude of the electric field in the cavity is given by:

$$E_c = \frac{V_c}{h} \tag{2.2}$$

The voltage across the cavity at which partial dicharges start to occur when the voltage is increased is called the inception voltage, and the corresponding stress is called the inception stress. When a partial discharge occurs at a voltage $V_{c,inception}$ across the cavity, the cavity is partly or completely discharged through a breakdown path in the field direction. When the discharge reaches the surface of the dielectric it is followed by discharges along the surface. After a few nano seconds the voltage across the void has dropped to the extinction voltage, also known as the remanent voltage, V_e and the PD is extinguished. A considerable part of the cavity surface is affected during the

PD and a surface charge is deposited on the surface of the cavity. Immediatly after discharge the electric field in the cavity will have a size of only a fraction of the field before the discharge occured. The cavity is once againg insulating until the voltage across it exceed $V_{c,inception}$ and a new partial discharge occur. [15] [14]

2.2.2 Partial Discharge under AC voltage

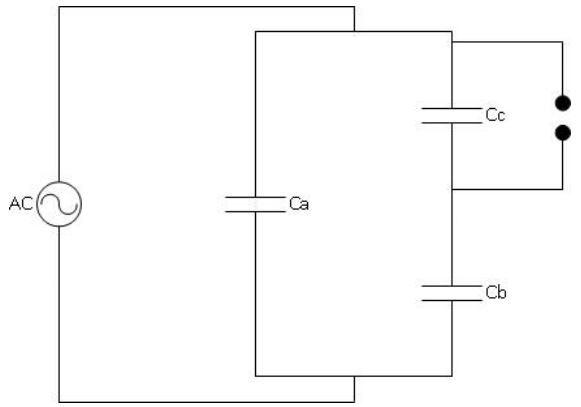

Figure 2.3: Internal discharge equivalent circuit under AC conditions [9]

Internal discharges at AC voltage can be described using the well-known abc equivalent circuit illustrated in Figure 2.3. The intact part of the dielectric is described by a capacitance C_a while the dielectric in series with the cavity is represented by C_b and the cavity is represented by a capacitance C_c, which is shunted by a breakdown path. [9]

2.2.2.1 Voltage distribution

The AC voltage across a cavity can be expressed by the following equation:

$$\hat{V}_{c,ac} = K_{AC}\hat{V}_{ac}sin(\omega t) \tag{2.3}$$

$\hat{V}_{ac}$ is the amplitude of the AC voltage with an angular frequency of ω=2πf applied across the dielctric and K_{AC} is given by the capacitances of the insulation and the cavity illustrated in Figure 2.3:

$$K_{AC} = \frac{C_b}{C_b + C_c} \tag{2.4}$$

The inception voltage for partial discharges measured over the terminals at AC voltage is defined as:

$$V_{PDIV,AC} = (\frac{1}{K_{AC}})V_{c,inception} \tag{2.5}$$

[6]

2.2.2.2 Recurrence of discharges

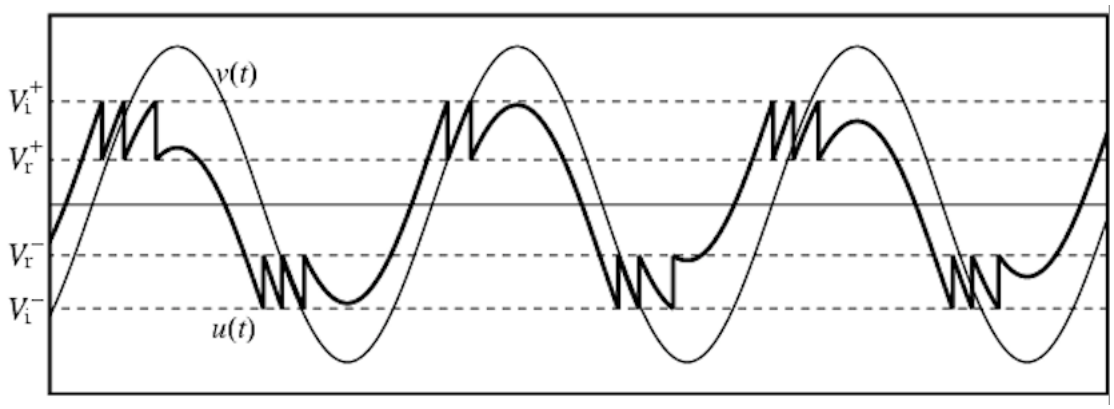

Figure 2.4: Discharge recurrence during AC voltage [17]

Figure 2.4 illustrates the PD activity in during AC voltage, the voltage across the cavity is given by v(t), the ignition voltage is V_i and the extingction voltage is denoted V_r. The voltage across a cavity when no partial discharges occur is given by Equation 2.3. After a partial discharge occur the voltage across the cavity drops and the voltage immediatly after discharge is given by superposition of the main electric field and the field of the surface charges at the cavity walls left by the PD. [9]

$$V_{c,ac,pd} = K_{AC}\hat{V}_{ac}sin(\omega t) - \Delta U \tag{2.6}$$

In this formula $\Delta U = V_{c,inception} - V_e$ is the voltage drop across the cavity during a partial discharge. A new PD will occur when the voltage in the cavity again reachs the critical value, $V_{c,ac,pd} \geq V_{c,inception}$. The same will occur in the negativ half period of the alternating voltage. [15]

For $V_{ac} \geq V_{PDIC,AC}$ the discharge frequency is given by:

$$f_{pd,ac} = \frac{4fK_{AC}\hat{V}_{ac}}{V_{c,inception}} \tag{2.7}$$

[6]

The repetition rate of partial discharges is difficult to determine since partial discharge inception and extinction voltage is strongly affected by the deposited discharge and the shape of the voltage applied. Ripple on the voltage may induce partial discharges at

an applied voltage below the inception voltage and the waiting time for free electrones may delay the discharge, letting the voltage increase to a level above breakdown voltage before an avalanche occurs.

The partial discharge inception voltage have been obseved to be dependent on the frequency of the AC voltage and increase at higher frequencies. The frequency dependence can be described by certain parameters; the statistical time lag, charge transport in the dielectric and the cavity surface decay. If the waiting time for a free electron is much shorter than the period time of the voltage there is no frequency dependence in the PD. However if the statistical time lag is in the same range as the period, the partial discharges is shifted forward in phase and occur at higher voltage due to the lack of free electrons. The result is fewer partial discharges per period and larger magnitudes. The surface charges deposisted by previous partial discharges decay over time due to conduction and recombination and if there are significant surface charge decay the field in cavity decreases and hence decrease the number of partial discharges. If there is a significant transport of surface charge in the cavity from shallow traps to deeper traps it will reduce the surface emission of starting electrons. This effect is intensified by increased frequency and will reduce the number of partial discharges per period. [10] [18]

2.2.3 Partial Discharge under DC voltage

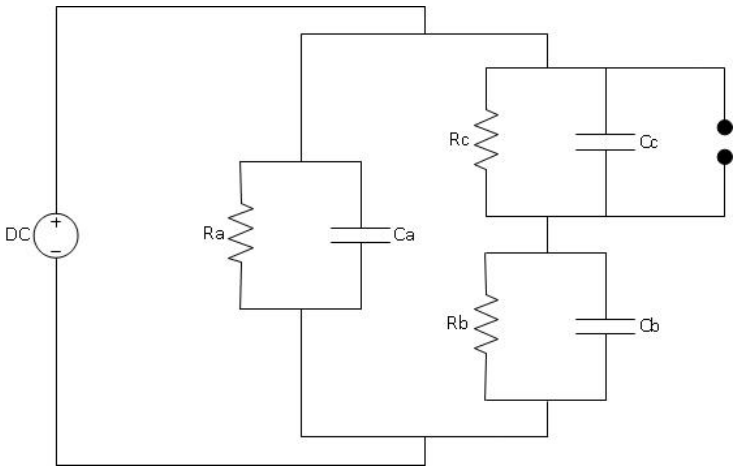

Figure 2.5: Internal discharge equivalent circuit under DC conditions [9]

To illustrate partial discharge under DC conditions, the well known abc circuit from AC partial discharge is extended with resistances, as seen in Figure 2.5. During AC voltage the capacitive voltage determine the field but at stationary DC voltage it is the resistive voltage that determine the field. During the increase and decrease of the applied DC voltage one will often get a capacitive voltage distribution across the insulation, and hence comparable conditions as during AC voltage. C_a and R_a

represent the properties of the entire dielectric between the cavity and the electrodes and C_b and R_b represent the properties of the dielectric in series with the cavity, C_c is the capacitance of the cavity and R_c represent the surface resitance of the void. [19] [12]

The time constant,τ, for charging of the cavity is given by:

$$\tau = (\frac{R_b R_c}{R_b + R_c})(C_b + C_c) = R_b C_b \frac{K_{DC}}{K_{AC}} = \frac{\epsilon_0 \epsilon_b}{\sigma_b} \frac{K_{DC}}{K_{AC}} \tag{2.8}$$

for a sylidrical cavity the time constant can be written:

$$\tau = \frac{D\epsilon_0 \epsilon_c + \epsilon_0 \epsilon_b}{D\sigma_c + \sigma_b} \tag{2.9}$$

Where ϵ_c and ϵ_b is the relative permittivity of the cavity and the dielectric respectively and σ_c and σ_b is the conducitivity cavity and the dielectric. D is given by the dimentions of the cavity:

$$D = \frac{H - h}{h} \tag{2.10}$$

2.2.3.1 Voltage distribution

The voltage distribution in the cavity under stationary DC conditions, assuming an extinction voltage V_e=0 is given by:

$$V_{c,dc} = (1 - e^{\frac{-t}{\tau}}) K_{DC} V_{dc} \tag{2.11}$$

where V_{dc} is the applied DC voltage across the test sample and K_{DC} is given by Equation 2.12.

$$K_{DC} = \frac{R_c}{R_c + R_b} \tag{2.12}$$

.

The partial discharge inception voltage during applied DC voltage is given by:

$$V_{PDIV,DC} = (\frac{1}{K_{DC}}) V_{c,inception} \tag{2.13}$$

The inception voltage for DC is not well defined, because there will be no discharges at the inception voltage, $V_{c,dc}$=$V_{PDIV,DC}$. In practice, the inception voltage for partial discharges under applied DC voltage is better defined as the voltage that will give a certain number of discharges per time. It can be accepted that the DC voltage across the cavity must be well above the inception voltage before discharges occur. [6]

2.2.3.2 Recurrence of discharges

When the DC is applied the field is capacitively graded. In this area the PD repetition rate is high and follows the polarization current closely. After all the polarization processes are completed, the field in the cavity is resistive and discharges only occur infrequently. Because of the resistances located around the cavity is finite the surface charge from the previous PD will decay and a new discharge will occur. The frequency of which these discharges occur is given by the local resistances. [9] [19]

After a discharge occur the next one can take place after a recovery time t_r'. The statistical timelag t_L is assumed equal to zero, hence there is no waiting time for free electrons. The equation below is an expression for the minimal time between discharges. [19] [6]

$$t'_r = -\tau ln[1 - \frac{V_{PDIV,DC}}{V_{DC}}] \tag{2.14}$$

for $V_{DC} > V_{PDIC,DC}$.

The repetition rate is given by equation 2.15 and is found using the first term in the Taylor series.

$$n = \frac{1}{t'_r} \tag{2.15}$$

$$n \approx \frac{1}{\tau}\frac{V_{dc}}{V_{PDIV,DC}} \tag{2.16}$$

The repetition rate during DC voltage is proportional to $V_{c,dc}$ and hence the external voltage. It can be seen from Equation 2.16 that the repetition rate during DC voltage is dependent of the time constant for the charging of the cavity. The charging time is a function of both the permittivity and the conductivity of the involved materials. Since the conductivity of a material is strongly dependent of the temperature and the applied electric field, so is the repetition rate. The conductivity of a dielectric changes by many orders of magnitude when the temperature is raised from a temperature of 20°C to a temperature between 60 and 90°C. The repetition rate is directly affected by the increase in conductivity. If the conductivity is increased by two orders, so would the repetition rate. [19] The repetition rate will also vary with time from the decrease in the volume conductivity and reach a stable level after some time has passed. The stable repetition rate is reached after a time dependent of the temperature. [9] [19] [20]

The repetiton rate under DC stress is several order of magnitude less than at AC voltage. Only at very high stresses the repetition rate during DC reaches a level close to the repetition rate at AC voltage. [19]

2.2.4 Partial discharge under combined AC and DC voltage

The abc equivalent for combined DC and AC voltage is the same as the one illustrated in Figure 2.5 with resistances to take into account the stationary DC voltage and capacitances for the alternating voltages.

2.2.4.1 Voltage distribution within the dielectric

A combined DC and AC voltage applied across the experimental set-up can be expressed as:

$$V_{input} = V_{dc} + \hat{V}_{ac} sin\omega t \tag{2.17}$$

where V_{dc} is the DC voltage and $\hat{V}_{ac}$ is the amplitude of the AC voltage with an angular frequency of ω=2πf.

The resulting peak voltage over the cavity, V_c, will be given by superposition of the combined voltages across the cavity.

$$V_c = V_{c,dc} + \hat{V}_{c,ac} = (1 - e^{\frac{-t}{\tau}}) K_{DC} V_{dc} + K_{AC} \hat{V}_{ac} sin(\omega t) \tag{2.18}$$

2.2.4.2 Repetition rate

The equation for the repetition rate under applied DC voltage, Equation 2.14 can be modified to take into account the AC voltage. Since the frequency of the AC voltage is much higher than the time constant given by Equation 2.8, it will appear as if the DC voltage is offset by the peak voltage of Equation 2.3. The new time between discharges can be written as: [6] [19]

$$t_r = -\tau ln[1 - (\frac{V_{PDIV,DC}}{V_{DC}} - \frac{V_{c,ac}}{V_{c,dc}})] \tag{2.19}$$

which can be rewritten as

$$t_r = -\tau ln[1 - (\frac{V_{PDIV,DC}}{V_{DC}})(1 - \frac{V_{AC}}{V_{PDIV,AC}})] \tag{2.20}$$

.

The repetition rate n is the inverse of t_r and can be approximated by ignoring all terms after the first one in the Taylor series of n:

$$n = \frac{1}{t_r} \tag{2.21}$$

$$n \approx \frac{1}{\tau}(\frac{V_{dc}}{V_{PDIV,DC}})(\frac{1}{1-\frac{\hat{V}_{ac}}{V_{PDIV,AC}}}) \tag{2.22}$$

Equation 6.2 is similar to the repetition rate during DC voltage with an additional section to take into account the superimposed AC voltage. The repetition rate during combined DC and AC voltage will have a similar shape as the voltage during DC voltage, but will increase with an increased AC voltage. With an applied AC voltage of half the inception voltage during AC voltage the repetition rate during a combined DC and AC voltage will be twice the frequency at DC voltage. It also states that n goes to infinity when $\hat{V}_{ac}$ approaches $V_{PDIV,AC}$. Due to Equation 2.7 this is clearly not the case. [6]

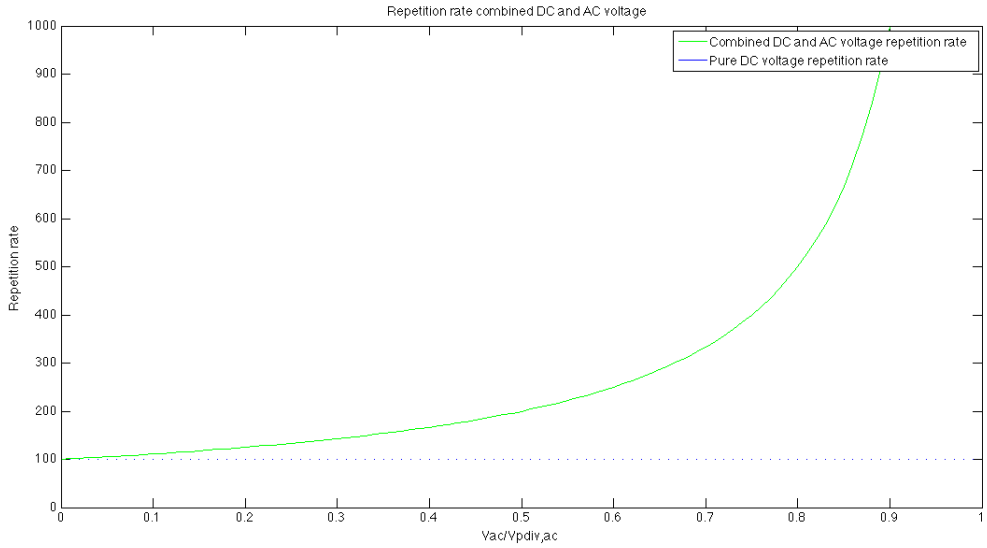

Figure 2.6: Repetition rate illustration for combined DC and AC voltage

3. Partial Discharge Detection

3.1 Detection circuit

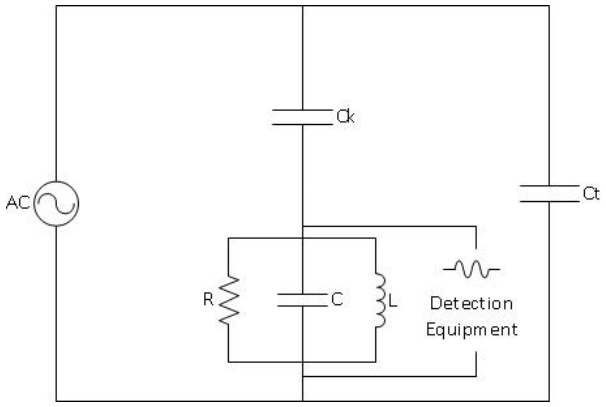

Figure 3.1: Equivalent circuit of straight detection circuit

Figure 3.1 illustrates a equivalent straight detection circuit. When discharges occur in the test object C_t the voltage across the test object experience a sudden voltage drop corresponding to the apparent charge. The coupling capacitor C_k in parallell with the test object will deliver a current into the test object to counteract the voltage difference that originate between them due to discharge, and create a low impedance circuit for the high frequency signals. The measuring impedance can be placed in series with either the coupling capacitor or the test object. The voltage drop during a discharge will result in a small transient current and the measuring impedance will result in a detectable voltage due to this current. The detection equipment is connected across the measuring impedance and must be high frequency detection equipment due to the short duration and high frequency of the voltage. [12] [15]

The coupling capacitor should be larger than the capacitance of the testobject to get a good sensitivity. The measuringimpedance will affect the measured signal and the data possible to get out of the measurement, hence the choice in design is very important. [12]

3.1.1 Sensitivity and noise

During partial discharge measurements the sensitivity of the detection circuit must be very good. Generally the aim is to maximize the signal to noise ratio by minimizing the noise, maximizing the signal or a combination of both. The reliability and sensitivity of

detection circuits are strongly affected by interference. Interference can originate from the main delivering the voltage to the equipment, the circuit itself, contact noise or from the surrounding, since all wiring basically works as antennas when not connected. [9] Due to the low repetition rate during pure DC measurements the signal to noise ration should be very low to get a clear picture of the actual partial discharges occuring in the test object.

A majority of the noise problems can be solved using electro-magnetical shields/faraday cage, careful design and testing all the equipment for PD separately, and hence eliminating them as sources of partial discharge in the sample, since all types of discharges have its own characteristic signature. Radio noise can be attenuated using a faraday cage. Corona discharges can be eliminated using field grading spheres and torids on sharp edges. Ground loops can be eliminated by careful design, grid interference can be attenuated using a filter on the main and floating objects can be pretty much eliminated by having a neat and clean test cell. Choosing a frequency band where the external noise is low and the signal from the defect high is important to distinct PD from noise. [21]

3.1.2 Partial discharge magnitude

The magnitude of the detected discharges may vary in size. The magnitude depend on where in the dielectric the discharges occur.

The apparent charge measured across the dielectric is not the same as the charge released in the cavity due to a partial discharge. The model during partial discharge detection is used to calculate the charge in the cavity rather than the one detected.

The capacitance of the dielectric is dependent of the permittivty and the dimentions of the cavity and test object,

$$C = \epsilon_o \epsilon_r \frac{A}{d} \tag{3.1}$$

where ϵ_o is the permittivity of vacuum=$8.854 \cdot 10^{-12}$ and ϵ_r is the reltive permittivity of the material. A is the area and d is the height of the different parts of the dielectric. Using the dimentions listet in table 4.2 one can calculate the capacitances of the test objects using equation 3.1 getting C_a=20.28 pF, C_b= 0.4867 pF and C_c=0.278 pF. The value of the coupling capacitor is C_k=800 pF.

The magnitude of the discharges across the entire cavity can be calculated. When a discharge occur all the components is considered to be capacitances due to the high frequency.

A charge Q is the product of the capacitance and the voltage across it.

$$Q = VC \tag{3.2}$$

Assuming a remanent voltage (extinction voltage) equal to zero the charge resulting from a partial discharge across the entire area of the cavity is found using Equation 3.3 where ΔV_c is peakvalue of the breakdown voltage $V_{paschen} \approx 950\ V_{peak}$.

$$Q_{cavity} = \Delta V_c C_c \tag{3.3}$$

Resulting in a charge Q_{cavity}=265.25 pC. The measured value for a discharge of this size at the breakdown voltage is given in Equation 3.4. The value of C_{eq} is given by the equivalent before discharge occur, and ΔV is given by voltage division.

$$Q_{measured} = C_{eq} \Delta V \tag{3.4}$$

$$C_{eq} = C_k + C_a + \frac{C_b C_c}{C_b + C_c} \tag{3.5}$$

$$\Delta V = \Delta V_c \frac{C_b}{C_b + C_a + C_k} \tag{3.6}$$

This gives a measured charge, corresponding to the cavity charge Q_{cavity}, $Q_{measured}$=452.3 pC.

3.2 Experimental set-up

The test circuit is based on a straight measuring circuit and is designed to able to apply both high frequency AC and DC voltage across the test cell. An equivalent circuit for the experimental set-up is illustrated in Figure 3.2. The experimental set-up is placed inside a faraday cage to attenuate the noise from the radiowaves, and corona toroids and spheres are connected at all the sharpe edges of the set-up to prevent corona discharges during testing. Pictures of the experimental set-up can be found in section A.1 in the appendix.

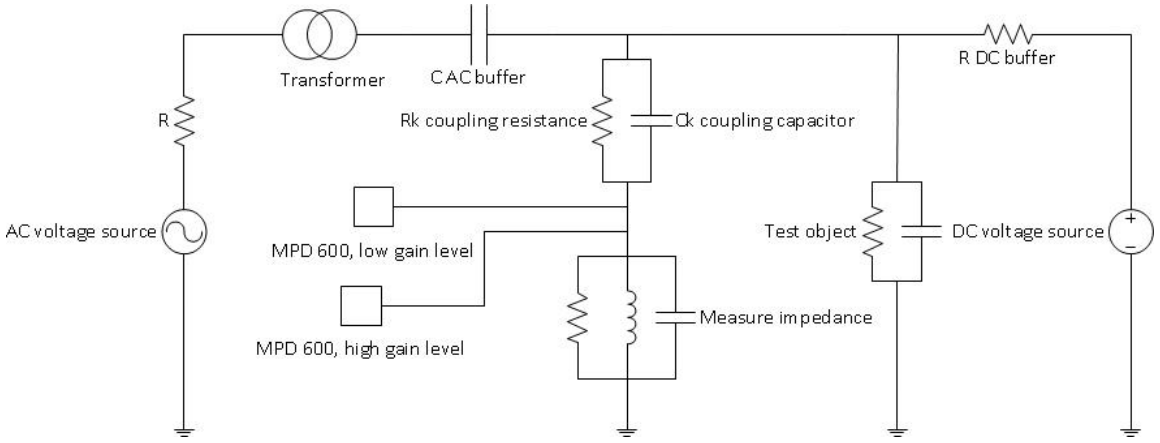

Figure 3.2: Equivalent circuit of the experimental set-up

C_{ac} is a buffer capacitance to prevent the DC current from entering the AC voltage side of the set-up. R_{dc} is a buffer resistance to prevent the AC current from entering the DC voltage source. One of the key parameters in a test set-up like this, with both AC and DC voltage source, is the buffer components and prevent creating a low impedance path for the transient currents from the partial discharge activity in another branch than through the measuring impedance.

Table 3.1: List of parameters in the experimental circuit

Parameter	**Definition**	**Value**
R	Series resitance	100 Ω
$C_{ac,buffer}$	Buffer capacitance	10 nF
$R_{dc,buffer}$	Buffer resistance	100 MΩ
C_k	Coupling capacitor	800 pF
R_k	Coupling resistance	280 MΩ
C_t	Testobject capacitance	200 nF
R_t	Testobject resistance	1 TΩ

The DC voltage across the test object can be expressed:

$$V_{DC,testobject} = V_{dc}\frac{R_k}{R_{dc,buffer} + R_k} \tag{3.7}$$

since $R_t \gg R_k$.

The AC voltage across the tesobject:

$$V_{AC,testobject} = V_{ac}\frac{C_{ac,buffer}}{C_{ac,buffer} + C_k + C_t} \tag{3.8}$$

The resulting voltage across the testobject is:

$$V_{testobject} = V_{AC,testobject} + V_{DC,testobject} \tag{3.9}$$

3.2.1 Hardware

Generation

- **Behlman Signal generator** a high frequency AC voltage source with a voltage range of 0-270 V_{RMS} and frequency range 45-10,000 Hz.
- **FUG** DC voltage source with a voltage output range of 0-35 kV
- **Messwandler Bau** Measuring Transformer

Some additional information on the hardware can be found in Section B.2 in the appendix.

Measurement

OMICRON MPD600 measurement and analysis tool for partial discharges is used for detection of the partial discharges. The OMICRON consist of a measuringshunt connected in the detection circuit. The measuring shunt is connected to the measuring unit that register and measures the size of the transient voltage signals. The analouge signal is converted to digital signals and transmitted to the computer through fiber optics for further treatment.

The detection limit will be limited by the sensitivity of the registrationinstrument and the noiseband. The design of the experimental laboratory set-up is very important with regard to interference reduction/elimination.

3.2.2 Test Cell

The set-up consist of a test cell with parallel plane Rogowski shaped electrodes with a surface area of approximately 19.62 cm^2. During testing the cell is filled with degassed mineral oil to prevent discharges at the edges of the electrodes. The oil is heated by a heat coil, to maintain a temperaterature within $\pm 0.1\%$ during testing. The pressure applied to the sample is controlled by weights and are set to 50 kN/mm^2 and 75 kN/mm^2. A picture of the test cell can be found in section A.2 in the appendix.

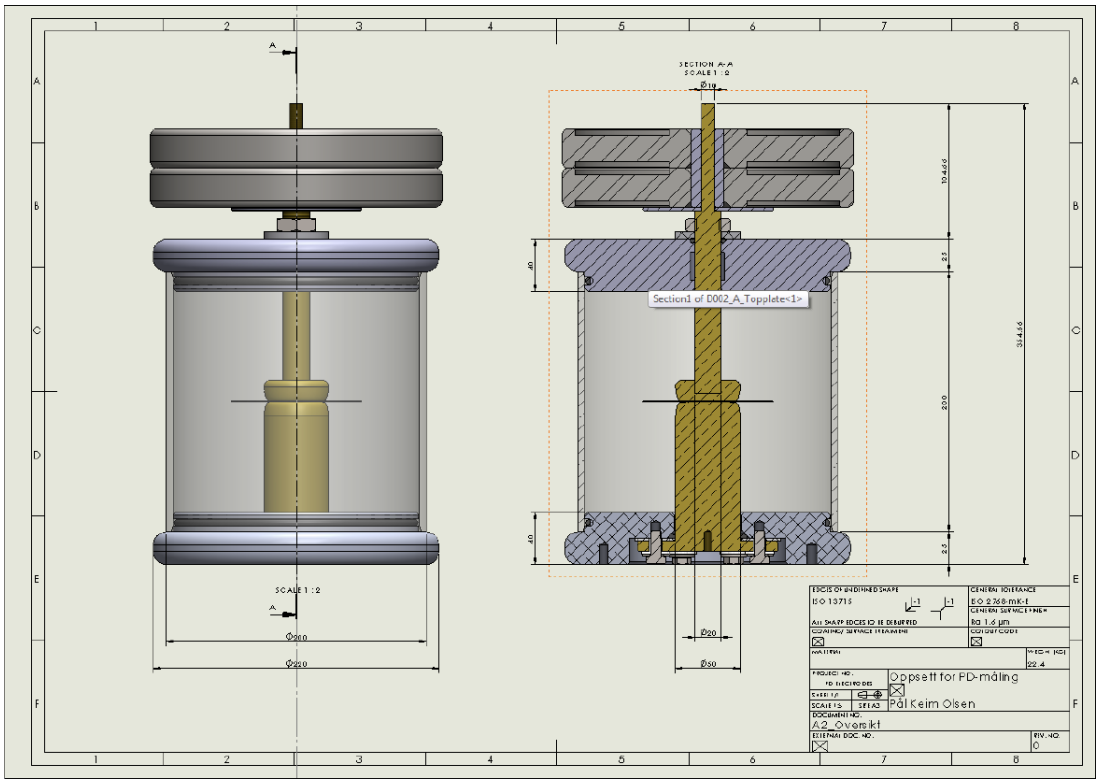

Figure 3.3: Test Cell

3.2.3 Security Measures

- A door switch is connected to a connection box between the voltage sources and the experimental set-up to eliminate the possibility of applying the voltage without a shut door and cut the connection if the door is opened during tests.
- A earthing rod is connected to the same security switch as the door. The rod must be placed on the circuit before handling it to prevent shock from charged components in the circuit.
- A smoke detector is connected to the circuit to detect any development of smoke from overheating in the oil.
- Two temperature sensors in the test cell is programmed to terminate the test if the temperate exceed 100°C.
- Oil level measurer are set to terminate the test if large amounts of oil is leaking from the test cell.

3.2.4 Calibration

The test circuit must be calibrated in order to measure the correct partial discharge magnitudes. This is done using a calibrator and applying a known charge pulse across the testcell with a test sample in place. The applied charge generates a current in the circuit and the voltage across the measuring impedance due to the charge is detected by the measuring equipment. The relation between the applied charge and related voltage transient measured is the calibrationfactor. When this is know the OMICRON detection program is able to convert the detected voltage signal to the correct charge magnitude. Calibrating must be preformed each time a test object of different height or material is used, since this changes the characteristics of the detection circuit and hence the detected transient voltage.

In the experimental set-up two OMICRON units are placed in parallell to detect partial discharges at two different gain levelse simultaneously. The two OMICRON MPD600 units in the experimental set-up is calibrated at 5 pC for the high gain unit and 50 pC for the low gain unit.

4. Experimental

The testing is performed to build a interference free experimental set-up illustrated in figure 3.2 for partial discharge testing and is performed in sections where the further work is based on the results from the previous test.

The testing on the experimental set-up is performed in a given order to eliminate problems as they arise.

- **Sub-system test;** testing on Behlman signal generator and transformers to find a low noise generation system for high frequency AC voltage.
- **System test;** testing of the external noise and interference originating from the circuit to eliminate them, and preforme tests on the layered samples without a cavity compared to solid samples to determine if discharge occur in the interfaces.
- **Main test;** tests on the layered samples described in Section 4.4 at different voltages and frequencies to further test the ability of the detection circuit by interpreting the results.

4.1 Sub-system test

The experimental set-up should be able to deliver both DC and high frequency AC across the test objects. The goal is to have a sinusoidal voltage with as little ripple as possible since they may lead to partial discharges at a lower applied voltage than the breakdown voltage. [9]. During the project assignment it was found that the Behlman signal generator is a viable choice for generating high frequency sinusoidal voltage. It is easy to regulate and can supply a wide range of frequencies with low distortion. The results from the project did not have a sufficiently high frequency resolution and a new test is nessesary to determine the distortion of the seemingly sinusoidal voltage. [22]

The voltage span of the Behlman signal generator is 0-270 V_{RMS} and a transformer is needed to reach the desired voltage for partial discharge testing.

The test is performed on both the Behlman Signal Generator and several transformers to be able to find a transformer able to handle the high frequencies, 1-5 kHz, and still reach a voltage of 2 kV_{RMS}. The difficulty with high frequency transformers is the risk of the core being saturated at higher frequencies distorting the output voltage. The transformers to be tested:

- The transformer design by Petter Nodeland [23] [24]
- Neon Transformer

- Messwandler Bau Measuring Transformer
- Arteche Measure Transformer

Some additional information on the transformers and the Behlman signal generator can be found in section B.1 in the appendix.

4.1.1 Experimental approach

The analysis to determine the quality of the output voltage were performed by connecting the Behlman source and the transformer in series with a resitance on the primary side of the transformer and a capacitor of 800 pF on the transformers secondary side. The capacitor on the secondary side is ment to simulate a load similar to the one it is subjected to during the partial discharge detection tests. The resistance is placed in series with the primary side of the transformer to limit the current to the transformer, get a higher voltage from the Behlman and a less sensitive controlsystem.

Initially a preliminary test is performed by observing the transformer ratios and the voltage shape on the secondary side by placing a high voltage measurment probe across the capacitor connected to a high resolution Yogogawa oscillioscope. The transformer with the most promising results during the observations done with the oscillioscope is investigated further with a fast fourier transform (FFT) of the signal.

The neccessary data for the FFT is collected using the yokogawa oscillioscope and the corresponing computerprogram Xviewer for saving the collected data as csv files. The text file is imported into a MATLAB script for plotting of the fast fourier transform and finding the total harmoinc distorition (THD) of the signal. To get an satisfactory analysis a suffiecient amount of data is needed to observe as much of the signals components as possible. A high sampling frequency must be used to detect the harmonic content of the voltages with high frequencies. The sampling where set to 62.5 MSamples and the aqusition time 20 ms at the yokogawa oscillioscope.

Tests are performed at 1 kHz, 2 kHz, 3 kHz, 4 kHz and 5 kHz at 1 $\mathrm{kV_{RMS}}$ and 2 $\mathrm{kV_{RMS}}$.

4.2 System test

All the system tests is performed using the OMICRON measurement system.

Noise and frequency band

Noise measurement tests are performed to eliminate the sources of interference if possible. The tests are performed with individual parts connected both with and without applied voltage to detect whether discharges occur. The testobject used during the

noise tests is a teflon plate to assure that no discharges occur in the sample and only the set-up is tested.

A measurement on the noise band is performed to ascertain at what limit partial discharges can be detected and not be strongly affected by underlaying noise. This is done by turning all the circuit equipment on, with no applied voltage and using the OMICRON program to detect the limit.

Finding the appropriate frequency band to preforme the tests are done using the OMICRONS FFT function and is done in the same manner as detecting the noiseband, observations and choosing an area where the noise content is low.

When the noise is at low level and all the segments of the circuit is tested and approved the experimental circuit is completed and approved for further testing.

Benchmarking

The benchmarking will give an indication of the partial discharge behaviour in a layered sample compared to a solid one to assure that no discharges occur in the interfaces of the test objects decribed in section 4.4. The set-up tests are done using solid layered test sample and a solid PET sample with a thickness of 250 μm without cavity.

The tests are performed applying a combined DC and AC voltage, V_{dc}=10 kV and V_{AC}=1 kV at 50 Hz and a pressure of 50 kN/mm.

4.3 Main test

All the main tests is performed using the OMICRON measurement system.

The test are ment to be a frame of reference by observing the discharge magnitudes and repetition rates at different applied voltages to be able to have some data to compare to the expected results based on theory. The results is used for a comparison to determine the capability and reliability of the experimental set-up.

The further testing is performed on the 3×100 μm samples with and without cavity r= 1 mm. The tests are performed under equal conditions, a temperature of 60°C and a pressure of 75 kN/mm.

Table 4.1: Main tests

Applied voltage	**Run time**
Pure AC voltage, V_{ac}=500 V_{rms}, f=50 Hz	24 hours
Pure DC voltage, V_{dc}=10 kV_{dc}	24 hours
Combined AC and DC voltage, V= 10 kV_{dc} +500 $V_{ac,rms}$, f=50 Hz	24 hours
Combined AC and DC voltage, V= 10 kV_{dc} +500 $V_{ac,rms}$, f=1 kHz	12 hours

4.4 Test Objects

The test objects are created out of Polyethylene Terephthalatem (PET) sheets. The choice of using PET sheet is due the consistent thickness, low amount of contaminants and constant dielectric properties. This makes the test objects simpler to create without large variations in characteristics of the samples.

The test objects consist of three circular layers of the PET sheet glued together at the edges. The middle sheet can be altered to either make a sample without or with a cavity of a given radius. The thickness of the PET sheet is 100 μm so the thickness of the finished sample will be 300 μm and the radius of the cavity can easily be changed based on the desired size of the artificial cavity for the test.

Table 4.2: List of parameters for the test objects

Parameter	**Definition**	**Value**
ϵ_b	Relative permittivity of dielectric	3.5 [F/m]
ϵ_c	Relative permittivity of cavity	1 [F/m]
σ_b	Conductivity of dielectric	1.65e^{-15}[S/m] at 80°C
σ	Conductivity of dielectric	1e^{-15}[S/m]
H	height of test object	300 [μm]
h	height of cavity	100 [μm]
R	effective radius of electrodes	25 [mm]
r	radius of cavity	1 [mm]

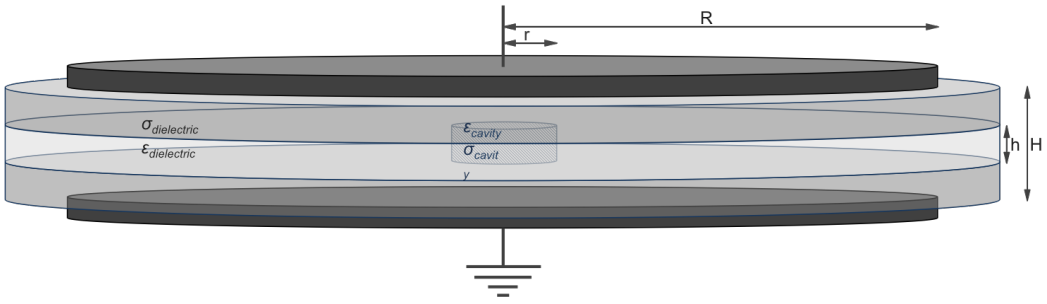

Figure 4.1: Test Object

4.4.1 Manufacturing of the samples

A stensil and press are used to create the circular objects from the PET sheet. The middle layer is either solid or have a hole drilled in the middle to create a cylindrical cavity filled with atmospheric air.

The samples with the drilled hole is inspected in a microscope in order to discard the object with sharp edges or irregularities around the cavity that may lead to local field

enhancements. The samples are sorted into categories A, B and discarded, based on the findings. This gives a more correct reading of the relevant partial discharges, e.i the ones occuring due to the artificial air cavity.

Since partial discharges occur in the imperfections in a dielectric it is important to manufacture the samples in a clean environment.

- The three PET sheets are cleaned using isopropanol and dryed.
- A catalyser (770) is applied along the edges and allowed to dryed before the sheets are placed together.
- The sheets are placed in a press and a pressure of approximately 3 bar is applied
- When the objects is placed under pressure, glue (406) is applied between all the layers along the edges.
- After 2-3 hours the glue have sufficiently hardened and the test object is complete.

The final samples are visually examined for contaminants before they are approved and numbered.

4.5 Test procedure

The test object to be tested is cleaned with isopropanol and dryed to remove any contaminants before it is lowered into oil in the testcell. Here it is moved around to remove airbubbles before being placed on the bottom electrode. The upper electrode must be partially lowered into the oil at an angle to let the airbubbles rise to surface. When the airbubbles have risen the lid is put in place and the electrode is lowered firmly in a vertical angle onto the sample to prevent the sample of sliding away. When the electrode is in place with the sample in the correct position the pressure needed is applied using the weights before connecting the electrode to the circuit and connecting the corona toroid before closing the faraday cage.

If the equipment have been in off posistion for a long time the sources are turned on, but with no voltage applied to reach operating temperature before applying the voltage. When the equipment have been on for at least an hour the voltage is applied. The DC voltage is tuned up slowly not induce any partial discharges.

5. Results

The results from the tests prefomed using the OMICRON measuring equipment a digital filter is used on the raw data. The filter takes out symmetrical, high frequency discharges out of the raw data. High frequency in this context is above 1 Hz, most of the discharges detected have a repetition rate of 180 per hour and lower, i.e. with a frequency well below 1/20 Hz. The filter was able to take out a small portion of the discharges responsible for sudden jumps in the repetition rate.

5.1 Sub-system test

The preliminary testing of the Behlman source and the transformers gave som unexpected results. The Petter Nodeland transformer showed a high current in the transformer, resulting in a high temperature in the windings, measured to be 97°C, at a voltage of 564 V at the secondary side of the transformer at 5 kHz.

The test on the neon transformer showed a transformer ratio of 1:100 in the 750 Hz area but that the transformer ratio declined rapidly with increased frequency with a 1:3 ratio at 5 kHz. Due to the ratio, the transformer cannot be used to reach 2 kV_{rms} with the Behlmans maximum output of 270 V_{rms}.

During the preliminary tests on the Arteche Measure Transformer it is revealed that the ratio between the primary and secondary side are very dependent on the frequency applied. The ratio differs from 1:500 at around 1 kHz to 1:11 at 5 kHz. The voltage looks good, but due the low ratio at higher frequencies it cannot be used to deliver the desired voltage.

In the preliminary tests performed on Messwandler Bau Measuring Transformator it became clear that both the voltage and the ratio looks good. Across the entire frequency range of 1 kHz- 5 kHz the ratio ranges between approximately 1:100 and 1:400. The Messwandler Transformer is used for further testing.

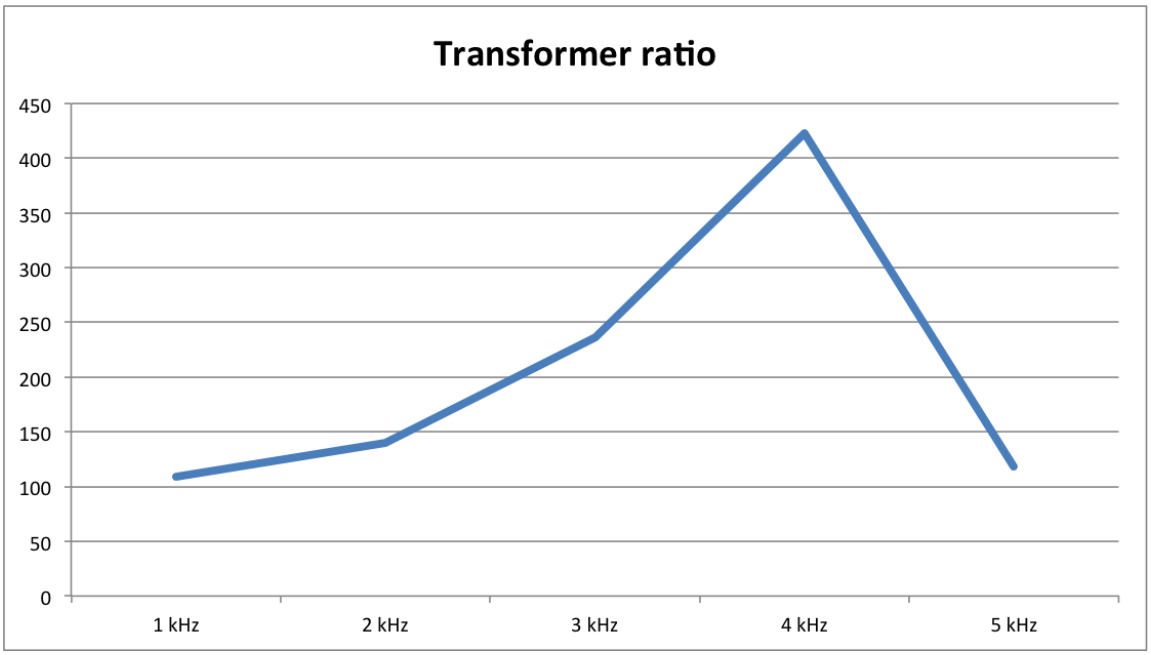

Figure 5.1: Transformer ratio of the Messwandler Bau

5.1.1 Harmonics analysis

The total harmonic distortion (THD) of the Messwandler Bau measuring transformer is calculated on harmonics of the voltage signal.

Table 5.1: Total harmonic distortion for the Messwandler Bau at 1 kV and 2 kV at frequencies 1 kHz - 5 kHz.

	THD	
Frequency	**1 kV_{rms}**	**2 kV_{rms}**
1 kHz	0.90 %	0.73 %
2 kHz	0.81 %	0.47 %
3 kHz	0.70 %	0.50 %
4 kHz	0.58 %	0.33 %
5 kHz	0.40 %	0.29 %

Figure 5.2 and Figure 5.3 on the two next pages illustrates the results from the FFT of the signal on the secondary side of the transformer during the testing at 1 kHz and 1 kV and 2 kV, respectively.

The total harmonic distortion is below 1% for all the voltages and frequencies tested. It is determined that a filter is not neccessary before continuing with the design of the experimental set-up. The figures and additional data for the tests across the entire tested range of frequencies and 1 and 2 kV can be found in appendix C.

FFT analysis plot 1 kHz and 1 kV

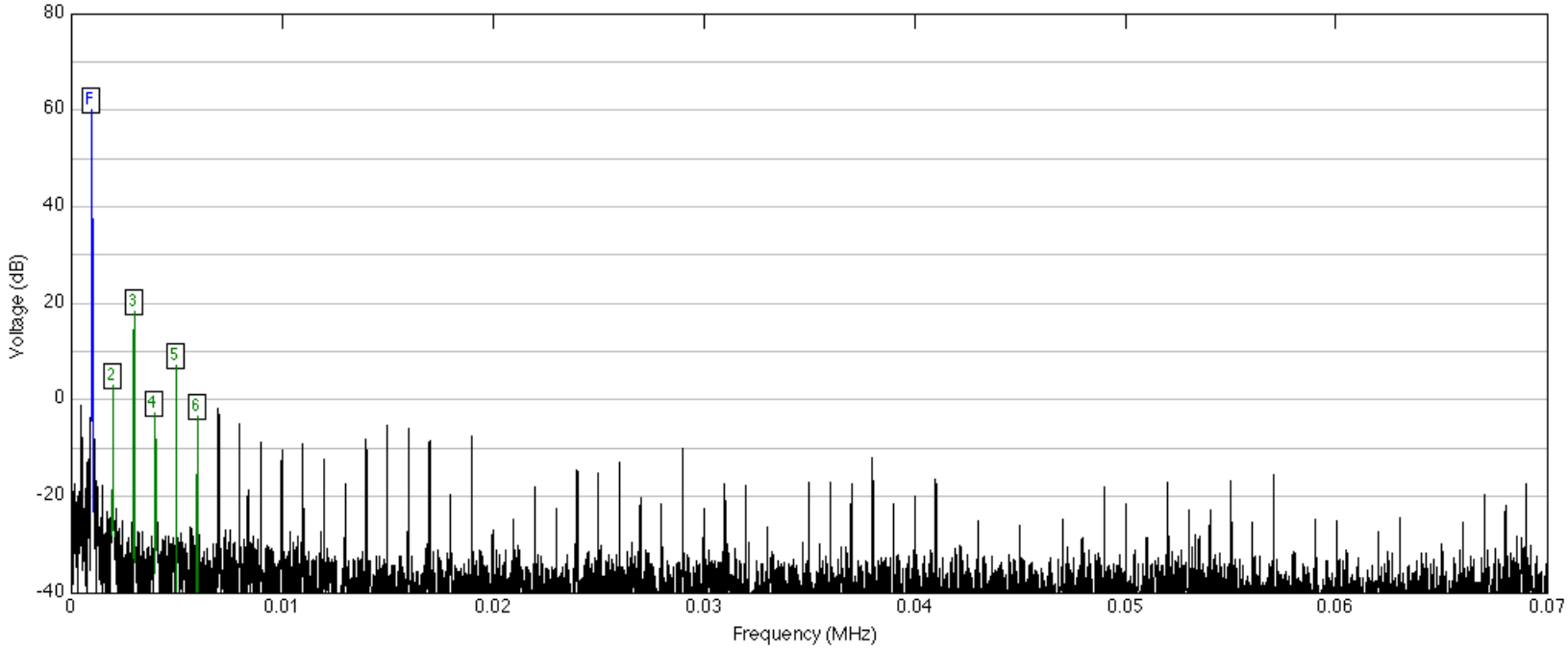

Figure 5.2: FFT plot 1 kHz and 1 kV

FFT analysis plot 1 kHz and 2 kV

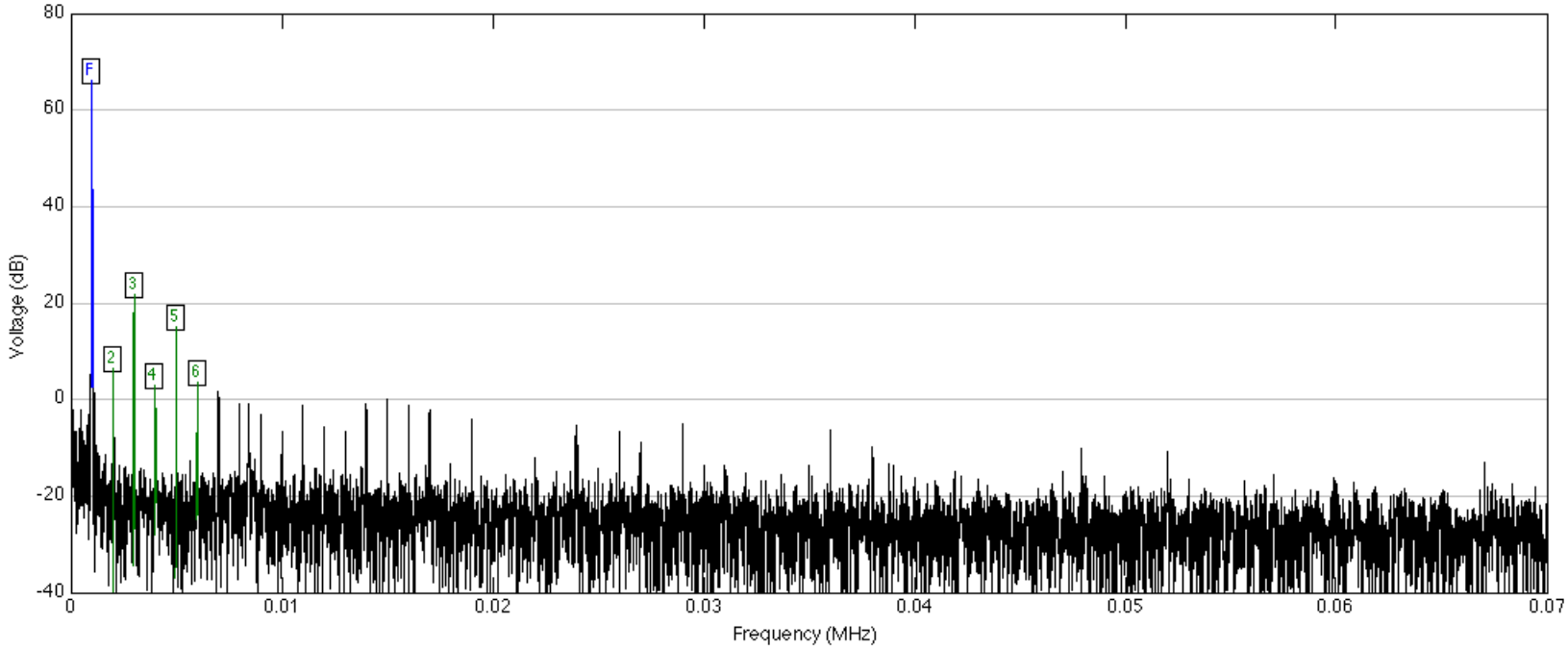

Figure 5.3: FFT plot 1 kHz and 2 kV

5.2 System test

5.2.1 Noise testing

The tests on the different segments of the circuit were carried out and alterations were done to lower the noise band. Resulting in a noise level of approximately 0.6 pC and a very good starting point for further testing. Figure 5.4 and 5.5 show the noise content and the FFT on the PD input, respectively. The frequency integrating range is set in a low noise area 1.15 -1.45 MHz and is marked in purple in the FFT illustration. The two peaks in the FFT plot, one small to the left of the frequency band and the larger one to the right, originate from an external noise source and have a sporadic occurence.

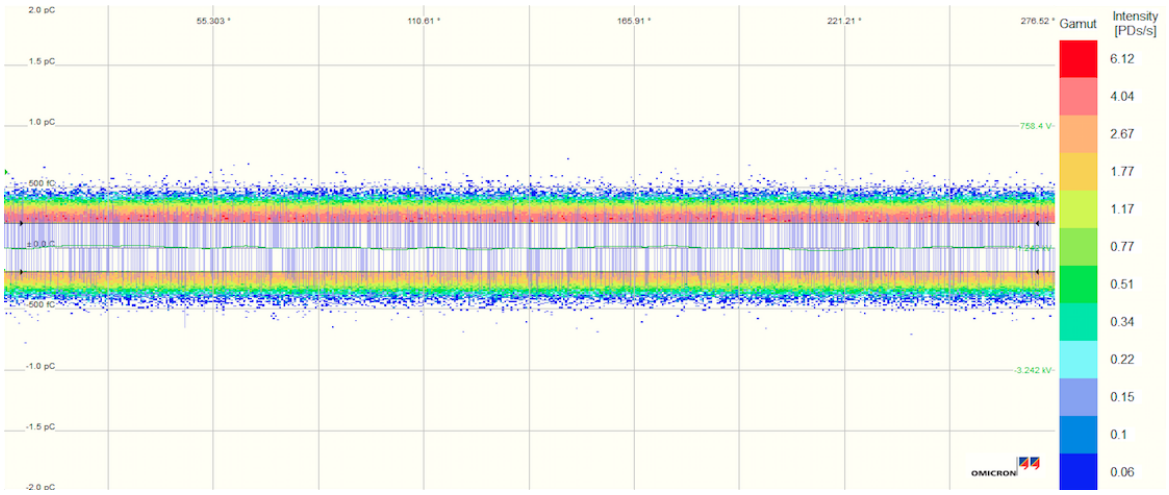

Figure 5.4: Noise content when all equipment is connected and in on state, but no voltage applied

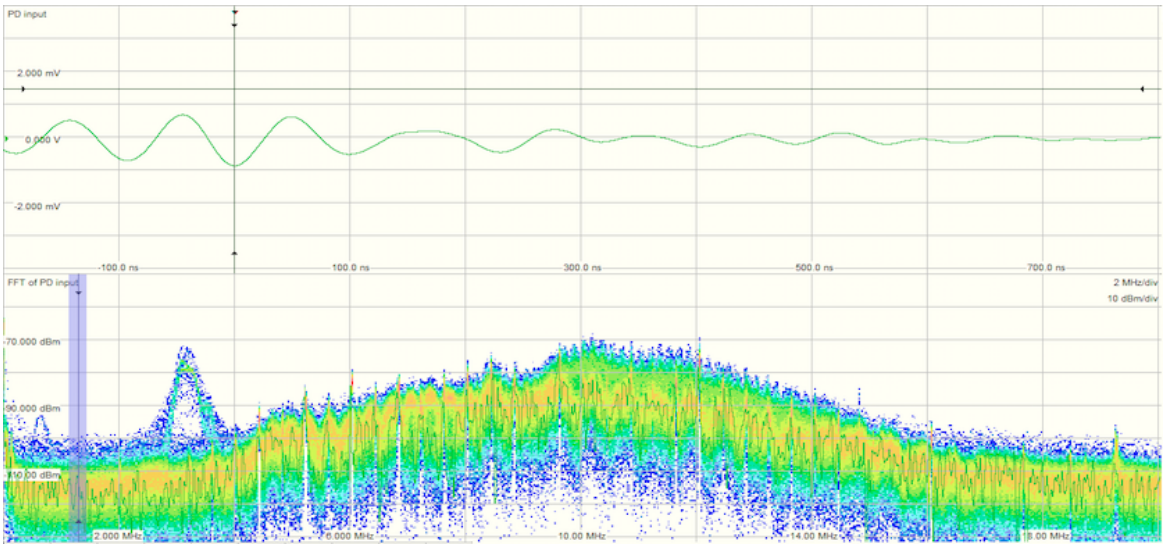

Figure 5.5: FFT and frequency band choice for the circuit. All equipment is connected and in on state, but no voltage applied

5.2.2 Combined 10 kV_{dc} and 50 Hz 1 $kV_{ac,rms}$ Voltage

P = 50 kN/mm

Table 5.2: PD data for PET 2, Solid 250 μm sample without cavity, 10 kV_{DC}, 1 $kV_{AC,RMS}$, f= 50Hz, P=50 kN/mm, t=18 hours, T=40°C

PD data for sample 2, without cavity	
Total number of discharges	81
Maximum magnitude	5.4893 pC
Minimum magnitude	-5.4565 pC
Mean discharge magnitude	-1.3283 pC
Median discharge magnitude	-1.1444 pC

Table 5.3: PD data for 3×100 μm layered samples without cavity, 10 kV_{DC}, 1 $kV_{AC,RMS}$, f= 50Hz, P=50 kN/mm, t=24 hours, T=60°C

PD data for layered samples, without cavity			
	Sample3	**Sample 4**	**Sample 5**
Total number of discharges	585	2595	4123
Maximum magnitude	7.0461 pC	75.6414 pC	84.7723 pC
Minimum magnitude	-30.94842 pC	-296.452 pC	-466.121 pC
Mean discharge magnitude	-1.1456 pC	-11.9983 pC	-21.3473 pC
Median discharge magnitude	-1.3518 pC	-2.8603 pC	-5.1317 pC

The plots of the discharge magnitude and repetition rate of sample 2 and sample 3 can be seen on the next two pages in Figure 5.6 and 5.7, respectively. It should be observed that the sampling time for sample 2 is 18 hours and the temperature is 40°C. The plots for sample 4 and 5 can be found in Figures D.1 and D.2 in section D.1 in the appedix.

From the data displayed in Table 5.3 above it can be seen that a high amount of discharges were detected in the layered samples without a cavity. In addition the discharges in the layered samples have a high magnitude compared to the discharges observed in sample 2, displayed in Table 5.2. Since these samples does not include a cavity these observations rises suspecion of discharges in the interfaces between the layers. The weight on the samples were increased to a corresponing pressure of 75 kN/mm for the continued testing.

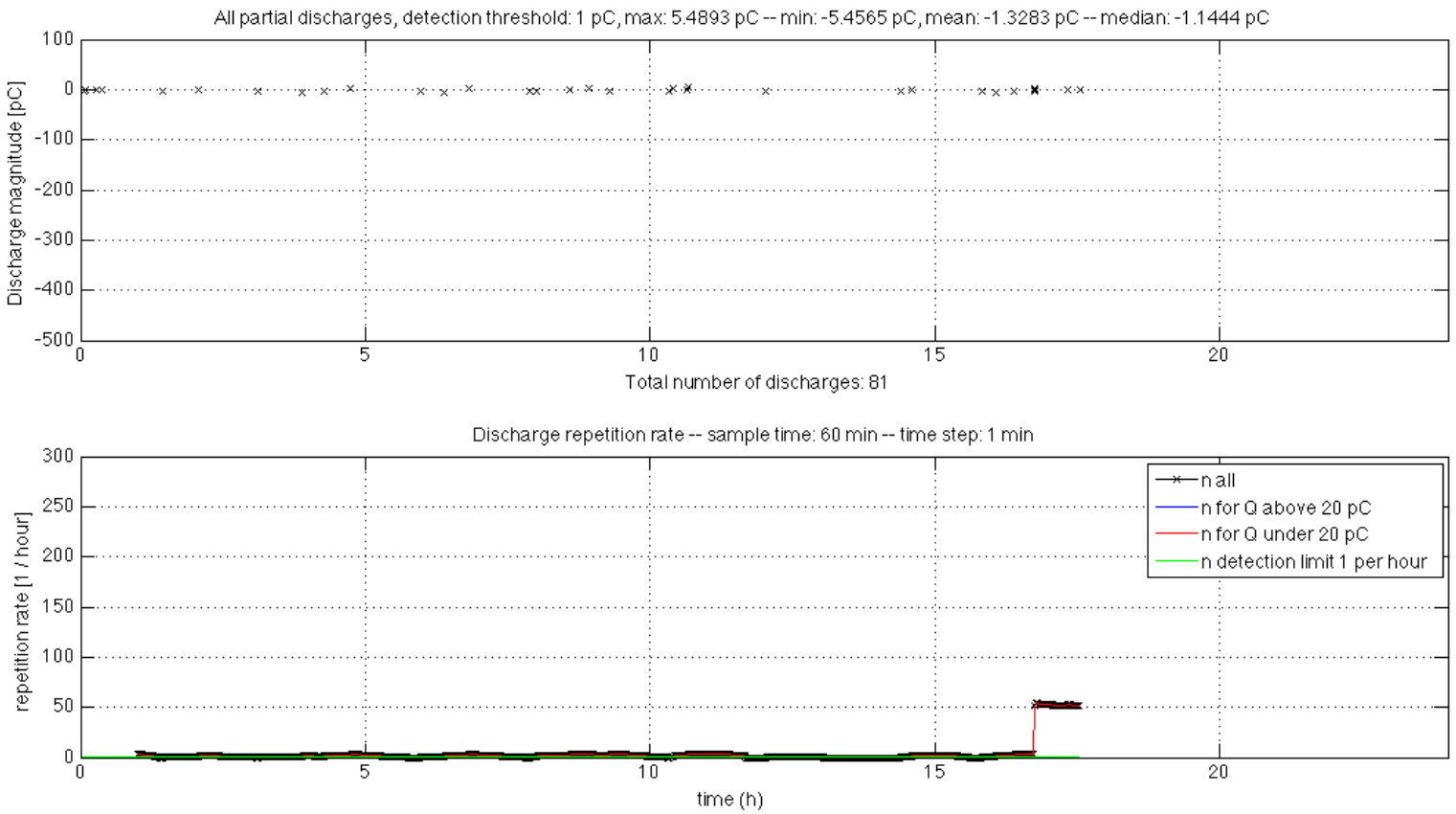

Figure 5.6: PET 2 plot. Solid 250 μm sample without cavity, 10 kV_{DC}, 1 $kV_{AC,RMS}$, P=50 kN/mm, t=18 hours, T=40°C

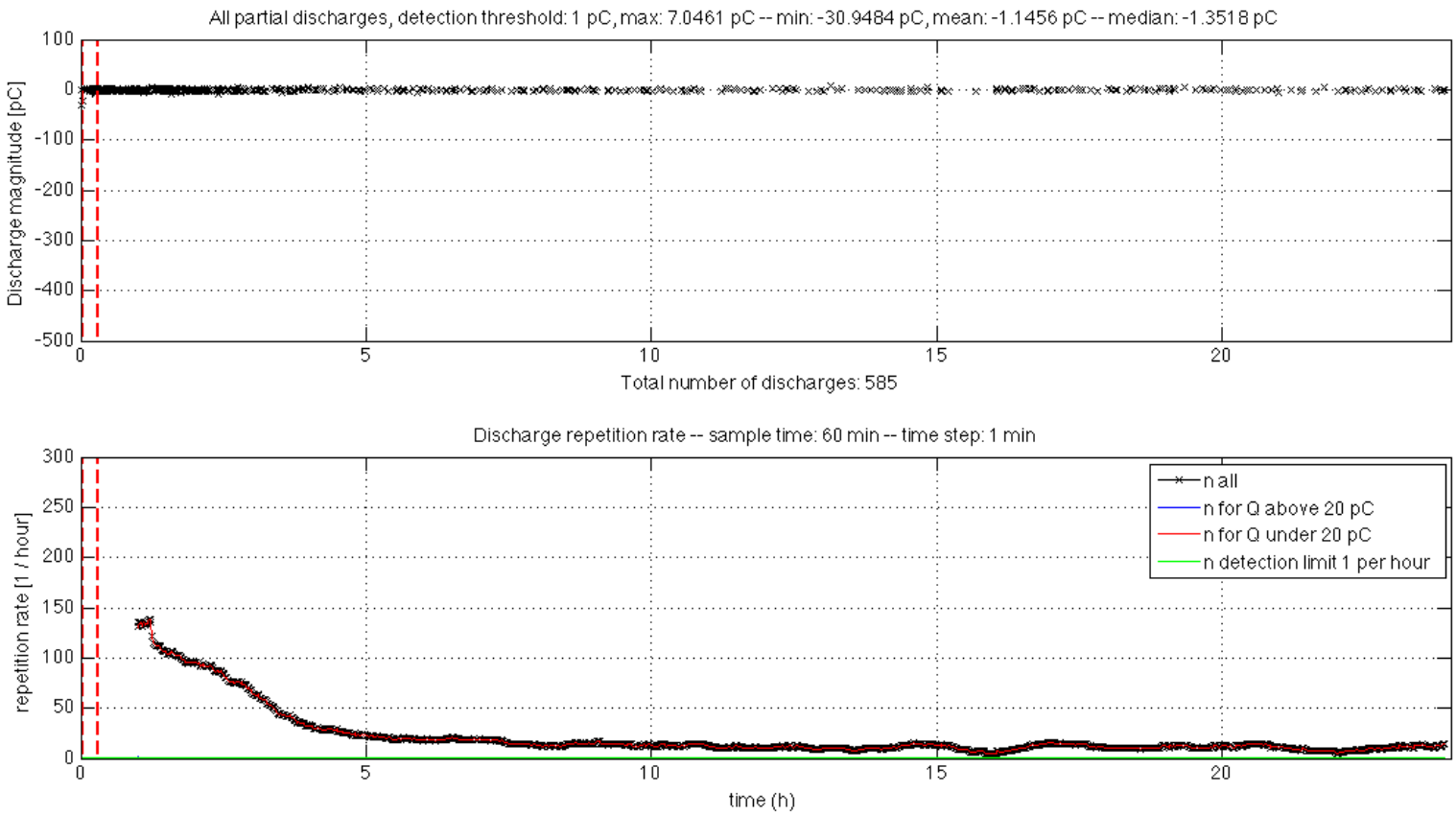

Figure 5.7: PET 3 plot. 3×100 μm layered sample without cavity, 10 kV_{DC}, 1 $kV_{AC,RMS}$, f=50 Hz, P=50 kN/mm, t=24 hours, T=60°C

P= 75 kN/mm

Table 5.4: PD data for PET 2.2, Solid 250 μm sample without cavity, 10 kV_{DC}, 1 $kV_{AC,RMS}$, f=50Hz, P=75 kN/mm, t=24 hours, T=60°C

PD data for sample 2.2, without cavity	
Total number of discharges	484
Maximum magnitude	2.9047 pC
Minimum magnitude	-26.5334 pC
Mean discharge magnitude	-1.3434 pC
Median discharge magnitude	-1.1061 pC

Table 5.5: PD data for PET 6, 3×100 μm sample without cavity, 10 kV_{DC}, 1 $kV_{AC,RMS}$, f= 50Hz, P=75 kN/mm, t=24 hours, T=60°C

PD data for sample 6, without cavity	
Total number of discharges	442
Maximum magnitude	13.0494 pC
Minimum magnitude	-22.5497 pC
Mean discharge magnitude	-2.4774 pC
Median discharge magnitude	-1.3589 pC

The plots of the discharge magnitude and repetition rate of sample 2.2 and sample 6 can be seen on the next two pages in Figure 5.8 and 5.9 respectively.

From the data diplayed in table 5.4 and table 5.5 above it can be suggested that increase of the pressure did not have an effect worth mentioning. Only a marginal reduction in magnitude and number of discharges for the layered sample 3 in the previos section and 6 can be observed by the data. However, looking at the plot for sample 3, Figure 5.7, and for sample 6, Figure 5.9, a noticable reduction in the repetition rate after some time has passed can be observed, and may indicate that the increased pressure did have some effect.

It was decided to apply a lower AC voltage for the main test, since the ignition voltage of the air cavity is approximately 1 $kV_{ac,rms}$ and the further tests are applied a voltage of 0.5 $kV_{ac,rms}$

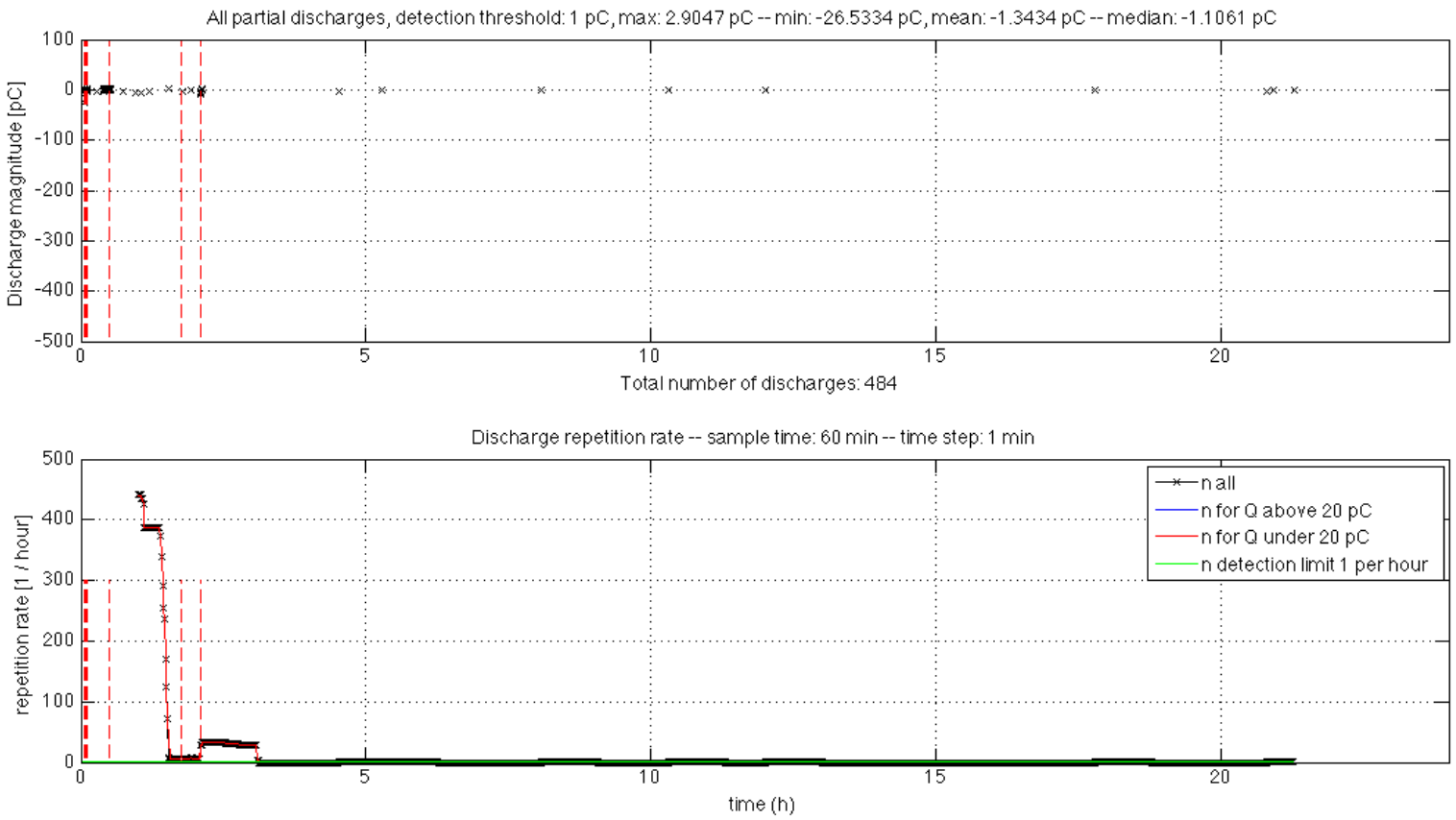

Figure 5.8: PET 2.2, Solid 250 μm sample without cavity, 10 kV_{DC}, 1 $kV_{AC,RMS}$, f=50 Hz, P=75 kN/mm, t=24 hours, T=60°C

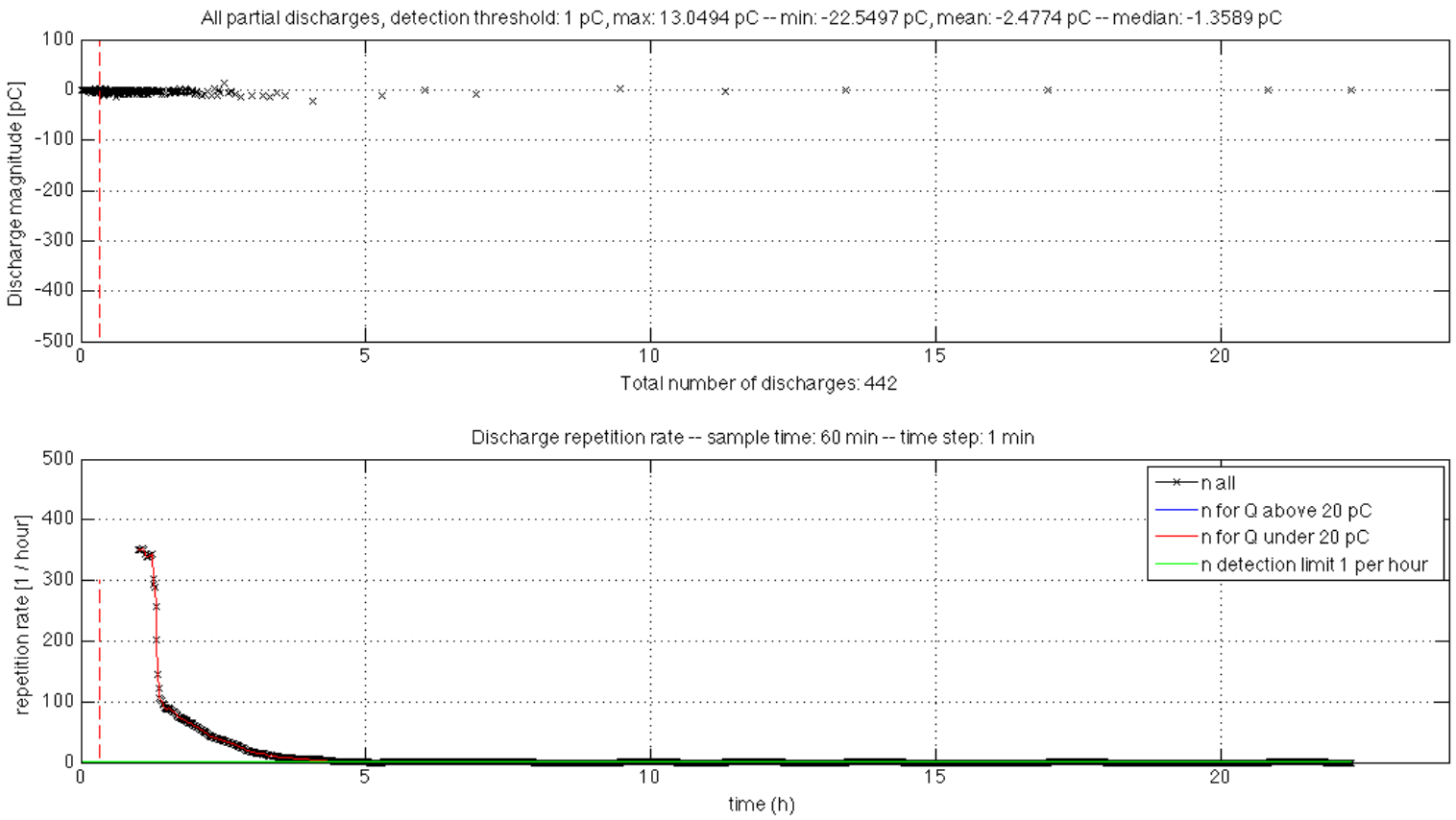

Figure 5.9: PET 6, 3×100 μm layered sample without cavity, 10 kV_{DC}, 1 $kV_{AC,RMS}$, f=50 Hz P=75kN/mm, t=24 hours, T= 60°C

5.3 Main test

5.3.1 50 Hz 0.5 $kV_{ac,rms}$

The inception voltage of the cavity was found to be approximately 1 kV_{rms} and the applied voltage across the dielectric was reduced to 500 V_{rms}.

Table 5.6: PD data for PET 17, 3×100 μm without cavity, 0.5 $kV_{AC,RMS}$, f=50Hz, P=75 kN/mm, t=24 hours, T=60°C

PD data for sample 17, without cavity	
Total number of discharges	15
Maximum magnitude	141.047 pC
Minimum magnitude	-41.3945 pC
Mean discharge magnitude	11.1082 pC
Median discharge magnitude	-1.2089 pC

Table 5.7: PD data for PET 16, 3×100 μm with cavity r=1 mm, 0.5 $kV_{AC,RMS}$, f=50 Hz, P=75 kN/mm, t=24 hours, T=60°C

PD data for sample 16, cavity r=1 mm	
Total number of discharges	40
Maximum magnitude	1.1612 pC
Minimum magnitude	-1.7126 pC
Mean discharge magnitude	-1.0086 pC
Median discharge magnitude	-1.1556 pC

The plots of the discharge magnitude and repetition rate of sample 17 and sample 16 can be seen on the next two pages in Figure 5.10 and Figure 5.11, respectively.

At a applied voltage of 500 $V_{ac,rms}$ there should be no discharges in either sample, as the applied voltage is below the inception voltage. The discharges in the sample with a cavity have a low magnitude and occur in the first 2 hours of the measurements.

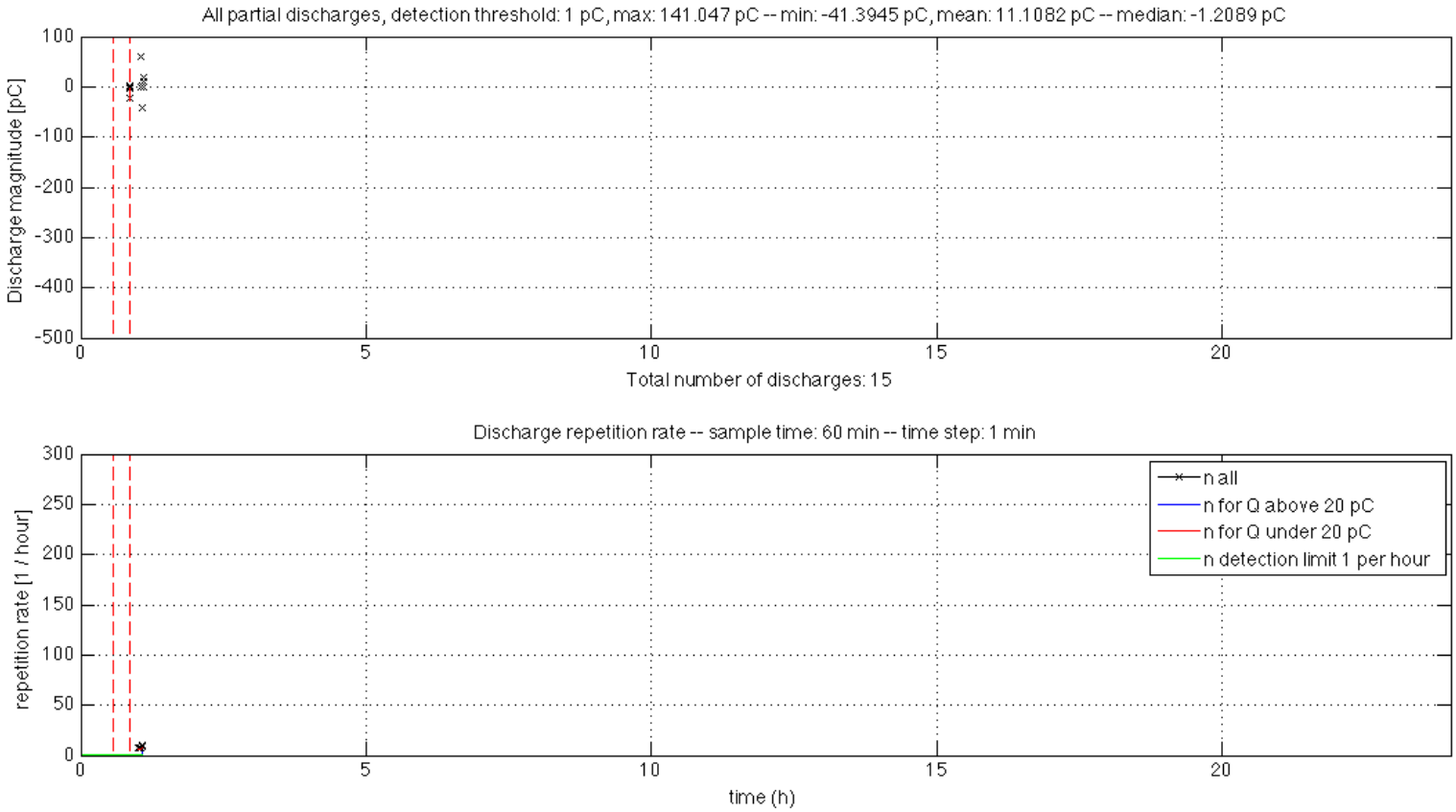

Figure 5.10: PET 17, 3×100 μm sample without cavity, 0.5 $kV_{AC,RMS}$, f=50 Hz, P=75 kN/mm, t=24 hours, T=60°C

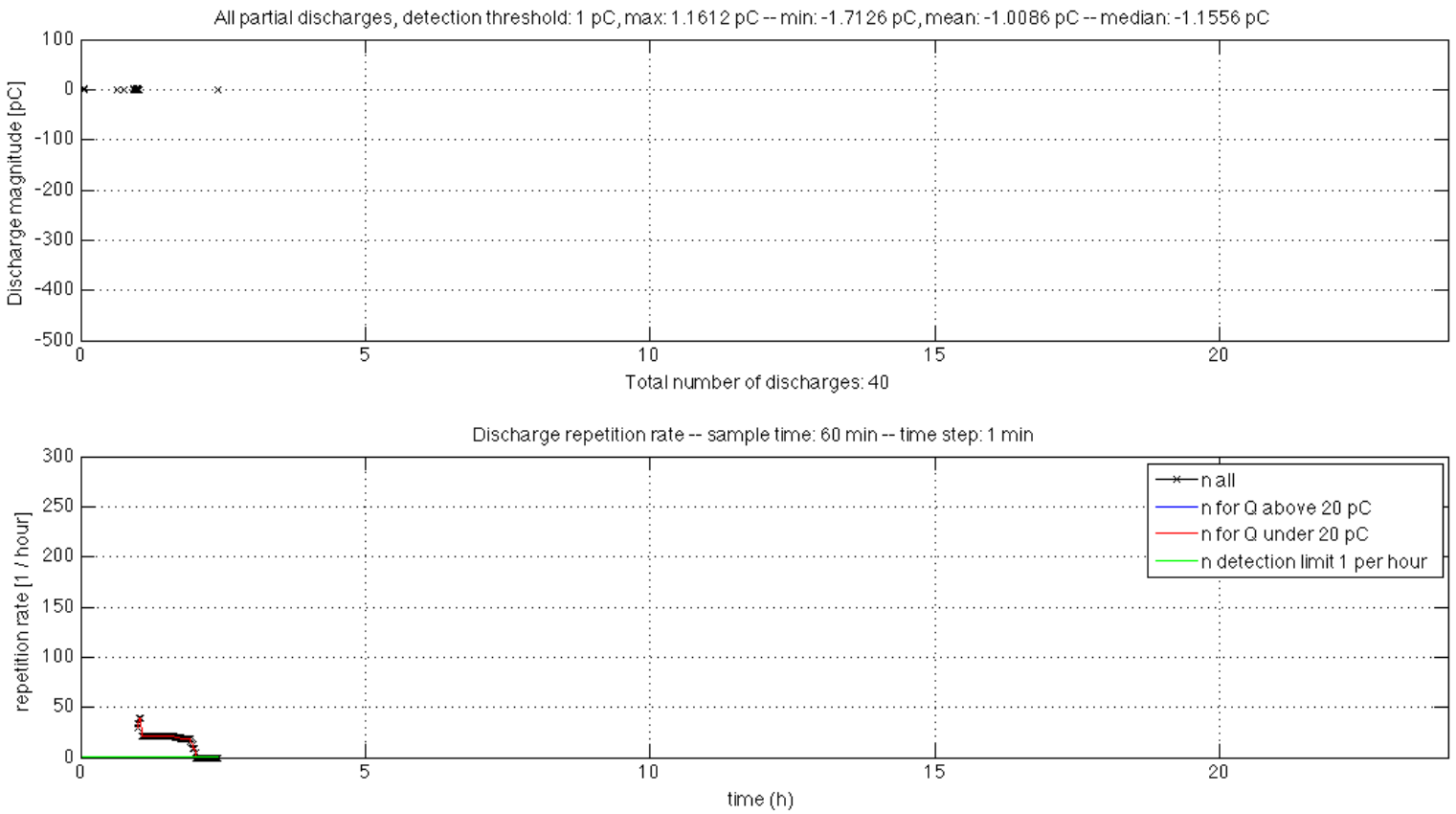

Figure 5.11: PET 16, 3×100 μm sample with cavity r=1 mm, 0.5 $kV_{AC,RMS}$, f=50 HZ, P=75 kN/mm, t=24 hours, T=60°C

5.3.2 10 kV_{dc}

The tests are preformed applying a pure DC voltage, V_{dc} =10 kV.

Table 5.8: PD data for PET 19, 3×100 μm without cavity, 10 kV_{DC}, P=75 kN/mm, t=24 hours, T=60°C

PD data for sample 19, without cavity	
Total number of discharges	12
Maximum magnitude	1.7231 pC
Minimum magnitude	-2.2113 pC
Mean discharge magnitude	-0.57098 pC
Median discharge magnitude	-1.1208 pC

Table 5.9: PD data for samples, 3×100 μm with cavity r=1 mm, 10 kV_{DC}, P=75 kN/mm, t=24 hours, T=60°C

PD data for samples with cavity r=1 mm			
	Sample 18	**Sample 21**	**Sample 22**
Total number of discharges	5	5556	30
Maximum magnitude	-1.159 pC	5.4882 pC	2.2333 pC
Minimum magnitude	-1.8398 pC	-12.1492 pC	-2.596 pC
Mean discharge magnitude	-1.48 pC	-1.3657 pC	-0.4779 pC
Median discharge magnitude	-1.4974 pC	-1.3814 pC	-1.052 pC

The plots of the discharge magnitude and repetition rate of sample 19 and sample 18 can be seen on the next two pages, in Figure 5.12 and Figure 5.13 respectively. The plots for Sample 21 and 22 is found in figure E.1 and figure E.2 in the appedix.

As can be observed in both the tables above and the figures, there is a large variation. No clear distinction between two of the samples with a cavity and the one without a cavity can be observed. However, sample 21 have a high number of discharges. A test were preformed to try to induce the same at 20 kV_{dc}, data and plots from this measurement can be found in the appendix in Table E.1 and Figure E.3. Even at a voltage twice as high, the same occurence could not be induced to the same extent.

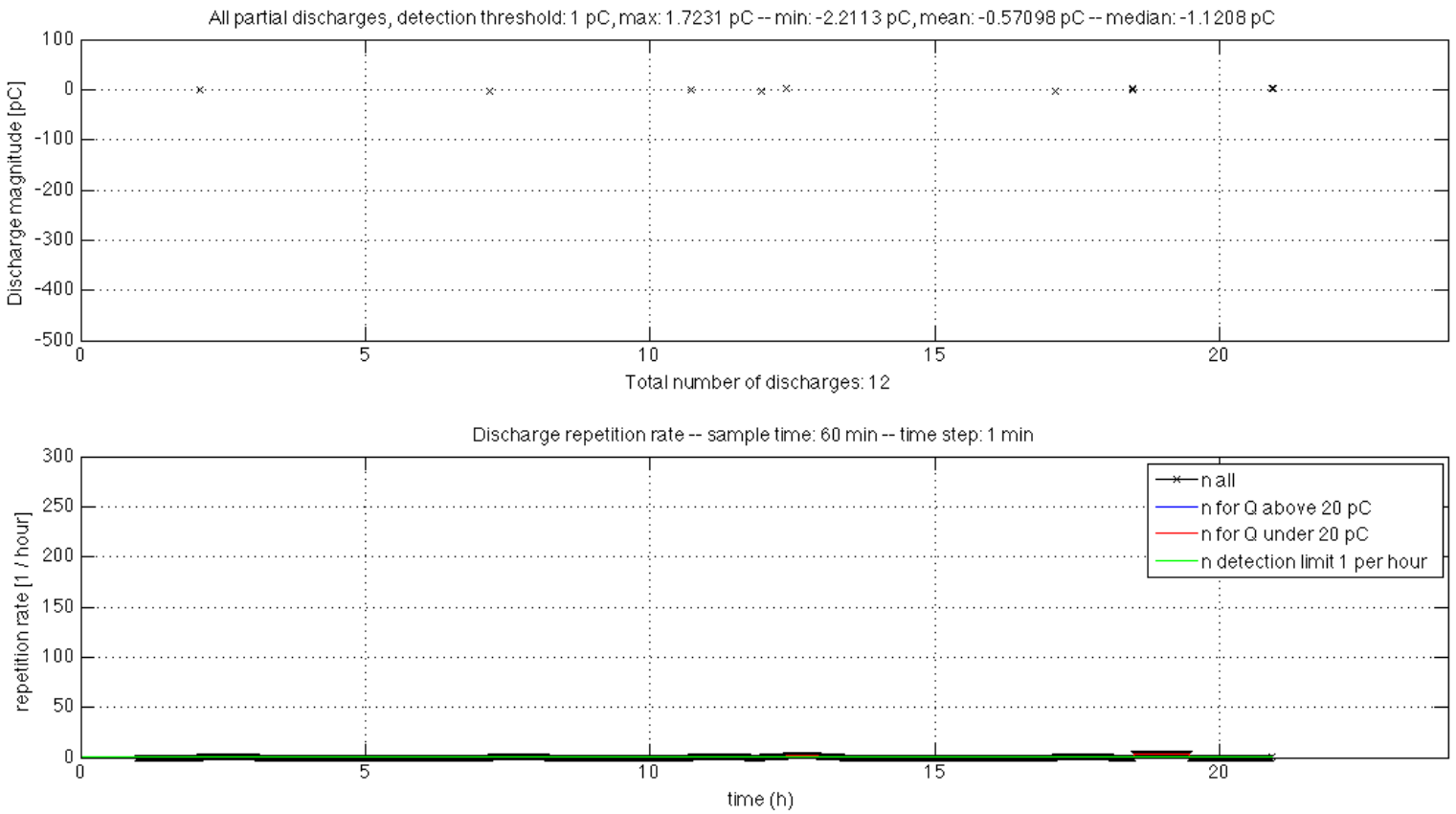

Figure 5.12: Pet 19, 3×100 μm sample without cavity, 10 kV_{DC}, P=75 kN/mm, t=24 hours, T=60°C

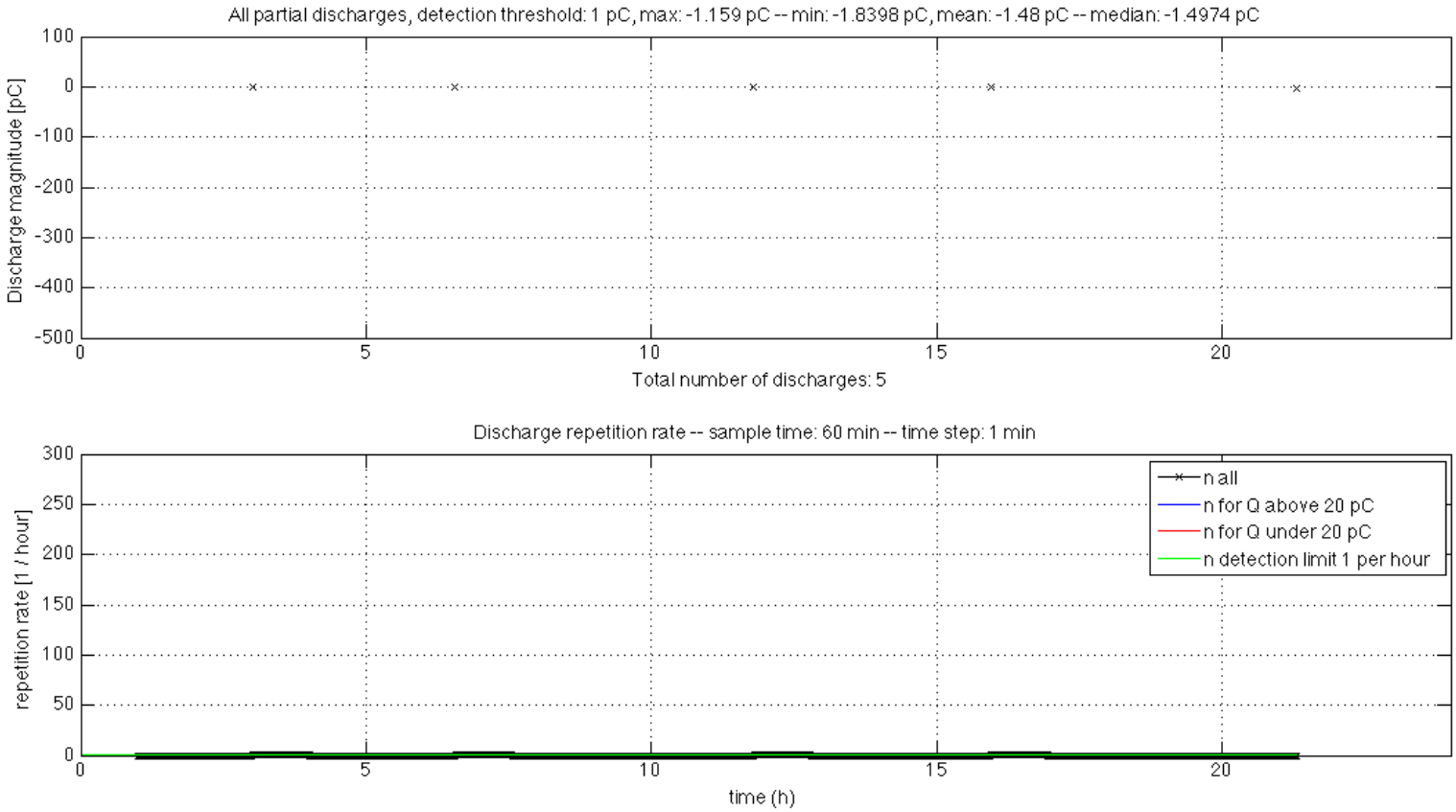

Figure 5.13: PET 18, 3×100 μm sample with cavity r=1 mm, 10 kV_{DC}, P=75 kN/mm, t=24 hours, T=60°C

5.3.3 Combined 10 kV_{dc} and 50 Hz 0.5 $kV_{ac,rms}$

The tests are preformed during combined DC and AC voltage applied, V_{dc} =10 kV, V_{ac}=500 V_{RMS} and f=50 Hz

Table 5.10: PD data for samples, 3×100 μm without cavity, 10 kV_{DC}, 0.5 $kV_{AC,RMS}$, f=50 Hz, P=75 kN/mm, t=24 hours, T=60°C

PD data for samples without cavity			
	Sample 13	**Sample 12**	**Sample 20**
Total number of discharges	75	30	60
Maximum magnitude	1.3749 pC	1.0466 pC	39.7632 pC
Minimum magnitude	-3.546 pC	-3.6006	-13.3236 pC
Mean discharge magnitude	-1.48 pC	-1.3867 pC	-1.05808 pC
Median discharge magnitude	-1.1184 pC	-1.3631 pC	-1.7244 pC

Table 5.11: PD data for samples, 3×100 μm with cavity r=1 mm, 10 kV_{DC}, 0.5 $kV_{AC,RMS}$, f=50 Hz, P=75 kN/mm, t=24 hours, T=60°C

PD data for samples with cavity r=1 mm			
	Sample 9	**Sample 8**	**Sample 15**
Total number of discharges	3435	2180	774
Maximum magnitude	108.931 pC	14.6515 pC	27.4434 pC
Minimum magnitude	-506.375 pC	-132.17	-183.937 pC
Mean discharge magnitude	-16.3414 pC	-9.2282 pC	-23.5858 pC
Median discharge magnitude	-3.949 pC	-4.2035 pC	-10.6381 pC

The plots of the discharge magnitude and repetition rate of sample 13 and sample 9 can be seen on the next two pages, in Figure 5.14 and Figure 5.15 respectively. The additional plots for sample 12, sample 20, sample 8 and sample 15 can be found Section E.3 in the appendix.

It can be observed in both the tables and the corresponing figures that there is a significant difference in both the total number of discharges and their magnitude between the solid samples and the ones with a cavity. The repetition rate for the samples with a cavity decrease from the moment voltage is applied, and after about 3-4 hours the discharges rate reaches a approximate stable level of discharges per hour. This steady level however varies from sample to sample.

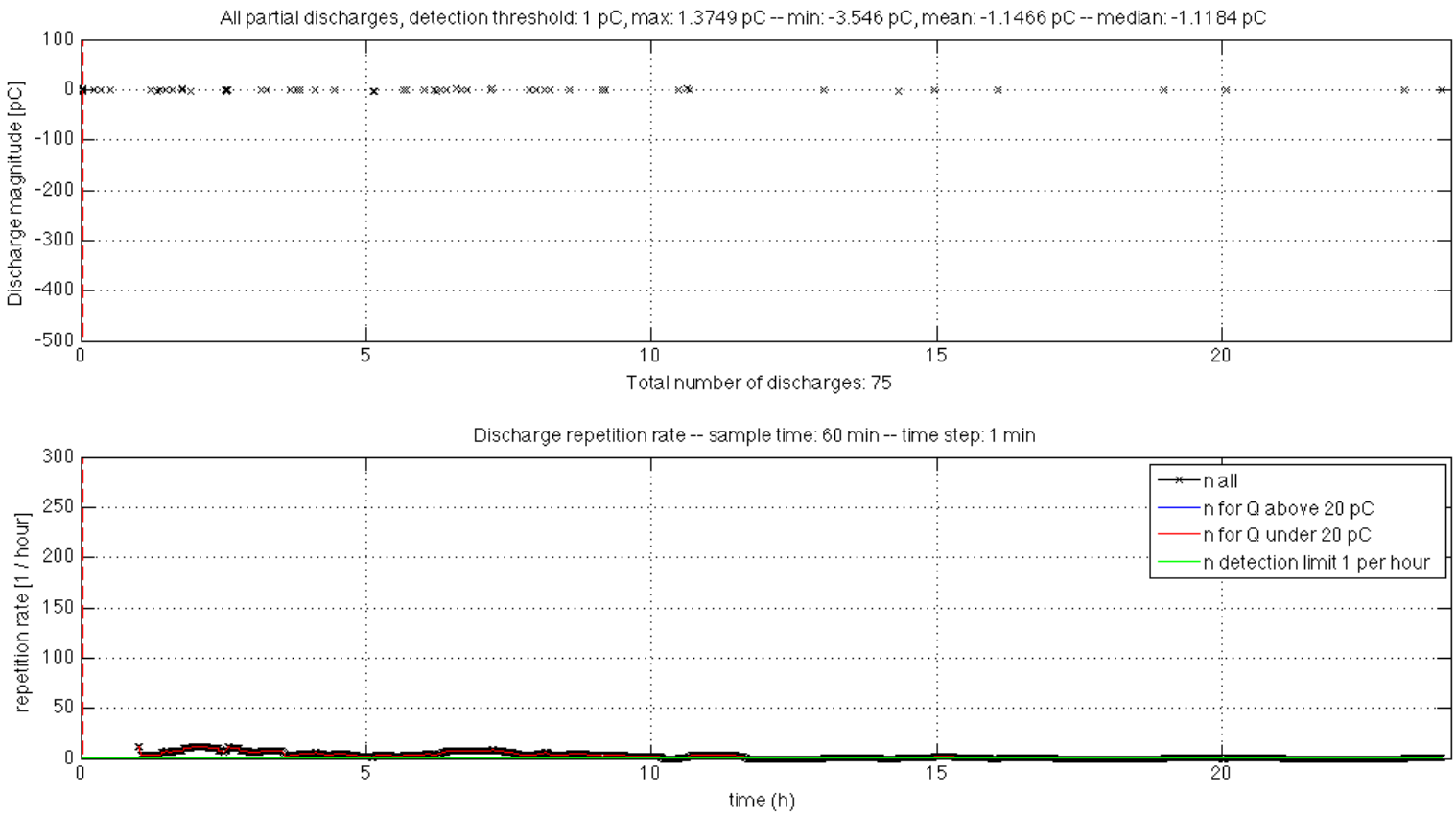

Figure 5.14: PET 13, 3×100 μm sample without cavity, 10 kV_{DC}, 0.5 $kV_{AC,RMS}$, f=50 Hz, P=75 kN/mm, t=24 hours, T=60°C

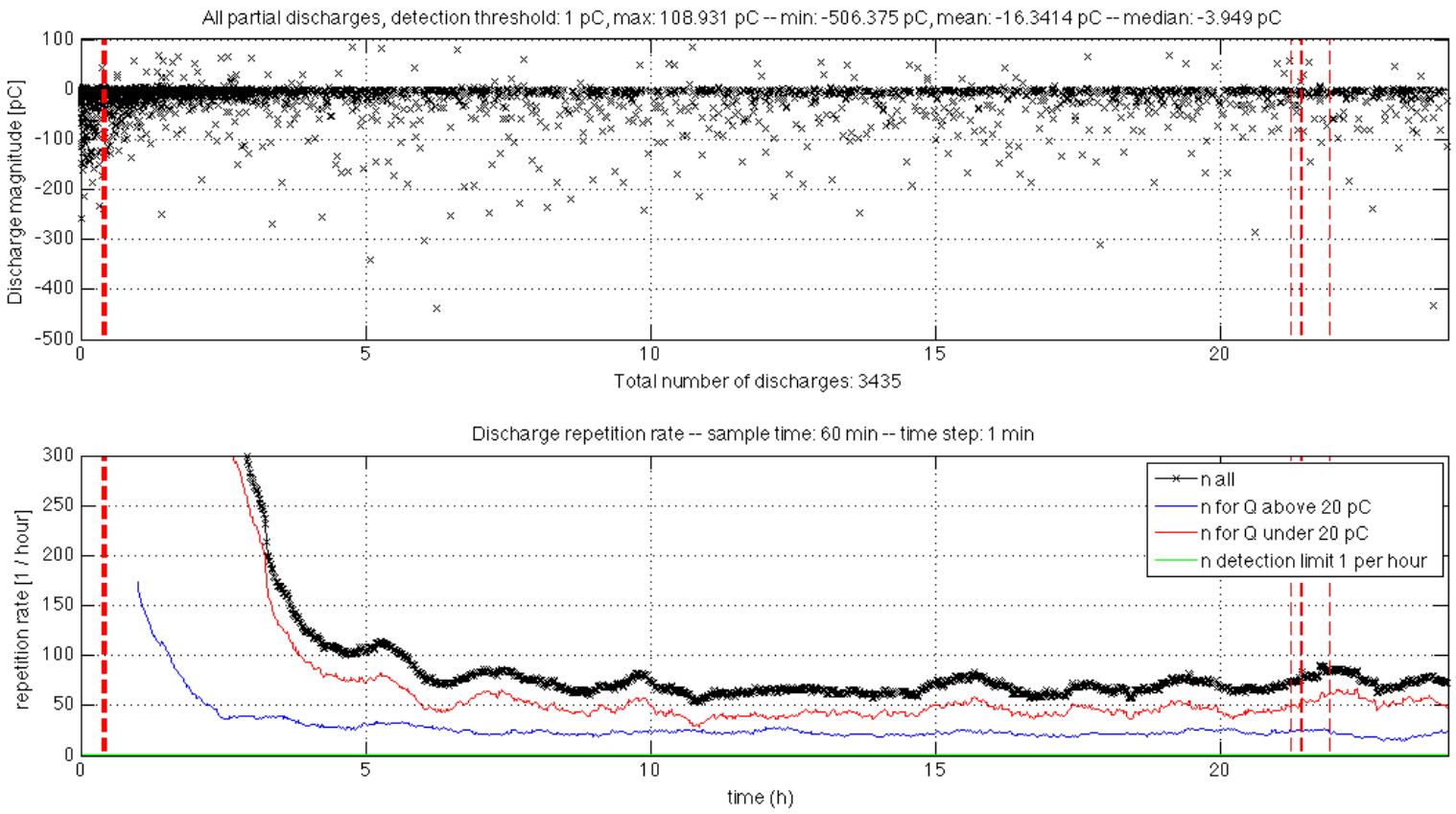

Figure 5.15: PET 9, 3×100 μm sample with cavity r=1 mm, 10 kV_{DC}, 0.5 $kV_{AC,RMS}$, f=50 Hz, P=75 kN/mm, t=24 hours, T=60°C

5.3.4 Combined 10 kV_{dc} and 1 kHz 0.5 $kV_{ac,rms}$

The tests are preformed under combined DC and AC voltage, V_{dc} =10 kV, V_{ac}=500 V_{RMS} and f=1000 Hz for 12 hours.

Table 5.12: PD data for PET 26, 3×100 μm without cavity, 10 kV_{DC}, 0.5 $kV_{AC,RMS}$, f= 1kHz, P=75 kN/mm, t=12 hours, T=60°C

PD data for sample 26, without cavity	
Total number of discharges	9
Maximum magnitude	1.1281 pC
Minimum magnitude	-1.5262 pC
Mean discharge magnitude	-0.81043 pC
Median discharge magnitude	-1.4325 pC

Table 5.13: PD data for samples, 3×100 μm with cavity r=1 mm, 10 kV_{DC}, 0.5 $kV_{AC,RMS}$, f=1 kHz, P=75 kN/mm, t=12 hours, T=60°C

PD data for samples with cavity r=1 mm			
	Sample 24	**Sample 27**	**Sample 25**
Total number of discharges	171	447	7
Maximum magnitude	53.11 pC	15.4275 pC	-1.0078 pC
Minimum magnitude	-291.093 pC	-253.672 pC	-2.2009 pC
Mean discharge magnitude	-35.1944 pC	-23.4936 pC	-1.4991 pC
Median discharge magnitude	-13.1498 pC	-10.7035 pC	-1.3598 pC

The plots of the discharge magnitude and repetition rate of sample 26 and sample 24 can be seen on the next two pages, in Figure 5.16 and figure 5.17 respectively. The additional plots for sample 27 and 25 can be found section E.4 in the appendix.

The tests at a combined DC and high frequency AC voltage have been run for 12 hours. The results have a large degree of variation. The results for sample 24 and 27 showed a similar shape of the repetition rate as during the 50 Hz combines test, but at a lower level.

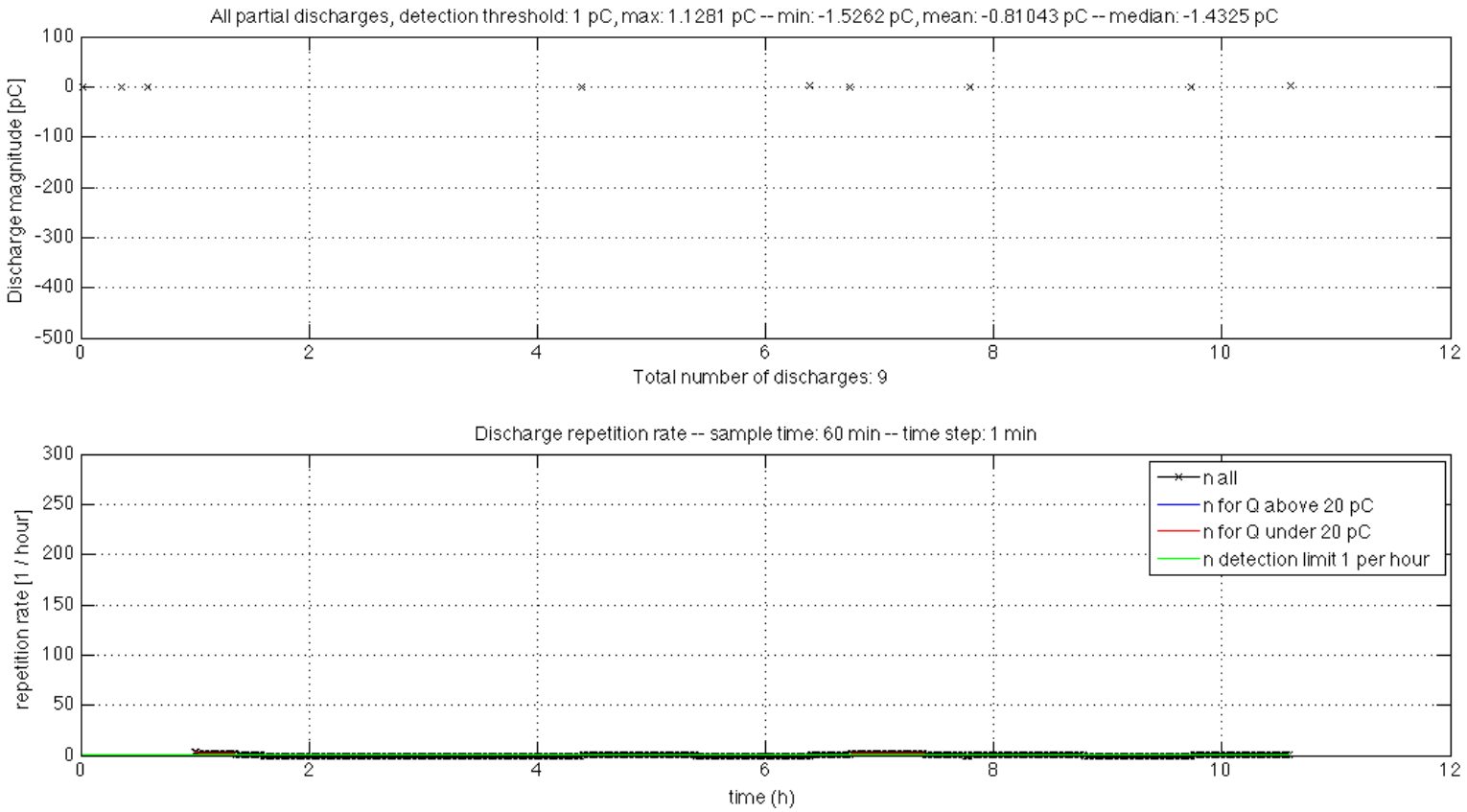

Figure 5.16: PET 26, 3×100 μm without cavity, 10 kV_{DC}, 0.5 $kV_{AC,RMS}$, f=1 kHz, P=75 kN/mm, t=12 hours, T=60°C

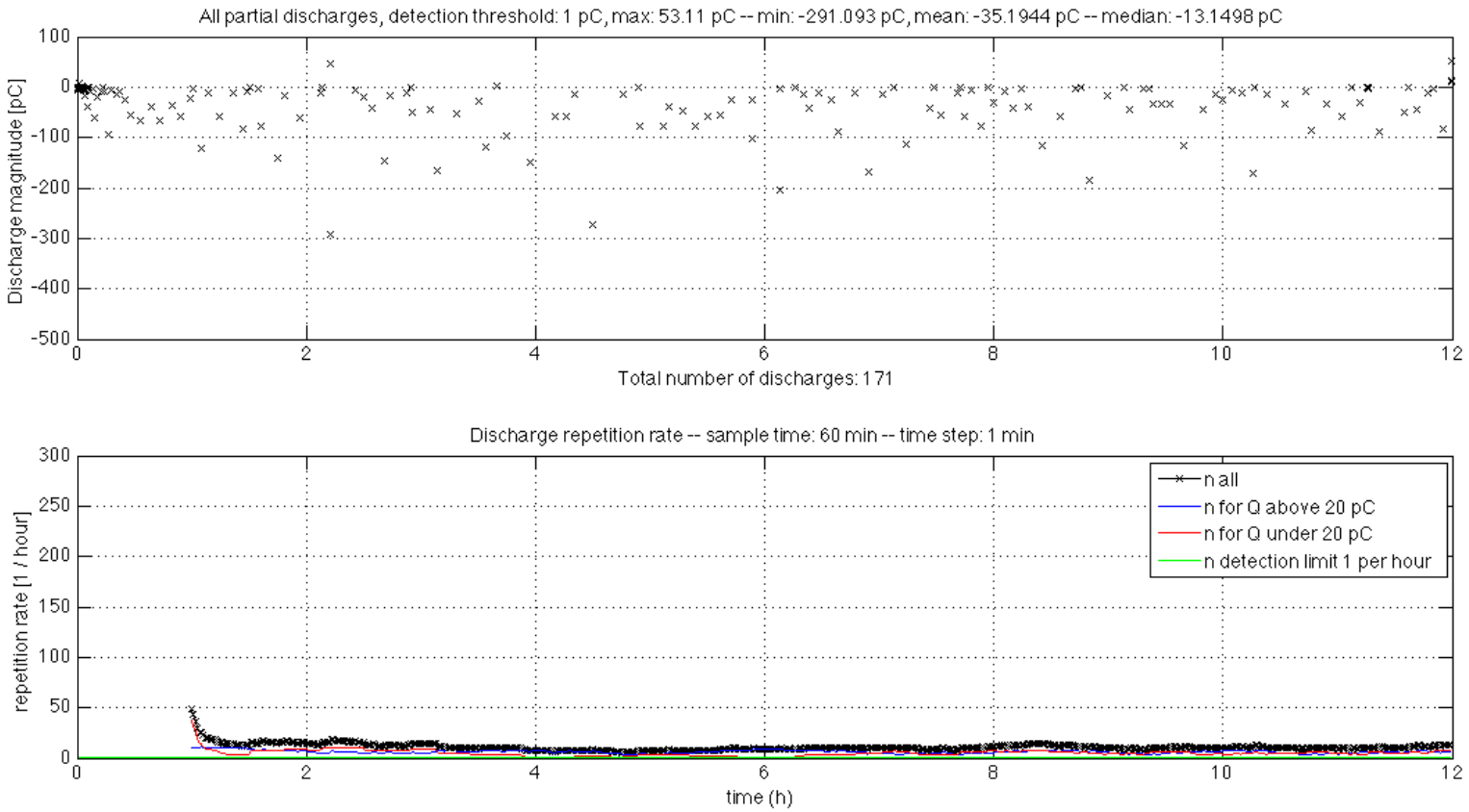

Figure 5.17: PET 24, 3×100 μm with cavity r=1 mm, 10 kV_{DC}, 0.5 $kV_{AC,RMS}$, f=1 kHz, P=75 kN/mm, t=12 hours, T=60°C

6. Discussion

6.1 Sub-system test

A number of transformers were tested. The results from the sub-system test proved three of the four transformer to have either a to low transform ratio or to much voltage distortion on the secondary side. At higher frequencies several of the transformers had difficulty reaching the 2 kV_{RMS}. The Messwandler Bau transformer proved to be the most promising transformer. It has a relatively high transformation ratio, which made it possible to deliver a voltage up to 2 kV_{rms} across the entire frequency spectrum of 1 kHz to 5 kHz. The transformer ratio may indicate that resonance occur at approximately 4 kHz. The FFT analysis results showed the harmonics from the source and transformer to be within a reasonable limit without extensive filtering, all have a THD below 1%. However the goal of reaching a voltage of 5 kV_{RMS} cannot be delivered with this equipment.

6.2 System test

6.2.1 Noise elimination

The initial testing of noise in the components in the experimental set-up was a time consuming part of the experimental work. The system test was conducted with sections of the set-up connected to the OMICRON to eliminate or attenuate the noise and a number of alterations were done.

- The coupling resistance and the buffer resistance were increased from 10 MΩ and 28 MΩ to 100 MΩ and 280 MΩ because noise from the DC source was detected and an error on the regulating controls of the DC source due to a induced voltage caused by the AC current across the buffer resistance.
- The control system of the heat coil were alterered due to noise.
- A part of the security system were moved, due to noise caused by movement.
- Ground loops due to the security system were eliminated.

The main supply can be a source of noise, but it is passed through a filter. Another source of noise, not solved in this task, is the voltage sources situated outside the faraday cage. Having all current carrying wiring inside the faraday cage eliminates the wiring picking up noise from the surroundings and creating noise in the circuit.

The FFT on the PD input signal shown in Figure5.5 has two peaks. These originate from noise from the surroundings and appear at sporadic times of the day and the frequency band chosen for testing is placed in the lowest range possible between these peaks. The noise measurements show a distinct noise band at approximately 0.6 pC. However, this is the noise band measured in one time window. Not the entire time test is run and does not necessarily give a clear image of the noise during the whole day.

6.2.2 Benchmarking

A large amount of discharges was detected in the layered sample compared to the solid sample during the benchmarking with an applied pressure of 50 kN/mm. In addition the partial discharges in the layered samples had a higher magnitude. The repetition rate for two of the samples decreases after the voltage has been applied and stabilized on a relatively constant level, for sample 3 at approximately 20/hour and for sample 5 at approximately 120/hour. Since these samples do not include a cavity these observations raises the suspicion of discharges in the interfaces between the layers. Sample 4 have a large variation in repetition rate with an increase to a maximum of approximately 840 discharges per hour after about 2.5 hours.

The results from the benchmarking at 75 kN/mm indicate a decrease in magnitude and a reduction in the number of discharges. The results suggested that an increase of the pressure did have an effect since the results in the solid and layered sample are similar. Comparing the results to the data from the 50 kN/mm test show a small reduction in magnitude and number of discharges for the layered samples. However, a noticeable reduction in the repetition rate after some time has passed is observed and may indicate that the increased pressure did have an effect.

The benchmarking results showed some aspects which can be interpreted as interference. The limited control of the DC voltage amplification and a too low waiting time could be a contributor to the large repetition rates in the first hours of the tests. The results from samples with an increased weight may still indicate a problem with the applied pressure on the sample. The design of the electrodes does not distribute an even pressure across the entire sample and the pressure along the edges of the electrodes could be a problem. The applied AC voltage in the system tests of 1 kV_{rms} is the inception voltage of the air cavity and the voltage is decreased to 500 V_{rms} for the main test.

6.3 Main test

The results during the pure AC voltage tests showed a low number of discharges, all situated in the first 2.5 hours. There should be no discharges at this voltage level. In the no cavity sample the discharge also has a higher magnitude than the sample with

a cavity. The discharges may be due to startup noise or small contaminants on the electrode surface. The high discharge detected in the no cavity sample may be noise, but no noise at this level has been detected.

The results from the pure DC test were very varying and discussing the results with the data collected during these tests, is difficult. The test on the sample without a cavity and two of the samples with a cavity had a low number of discharges. The third sample with a cavity had a high number of discharges. The sample with the 20 kV_{rms} show a similar repetition rate. A low repetition rate during the first hours before the repetition rate increased. The discharge during applied DC voltage are all small in magnitude. Since the field is unipolar, it is more likely that charge accumulate on the cavity surface, creating a field in the opposite direction and a smaller voltage drop to the extinction voltage. [26] The small magnitude and a typically low repetition rate will make the DC test results more prone to noise. Another problem with the small magnitudes is the problem with the OMICRON, the detection system have proven to have some issues determining polarity at low magnitudes. The polarity of discharges during DC voltage should all be of the same polarity. [19] Without additional data it is impossible to explain the partial discharge occurence in the DC tests.

The results from the combined DC and AC voltage test at 50 Hz illustrated a significant difference between the samples with and without a cavity. The solid layered samples experienced a low number of discharges with a small magnitude. The results from the test performed with a cavity showed an increase in both the magnitude and repetition rate. The repetition rate is high in the initial hours before it decrease to a relatively stable level. The initial repetition rate and the stable level is different for the samples. Sample 9 stabilize at approximately 125 discharges/hour, Sample 8 stabilize at a level of approximately 75 discharges per/hour while sample 15 have a stable level of approximately 20 discharges/hour. The repetition rates for the samples with a cavity follow an expected shape indicated by the equation for the repetition rate during a combined DC and AC voltage. It is dependent of the time constant which is a function of the conductivity of the cavity and the dielectric which approaches a stable level after a time dependent of temperature.

$$\tau = \frac{D\epsilon_0\epsilon_c + \epsilon_0\epsilon_b}{D\sigma_c + \sigma_b} \tag{6.1}$$

$$n \approx \frac{1}{\tau}\left(\frac{V_{dc}}{V_{PDIV,DC}}\right)\left(\frac{1}{1 - \frac{\hat{V}_{ac}}{V_{PDIV,AC}}}\right) \tag{6.2}$$

The stable value of the repetition rate is affeced by the conductivity of the air in the cavity. This value is unknown since there is no information on the humidity, possible by-products or other contributing factors. The placement of the discharge detected by the low gain unit can be seen in Figure 6.1. It shows that discharges are concentrated near the peak value of the applied voltage.

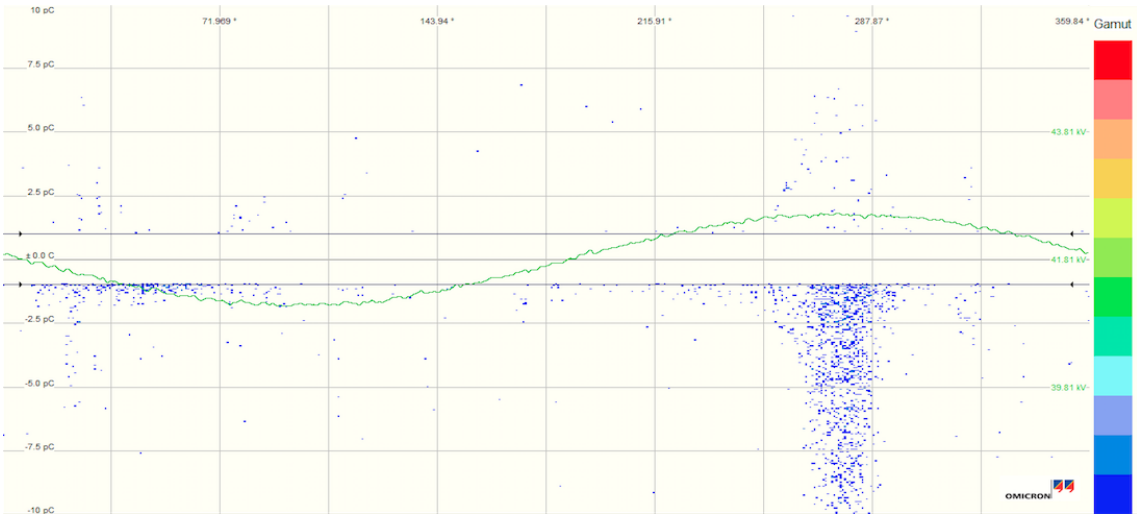

Figure 6.1: Picture from Omicron illustrating occurence of discharges, high gain for sample 8, 3×100 μm with cavity r=1 mm, 10 kV_{DC}, 0.5 $kV_{AC,RMS}$, f=50 Hz, P=75 kN/mm, t=24 hours, T=60°C

The results from the combined DC and AC voltage with a frequency of 1000 Hz gave some variations. The sample without a cavity gave a low number of discharges at low magnitude. The tests on the samples with cavity had a large variation in the number and magnitude of the detected discharges. It should, however, be observed that the repetition rate was overall lower at the high frequency test compared to the 50 Hz test. The stable level is approximately 10 discharges/hour for sample 24 and 40 discharges/hour in sample 27. The reduced number of discharges can be due to an alteration of the capacitance of the test object at higher frequencies because of the permittivity. A decrease of the capacitances result in a lower stress across the cavity and a lower repetition rate. But additional data must be collected to know the effect of the frequency on the permittivity and partial discharge behavior. An error source in the comparison between the 1 kHz tests and the 50 Hz tests is the fact that the Behlman source was not tested at 50 Hz, and might have a higher THD at 50 Hz, than at 1 kHz. In Figure 6.2 one can observe a slight shift in the placement of the voltage phase compared to Figure 6.1 for the 50 Hz comined voltage test. This may be due to the measuring shunt. The RLC measuring shunt might result in a phase shift at higher frequencies. It could also be explained by the statistical time lag.

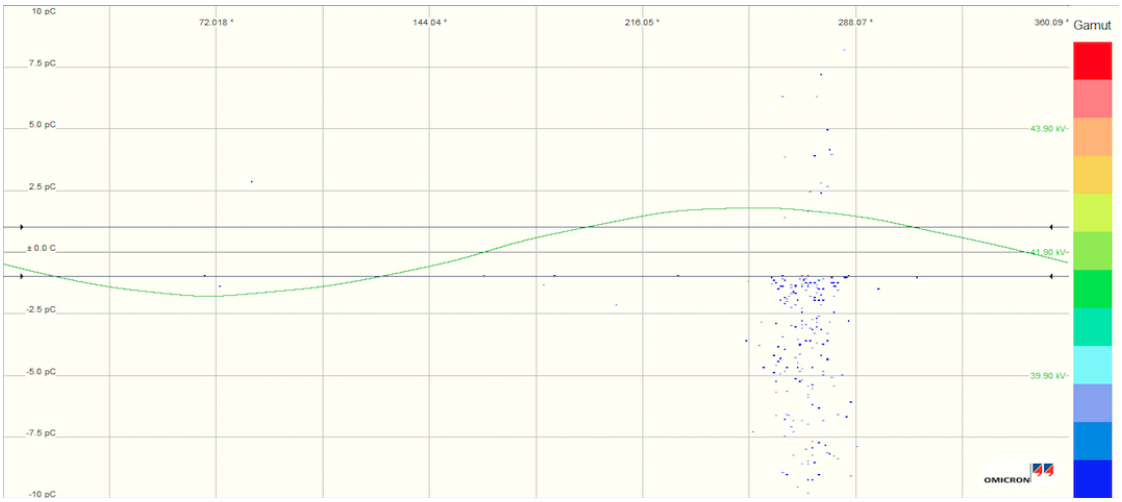

Figure 6.2: Picture from Omicron, high gain for sample 27, 3×100 μm with cavity r=1 mm, 10 kV_{DC}, 0.5 $kV_{AC,RMS}$, f=1 kHz, P=75 kN/mm, t=12 hours, T=60°C

The results from the discharge tests show a large variation in the number of discharges and magnitude throughout the samples with the same characteristics and voltage. There are a number of phenomenona that may contribute in explaining the variations in the number and magnitude of the discharges. The accumulation of space charge due to the resitive field may alter the field across the cavity. Production of by-products from the discharges in the cavity or on the cavity walls may alter the characteristics of the cavity, creating large varations in the breakdown strengt and the number of discharges.

Some observations have been made in several samples.

- Partial discharge with a high positive magnitude when a unipolar field is applied. This might indicate a flashback in the cavity or noise.
- Partial discharge magnitude above the calculated value for a discharge across the whole cavity area might be explained by the electrostatical forces on the test object, altering the dimentions and increasing the area. It might also be due to a too low pressure on the sample making the discharges bigger due to the intersections.
- High repetition rate in the first hours may be due to an insuffient waiting time for the voltage sources, or a too rapid increase of the DC voltage.
- Noise. The presence of noise is hard to determine, espesially when the OMICRON has difficulty determining the polarity of small discharges. Inconsistencies may also be caused by contaminants or airbubbels on the electrode surfaces.

Both the quantity and the quality of the results must be increased to get a clear image of the partial discharge activity in the samples. The inconsistencies in the results suggest that further improvements must be done with the experimental set-up to get a more reliable result.

6.4 Procedure

6.4.1 Test samples

The manufacturing of the test samples is in theory a simple procedure, but there are many possible error sources that can be caused by poor manufacturing. Oil leakage has been a problem that has occured during the testing and several samples have been discarded. It is very important to create them using a sharp blade to be able to get the glued surfaces to curve in the same direction to maximize the probability of successful glueing and hence minimize the chance of oil leakage into the sample.

The oil ingress can in most cases be observed as the samples are lowered into the mineral oil in the test cell, but in some instances the ingress had some kind of delay and cannot be discovered until the test finished and the whole measurement must be discarded. In the beginning the process of creating the samples took a minimum of 12 hours for the glue to hardened sufficiently before removing it from the press. In combination with the oil leakage problem the set-up stood still for days. Due to the limited time this proved to be an issue. The problem with the sample production time was however considerably reduced (to about two hours) by applying the catalysator 770 before the glue, 406. The problem with the oil leakage still occured, but with a significantly lowered production time it would only lead to a 2 hour delay rather than 12.

In addition to the problem with oil seeping into the samples, another issue to be addressed is the possible contaminants. Since a contaminant can lead to field enhancement it is a important to work in a clean environment when assembling the samples. The environment is reasonably clean, but still the occurrence of dust and other particles can easily occur. In some completed samples it has be observed imperfections and hence, the sample is scrapped. The assumption that samples are contaminated with small imperfections without it being discovered, is reasonable.

7. Conclusion

The main objective with this master thesis was to develop an experimental set-up able to detect partial discharge activity during a combined DC voltage superimposed a AC voltage. The sub-system tests showed that both the Behlman signal generator and the Messwandler Bau transformer functions to a satisfactory degree with a total harmonic distortion of 1 % in the voltage range 1-2 kV_{rms} and frequency range 1-5 kHz.

An experimental setup based on a straight detection circuit for partial discharge detection is built with the Behlman and Messwandler bau connected to generate the AC voltage.

The resulting noise band of 0.6 pC was found after a number of alterations in the system test, and the detection limit were set at 1 pC. The benchmarking of the layered test object indicated what could be interpreted as partial discharge in the intersection in the sample at a pressure of 50 kN/mm. The pressure is increased to 75 kN/mm before the main tests were conducted. But some observation may still indicate a too low or uneven pressure across the area of the electrodes.

The experiments conducted during the main tests were preformed for several voltages and test objects both with and without a cavity. The result from the main test varied to a large extent. The problem with the OMICRON and the issue with polarity determination makes the interpretations even harder. The AC test voltage was below the inception voltage and still discharges occured, implicating noise. The results during the DC tests varied to a large extent, making the results unreliable. Making any comparison between the tests with combined voltage and DC test is not possible with these results.

The combined DC and AC voltage test show a clear distinction between the samples with and without a cavity. The results during the cavity tests at 50 Hz AC and DC voltage are more reliable. The repetition rate had a high initial value, decreasing to a stable level. This is consistent with the expectations that repetition rate is dependent of the conductivity of the dielectric and the cavity. The 1 kHz AC and DC tests had a significantly lower repetition rate, both initially and the stable level, but the same shape is observed.

The statistical quality and the quantity of data are always of great importance when discussing experimental results. The results from the testing gave varied results with a large difference in both magnitude and repetition rate in similar samples at the same applied voltage. More test must be performed to get a better fundation for interpretation of the results. The varying results indicate some possible issues with noise and the design of parts in the set-up.

8. Further Work

There is a number of exciting possibilities for further work in the field of partial discharge detection and interpretation.

The results from the partial discharge tests indicated some sources of noise, and the high repetition rate during the first hours could be due to a low waiting time or to a rapid increase of the DC voltage. A control system should be developed to increase the reliability of these parameters. The possible noise originatinating from having the voltage sources outside the faraday cage should be addressed. A control system for both the DC voltage source and the Behlan signal generator must be made to be able to move all the current carrying parts of the set-up inside the faraday cage.

The problem with the OMICRON and determining the polarity of small partial discharges should be solved to increase the reliability. Changing the measuring shunt to an RC circuit, rather than an RLC circuit, could reduce the oscillations and possibly reduce the problem.

The discharge with a magnitude higher than the calculated value of a complete breakdown of the cavity surface indicated discharges being affected by the interfaces due to an unsufficient pressure or electrostatical forces. A new design of the testcell should be investigated to assure an even pressure. The problems with oil ingress into the test objects and indications of discharge activity in interfaces suggest that it should be researched to use a different approach for production of the test objects. Using Uglestad spheres or injecting air bubbles in an epoxy resin might be a direction worth looking at.

As stated above, a problem with the interpretation of the result is due to the limitations of the OMICRON. One possibility is to determine where the discharges occur can be done by modelling the partial discharges detected to look at the characteristic signatures. All the different types of partial discharges have a distinct characteristic. It has been done some research on analysing partial discharge and model the discharges based on their characteristics. This gives the opportunity to eliminate the discharges occurring in the surroundings, and focus on the discharges in the cavity. [9] [27] [13] To determine whether the discharges occur in the sample or originate from external sources it is aslo possible to use a balanced circuit rather than a straight used in this thesis. The balanced circuit is also known to have a higher sensitivity.

A natural path for further work is to continue the testing to increase the reliability of the results before continuing at additional voltage and frequency levels as well as investigating the temeprature dependence. The quantity and quality of the experimental results are the most critical parameters for laboratory reseach, and further studies are encouraged to validate and increase the credibility of the experimental results in the report.

Bibliography

[1] ABB, "ABB Review," *The corporate technical journal of the ABB Group*, vol. 22, March 2008.

[2] E. Spahic and G. Balzer, "Offshore Wind Farms - VSC-based HVDC Connection," *Power Tech IEEE Russia*, pp. 1–6, June 2005.

[3] N. Mohan, T. M. Undeland, and W. P. Robbins, *Power Electronics, Converters, Applications, and Design*. John Wiley and Sons, Inc, 3 ed., 2003.

[4] P. Bresesti, W. L. Kling, R. L. Hendriks, and R. Vailati, "HVDC Connection of Offshore Wind Farms to the Transmission System," *IEEE Transactions on Energy Conversion*, vol. 22, March 2007.

[5] C. H. Chien and R. W. G. Bucknall, "Analysis of Harmonics in Subsea Power Transmission Cables Used in VSC-HVDC Transmission Systems Operating Under Steady-State Conditions," *IEEE Transactions on Power Delivery*, vol. 22, October 2007.

[6] P. K. Olsen, F. Mauseth, and E. Ildstad, "The effect of DC superimposed AC Voltage on Partial Discharges in Dielectric Bounded Cavities," *International Conference on High Voltage Engineering and Application*, 2014.

[7] F. Mauseth, S. Hvidsten, H. H. Sæternes, and J. Aakervik, "Influence of DC stress Superimposed with High Frequency AC on Water Tree Growth in XLPE Insulation," *Nordic Insulation Symposium*, June 2013.

[8] W. Choo and G. Chen, "Electric Field Determination in DC Polymeric Power Cable in the Presence of Space Charge and Temperature Gradient under DC Conditions," *International Conference on Condition Monitoring and Diagnosis*, April 2008.

[9] F. R. Kreuger, *Partial Discharge Detection in High Voltage Equipment*. Butterworths and Co., 1989.

[10] C. Forssén, "Modelling of Cavity Partial Discharges at Variable Applied Frequency," *Doctorial Thesis in Electrical Systems*, 2008.

[11] K. D. Hammervoll, "Ikke-destruktiv tilstandskontroll av kabelskjøter i distribusjonsnett," *Master i energi og miljø, NTNU*, June 2010.

[12] L. Lundegaard, "Partielle utlandninger, Begreper, måleteknikk of mulige anvendelser for tilstandskontroll," *SINTEF Energy Research*, pp. 1–50, March 1996.

[13] L. Niemeyer, "A Generalized Approach to Partial Discharge Modeling," *IEEE Transaction on Dielectrics and Electrical Insulation*, vol. 2, pp. 510–528, August 1995.

[14] P. K. Olsen, F. Mauseth, and E. Ildstad, "Modelling of Partial Discharges in Polymeric Insulation Exposed to Combined DC and AC Voltage," *Nordic Insulation Symposium*, June 2011.

[15] E. Ildstad, *TET 4160 High Voltage Insulation Materials*. NTNU Department of Electric Power Engineering, 2012.

[16] E. F. Bere, "Innvirkning av fuktighet på dielektriske tap og risiko for partielle utladninger i innstøpte endeviklinger," *Master i energi og miljø, NTNU*, June 2014.

[17] H. Suzuki, K. Aihara, and T. Okamoto, "Complex behaviour of a simple partial-discharge model," *Europhysics Letters*, vol. 66, pp. 28–34, February 2004.

[18] D. Malec and T. Lebey, "Effects of the Voltage Waveform on Partial Discharges Activity in a Vented Sample(HDPD," *Conference on Electrical Insulation and Dielectric Phenomena, IEEE*, 2000.

[19] P. H. F. Morshuis and J. J. Smit, "Partial Discharges at DC Voltage: Their Mechanism, Detection and Analysis," *IEEE*, pp. 328–340, October 2005.

[20] B. Salvage and N. R. Steinberg, "Discharge Repetition in an Air Filled cavity in a Solid Dielectric under Direct Voltage Conditions," *Electronic Letters*, vol. 2, pp. 432–433, November 1966.

[21] S. Hvidsten, "Power cables, Partial discharge measurements," *ELK-30, Condition assessment of high voltage apparatur*, 2013.

[22] I. R. Velo, "Test setup for measuring partial discharge in polymer insulatin subjected to hvdc superimposed by high frequency ac," *Prosjekt i energi og miljø, NTNU*, June 2014.

[23] P. I. Nodeland, "Design av en høyfrekvent transformer for testing av hvdc kabler for flytende vindturbiner," *Prosjekt i energi og miljø, NTNU*, Desember 2009.

[24] P. I. Nodeland, "Utvikling av testoppsett for spenningsprøving av hvdc pex-kabler," *Master i energi og miljø, NTNU*, June 2010.

[25] S. Beg and B. Salvage, "Discharge Repetition in an Air Filled Cavity in Polythene under High Direct Electric Stresses at Elevated Temperatures," *Electronic Letters*, vol. 5, pp. 118–120, March 1969.

[26] U. Fromm, "Partial Discharges and Breakdown Testing at High DC Voltage," *Doctorial Thesis Delft University of technology*, september 1995.

[27] U. Fromm, "Interpretation of Partial Discharges at DC Voltages," *IEEE Transaction on Dielectrics and Electrical Insulation*, vol. 2, pp. 761–770, October 1995.

A. Experimental setup

A.1 Experimental circuit

Figure A.1: Picture of the experimental setup from outside the faraday cage with the voltage sources, top: DC source, bottom: Behlman

Figure A.2: Picture of the experimental setup inside the faraday cage with the testcell in the center

A.2 Test Cell

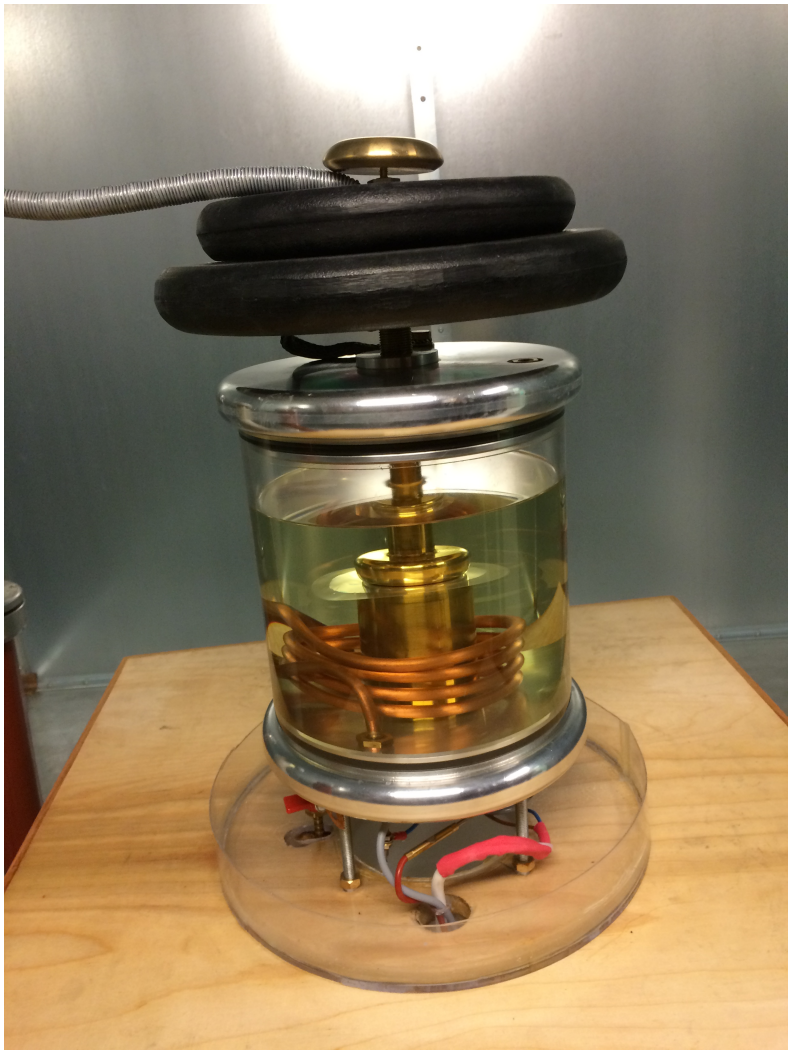

Figure A.3: Picture of the test cell

B. Hardware Data

B.1 Transformers

B.1.1 Petter Nodeland Designed Transformer

Transfromer was designed for 20 kHz - but has proven to work at its best at 15 kHz.

$V_{pri} = 350\ V_{RMS}$

$V_{sec} = 10\ kV_{RMS}$

$N_{pri} = 25$ turns

$N_{pri} = 724$ turns

		Primary Side		**Secondary side**	
Frequency	f	20	kHz	20	kHz
Voltage	V	350	V_{RMS}	10	kV_{RMS}
Current	I	5	A_{RMS}	0.18	A_{RMS}
Windings	N	25	turns	724	turns
Conductor crossection	A	3.17	mm^2	0.12	mm^2
Conductor diameter	d	1.78	mm	0.34	mm

[24] [23]

B.1.2 Neon Transformer

An alternative transformer was located in Frank Mauseths office- a neon transformer. Data:
NEONTRAFO TYPE
N 50/4 S

PRIM
$U_P = 230$ V, 50 Hz
$I_P = 1.13$ A
$\cos\phi = 0.55$

SEC
$U_S = 4000$ V - PE
$I_S = 50$ mA
$P_P = 260$ VA

IP00 ta40c
19.01.96
NEONCOMP OY
TURKU - FINLAND

B.1.3 MESSWANDLER BAU Measuring Transformator

Labnr.: B01-0967

Type: TRAFO MÅLE
Modell: REL 10
Serienr.: 89/932436
Fabrikat: MESSWANDLER BAU

Sp. min (P): 11 KV
Sp. max (S): 110 V
Ampere (S): 2 A
Effekt (P): 60 VA
Merkeverdi: 11KV - 110V 3A 60VA

B.1.4 ARTECHE Measure Transformer

Labnr.: B01-0800
Type: TRAFO MÅLE
Modell: UCN-36
Serienr.: 10012441 / 6
Sp. type: AC
Fabrikat: ARTECHE

Sp. min (P): 36 KV
Sp. max (S): 120 V
Effekt (P): 200 VA
Merkeverdi: 36KV - 0.5% - 200VA

B.2 Experminal setup equipment

B.2.1 DC Voltage Source

Labnr.:B02-0405
The DC voltage source is a high voltage DC source from Fug. It has the possibility of

a voltage output range from 0-35 kV and a current range of 0-4 mA. The source can be controlled externally.

B.2.2 AC Voltage Source

Labnr.:B02-0584
The AC voltage source is a Behlman signal generator. The Behlman ACM-3000 OSN-1-45/10000 is a high quality variable frequency AC power supply that produces low distortion sinusoidal wave power over a wide range of output frequencies and voltages. The Behlman voltage source available in the NTNU inventory is build up out of an ACM- 3000 and an OSN-1-45/10000. It has a maximum voltage range 0- 270 VRMS and a frequency bandwidth of 45- 10,000 Hz and the rated power is 3000 VA.

C. Sub-system test

C.1 Total harmonic distorition and FFT in Messwandler Bau Transformer

C.1.1 Harmonic analysis at 1 kHz

Table C.1: Harmonic magnitudes and THD at 1 kHz, 1 kV and 2 kV

1 kHz						
	1 kV			**2 kV**		
Harmonic	**dB**	**V[e+03]**	**f[e+04 Hz]**	**dB**	**V[e+03]**	**f[e+04 Hz]**
1st	60.0628	1.0073	0.1000	66.0274	2.0016	0.1001
2nd	3.3643	0.0015	0.2002	6.4260	0.0021	0.2002
3rd	18.4392	0.0084	0.3001	21.9879	0.0126	0.3002
4th	-2.4498	0.0008	0.4001	3.3423	0.0015	0.4002
5th	7.3337	0.0023	0.5002	15.3291	0.0058	0.5003
6th	-3.3104	0.0007	0.6003	4.0278	0.0016	0.6003
7th	-1.7252	0.0008	0.7003	1.7468	0.0012	0.7004
8th	-5.0208	0.0006	0.8003	-0.3070	0.0010	0.8001
9th	-8.8534	0.0004	0.9005	-2.8641	0.0007	0.9005
10th	-10.5893	0.0003	1.0004	-6.6331	0.0005	1.0005
11th	-9.0920	0.0004	1.1005	-1.1117	0.0009	1.1006
12th	-12.2572	0.0002	1.2005	-5.4013	0.0005	1.2006
13th	-17.3637	0.0001	1.3005	-6.5293	0.0005	1.3005
THD	**-40.8945**			**-42.7277**		

1 kV

x

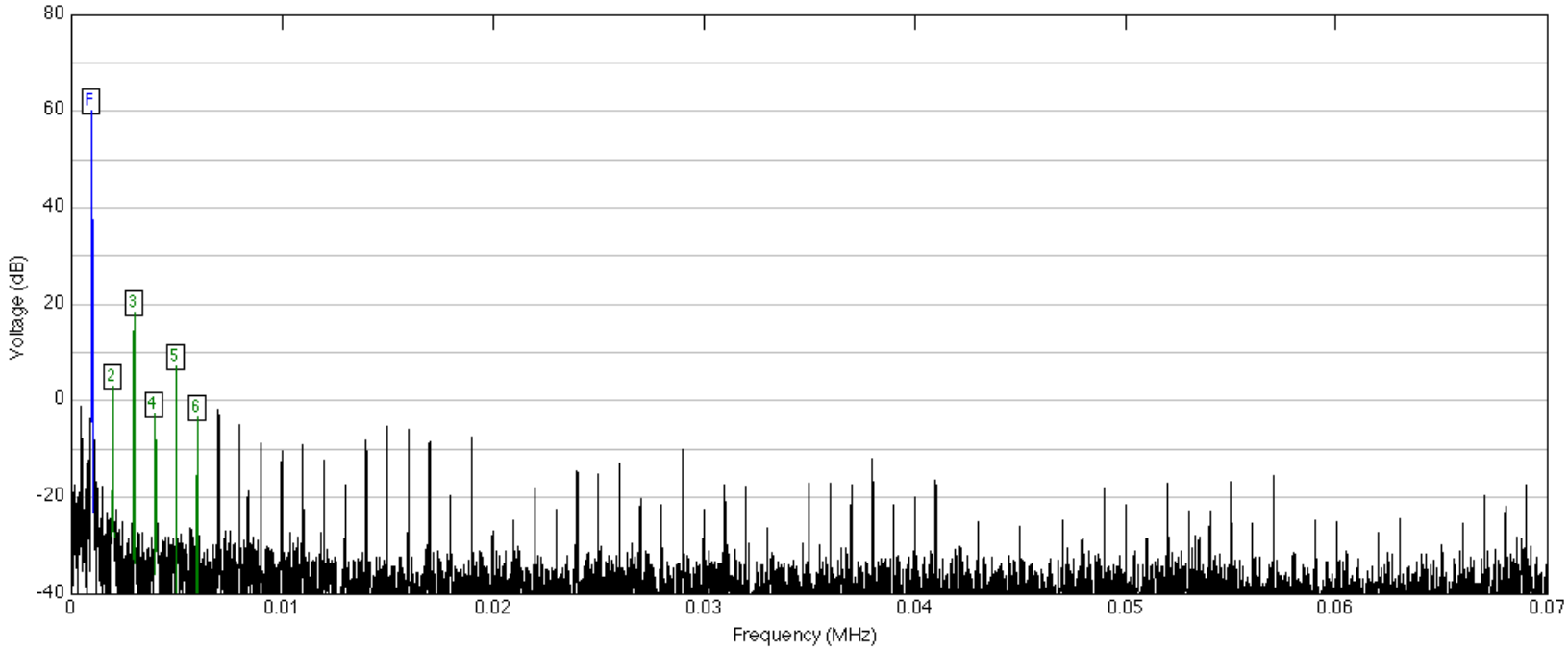

Figure C.1: FFT plot 1 kHz and 1 kV

2 kV

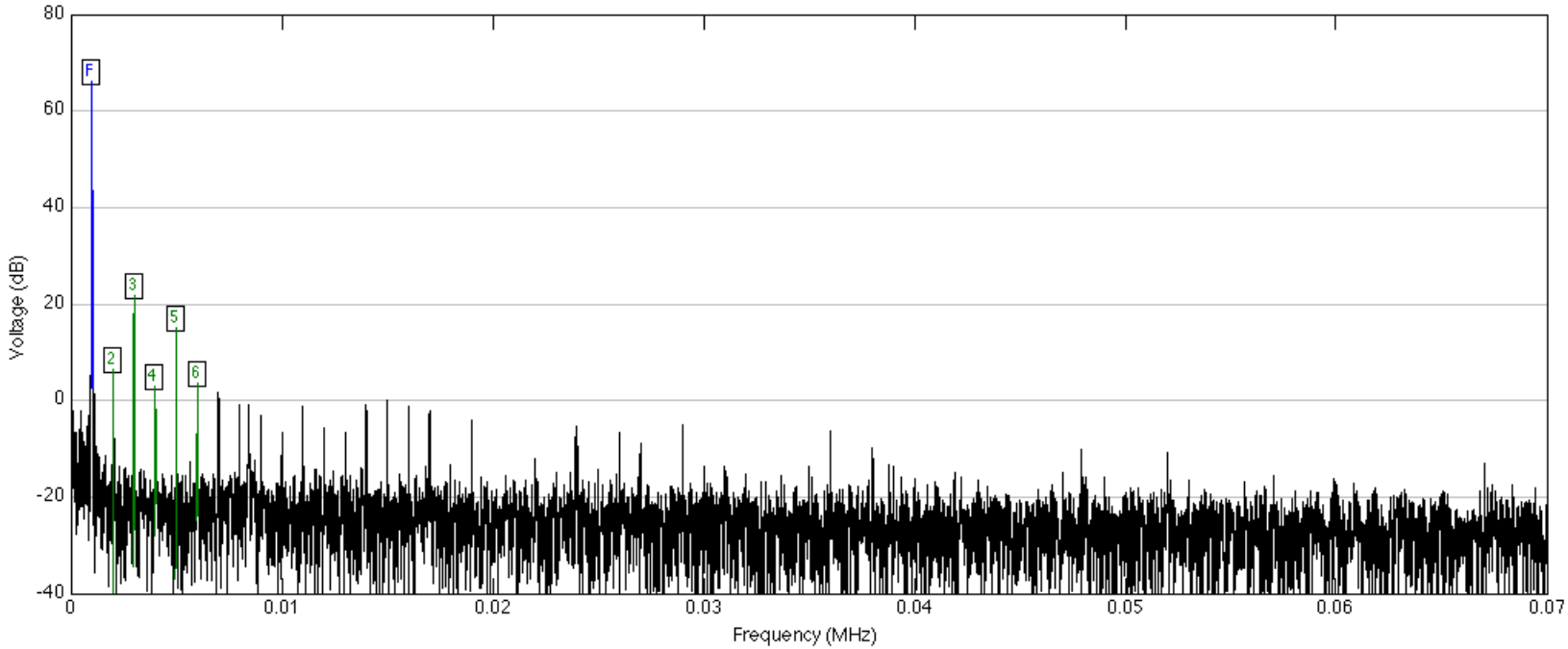

Figure C.2: FFT plot 1 kHz and 2 kV

C.1.2 Harmonic analysis at 2 kHz

Table C.2: Harmonic magnitudes and THD at 2 kHz, 1 kV and 2 kV

2 kHz						
	1 kV			**2 kV**		
Harmonic	**dB**	**V[e+03]**	**f[e+04 Hz]**	**dB**	**V[e+03]**	**f[e+04 Hz]**
1st	60.0237	1.0027	0.2002	66.0288	2.0019	0.2003
2nd	8.8042	0.0028	0.4004	0.6618	0.0011	0.4005
3rd	16.7532	0.0069	0.6006	18.1822	0.0081	0.6008
4th	0.8089	0.0011	0.8008	3.2071	0.0014	0.8010
5th	4.2506	0.0016	1.0012	7.8490	0.0025	1.0013
6th	-5.0607	0.0006	1.2011	-0.9325	0.0009	1.2015
7th	6.2978	0.0021	1.4015	3.6681	0.0015	1.4018
8th	-3.9066	0.0006	1.6014	0.6519	0.0011	1.6020
9th	2.7576	0.0014	1.8019	-3.1889	0.0007	1.8023
10th	-2.0617	0.0008	2.0021	-8.0325	0.0004	2.0026
11th	-5.5485	0.0005	2.2022	0.1525	0.0010	2.2030
12th	-14.2950	0.0002	2.4029	-11.2394	0.0003	2.4034
13th	-12.8451	0.0002	2.6030	-9.9830	0.0003	2.6037
THD	**-41.6788**			**-46.5906**		

1 kV

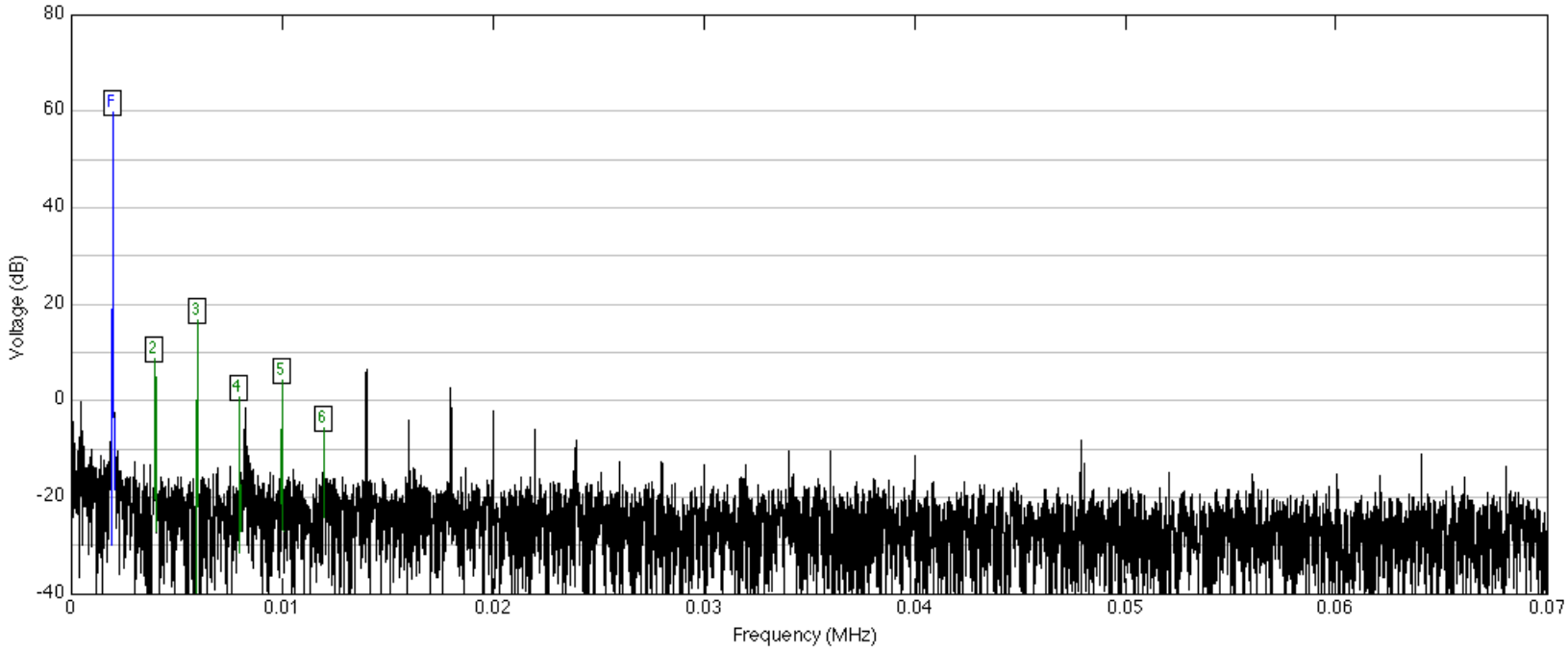

Figure C.3: FFT plot 2 kHz and 1 kV

2 kV

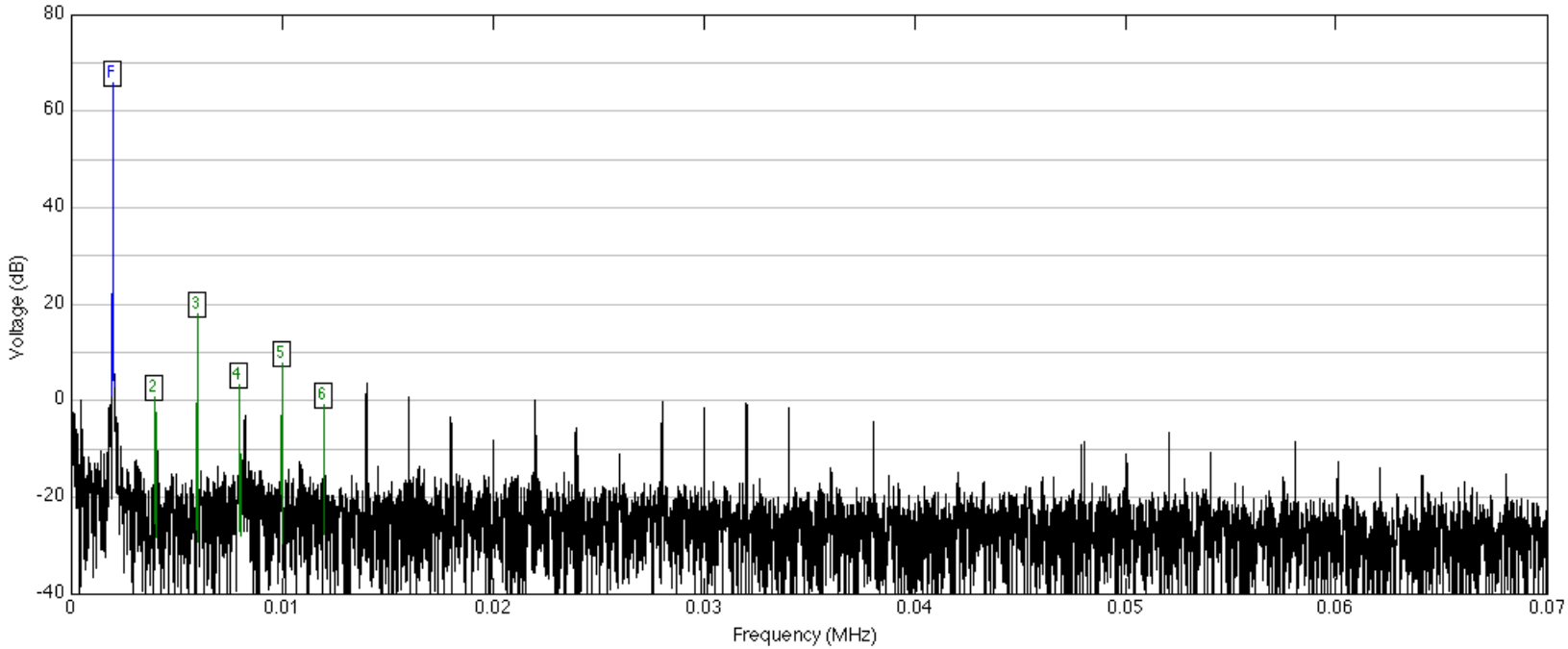

Figure C.4: FFT plot 2 kHz and 2 kV

C.1.3 Harmonic analysis at 3 kHz

Table C.3: Harmonic magnitudes and THD at 3 kHz, 1 kV and 2 kV

3 kHz						
	1 kV			**2 kV**		
Harmonic	**dB**	**V[e+03]**	**f[e+04 Hz]**	**dB**	**V[e+03]**	**f[e+04 Hz]**
1st	60.0028	1.0003	0.3001	66.0335	2.0030	0.3001
2nd	5.7832	0.0019	0.6002	5.0493	0.0018	0.6002
3rd	14.6357	0.0054	0.9003	15.5450	0.0060	0.9003
4th	-1.4349	0.0008	1.2005	0.1174	0.0010	1.2006
5th	-7.0954	0.0004	1.5011	10.6539	0.0034	1.5006
6th	-2.3237	0.0008	1.8011	-0.7087	0.0009	1.8007
7th	8.5450	0.0027	2.1009	-2.5797	0.0007	2.1012
8th	-1.1953	0.0009	2.4008	-1.8146	0.0008	2.4010
9th	1.2636	0.0012	2.7011	-6.2540	0.0005	2.7010
10th	-4.1652	0.0006	3.0013	-5.0623	0.0006	3.0016
11th	-1.6701	0.0008	3.3014	-2.7722	0.0007	3.3015
12th	-14.5575	0.0002	3.6008	-7.3699	0.0004	3.6015
13th	-13.3737	0.0002	3.9011	-4.7645	0.0006	3.9017
THD	**-43.1474**			**-47.9638**		

1 kV

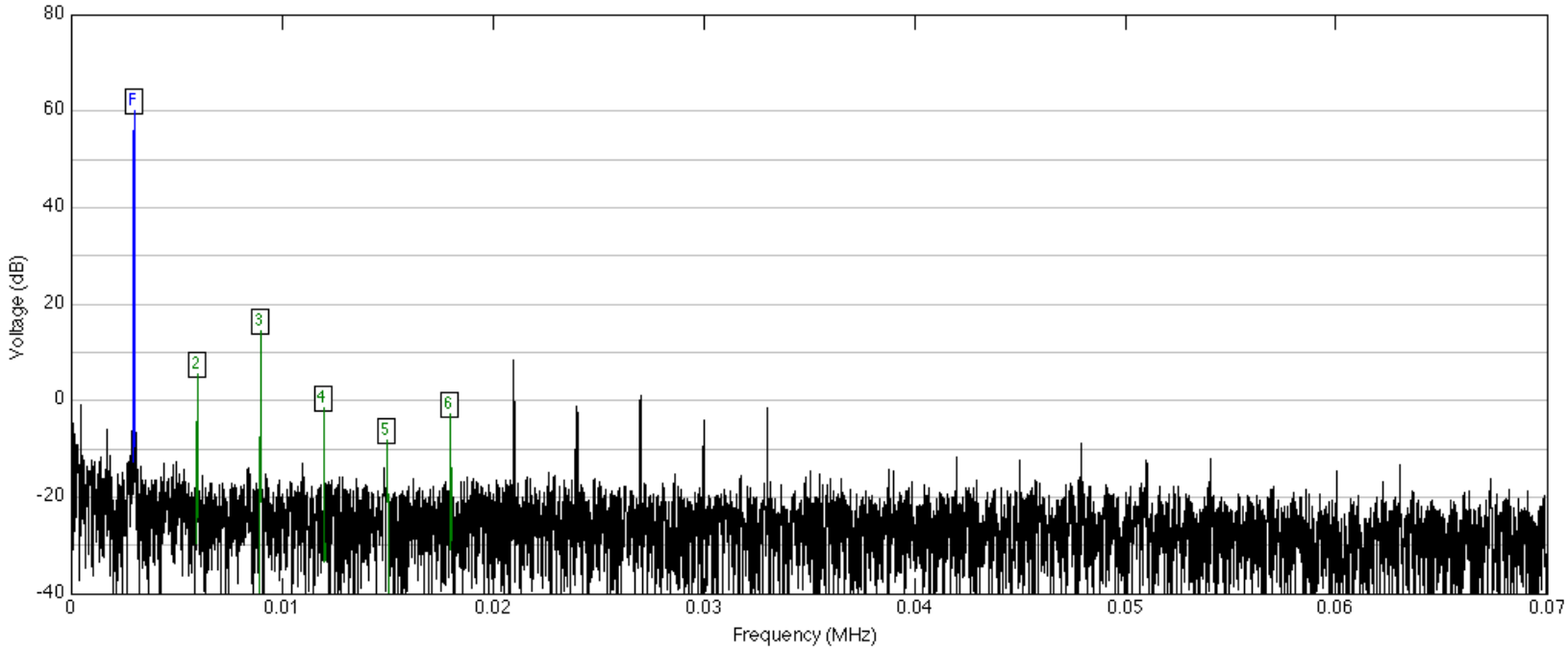

Figure C.5: FFT plot 3 kHz and 1 kV

2 kV

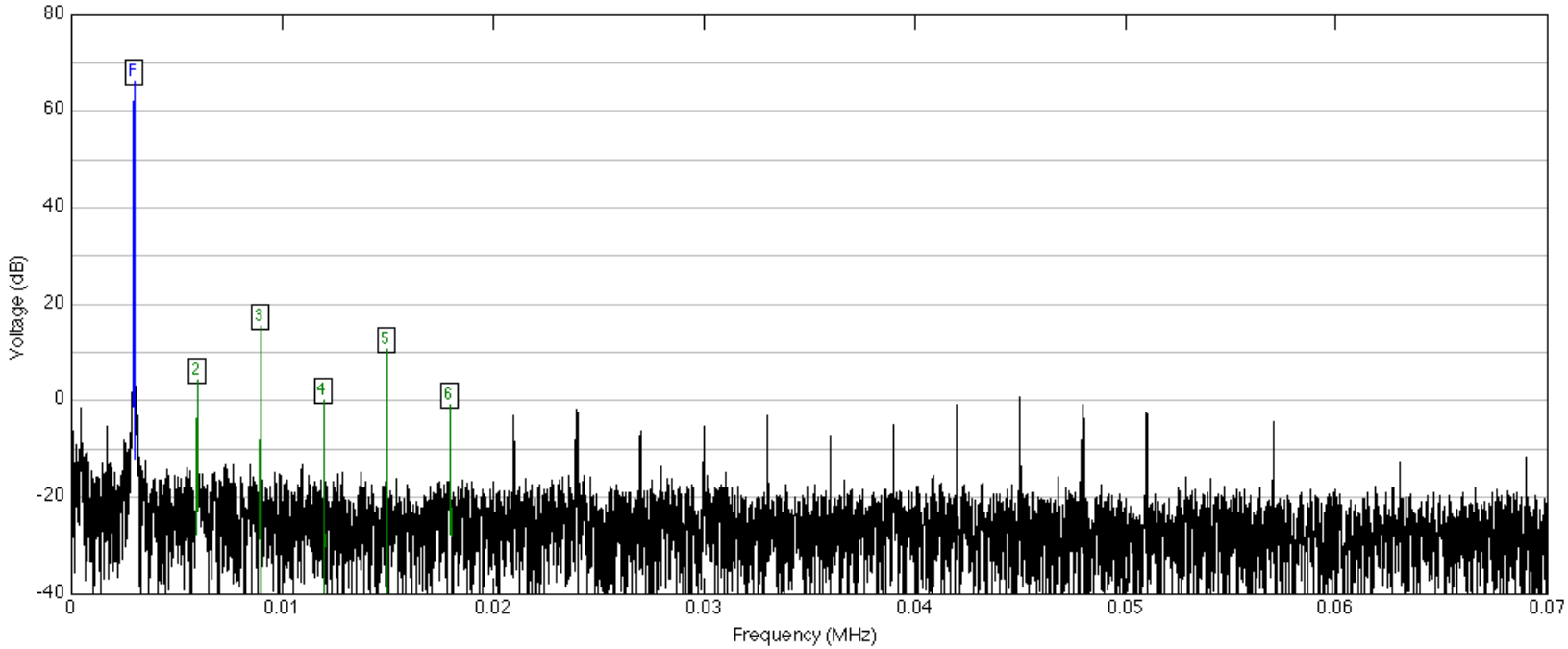

Figure C.6: FFT plot 3 kHz and 2 kV

C.1.4 Harmonic analysis at 4 kHz

Table C.4: Harmonic magnitudes and THD at 4 kHz, 1 kV and 2 kV

4 kHz						
	1 kV			**2 kV**		
Harmonic	**dB**	**V[e+03]**	**f[e+04 Hz]**	**dB**	**V[e+03]**	**f[e+04 Hz]**
1st	60.0060	1.0007	0.4003	66.0445	2.0055	0.4003
2nd	7.5078	0.0024	0.8005	0.3899	0.0010	0.8006
3rd	10.7621	0.0035	1.2009	11.2780	0.0037	1.2008
4th	0.3700	0.0010	1.6012	3.6066	0.0015	1.6011
5th	4.4964	0.0017	2.0013	12.1923	0.0041	2.0014
6th	-4.4983	0.0006	2.4016	-2.7910	0.0007	2.4017
7th	7.2793	0.0023	2.8020	-2.4285	0.0008	2.8021
8th	-1.0200	0.0009	3.2023	-0.8208	0.0009	3.2023
9th	4.7833	0.0017	3.6025	2.5330	0.0013	3.6027
10th	-3.1726	0.0007	4.0028	-4.9000	0.0006	4.0028
11th	-2.6680	0.0007	4.4030	-1.3152	0.0009	4.4032
12th	-24.9168	0.0001	4.8030	-9.3174	0.0003	4.8035
13th	-8.9505	0.0004	5.2036	-11.0249	0.0003	5.2038
THD	**-44.7482**			**-49.5494**		

1 kV

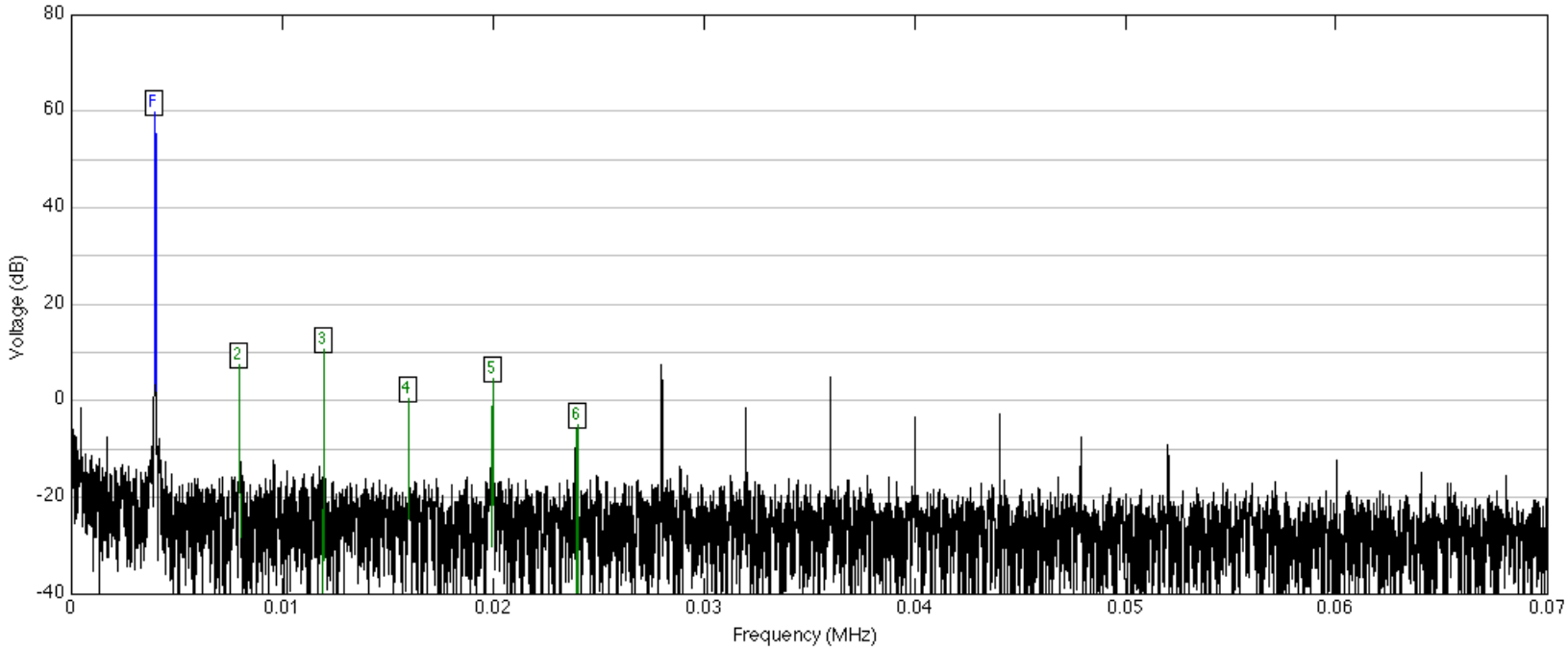

Figure C.7: FFT plot 4 kHz and 1 kV

2 kV

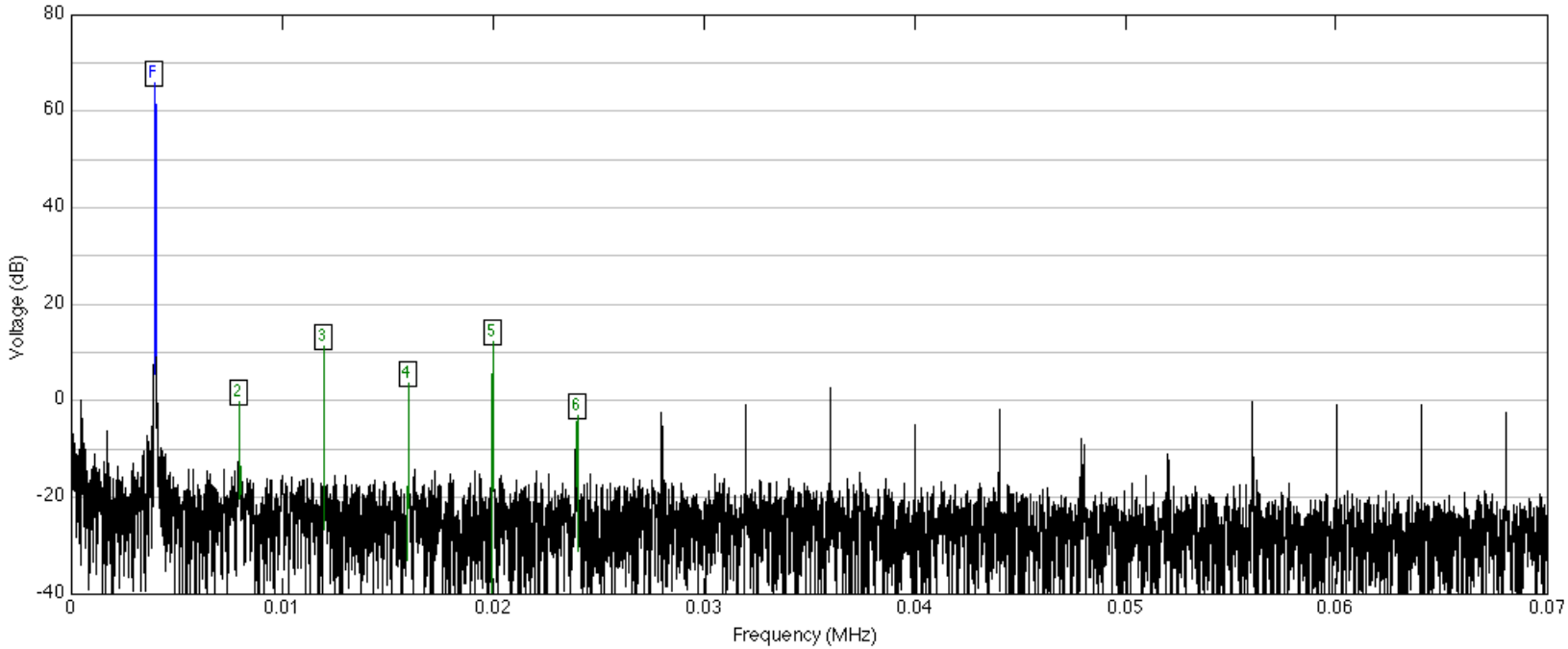

Figure C.8: FFT plot 4 kHz and 2 kV

C.1.5 Harmonic analysis at 5 kHz

Table C.5: Harmonic magnitudes and THD at 5 kHz, 1 kV and 2 kV

5 kHz						
	1 kV			**2 kV**		
Harmonic	**dB**	**V[e+03]**	**f[e+04 Hz]**	**dB**	**V[e+03]**	**f[e+04 Hz]**
1st	60.0297	1.0034	0.5001	66.0284	2.0018	0.5002
2nd	5.7813	0.0019	1.0002	1.4528	0.0012	1.0005
3rd	2.9841	0.0014	1.5005	3.4332	0.0015	1.5005
4th	1.7235	0.0012	2.0005	4.7544	0.0017	2.0006
5th	-2.1606	0.0008	2.5007	11.0826	0.0036	2.5010
6th	-6.8642	0.0005	3.0010	-1.4851	0.0008	3.0012
7th	4.0719	0.0016	3.5010	4.3206	0.0016	3.5013
8th	-0.5190	0.0009	4.0012	0.4570	0.0011	4.0014
9th	3.8102	0.0016	4.5014	1.0204	0.0011	4.5017
10th	-2.3777	0.0008	5.0015	-3.4791	0.0007	5.0019
11th	-5.0659	0.0006	5.5015	-0.4978	0.0009	5.5020
12th	-26.1117	0.0000	6.0026	-7.6613	0.0004	6.0022
13th	-18.1499	0.0001	6.5020	-5.1565	0.0006	6.5024
THD	**-47.8961**			**-50.7887**		

1 kV

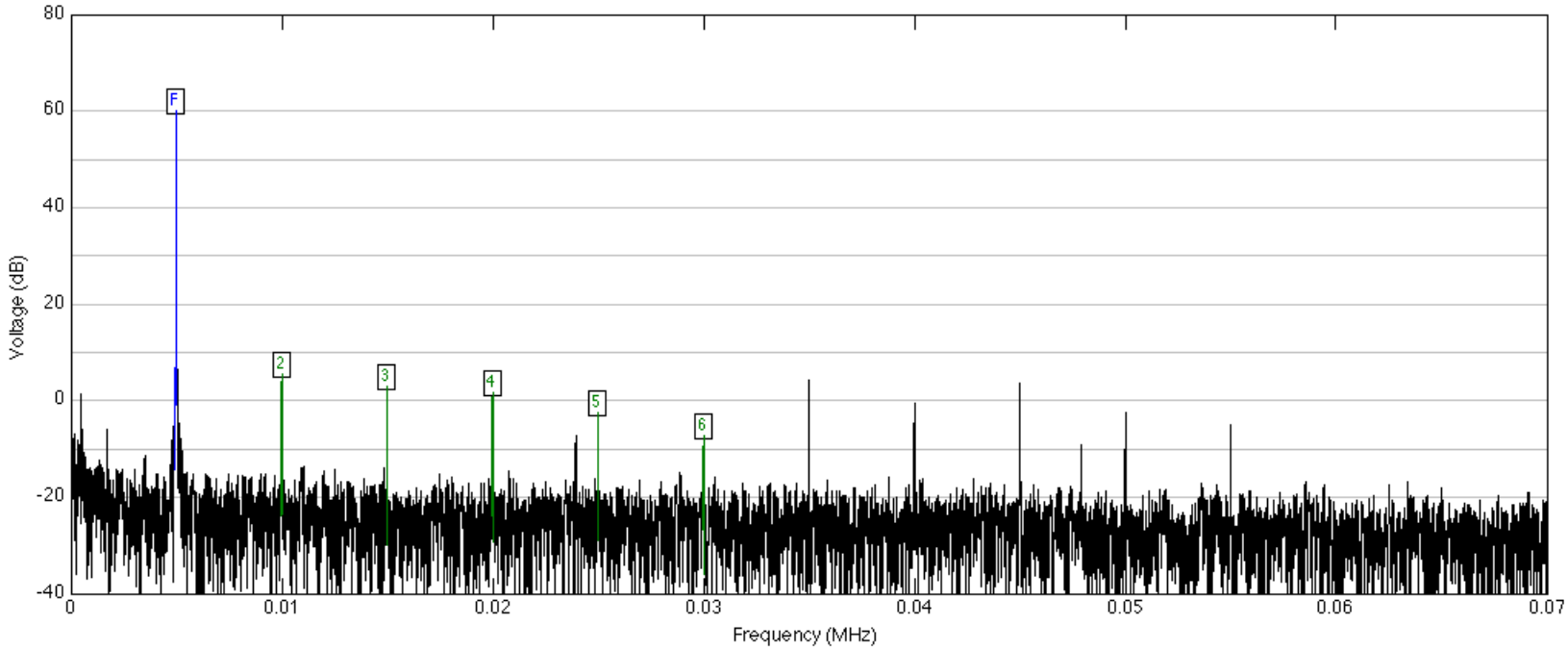

Figure C.9: FFT analysis plot 5 kHz and 1 kV

2 kV

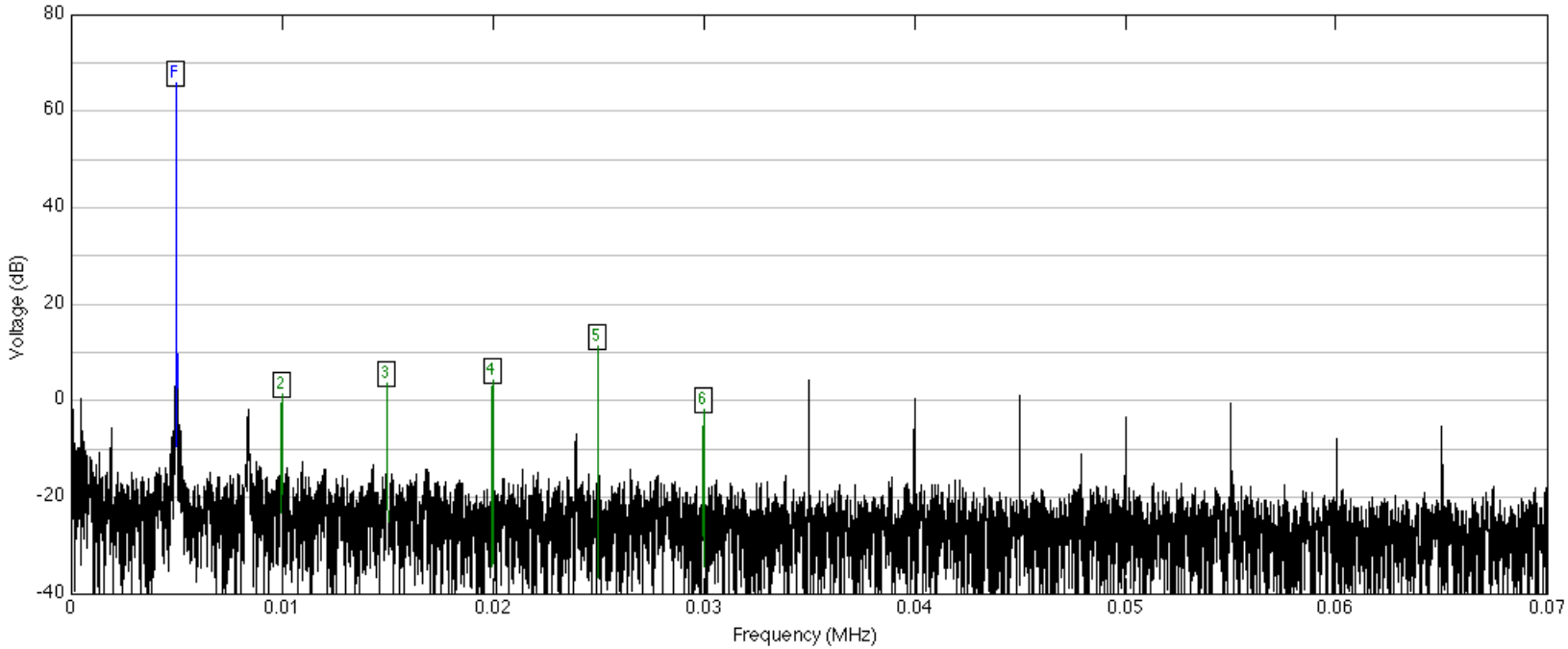

Figure C.10: FFT analysis plot 5 kHz and 2 kV

D. System test

D.1 Partial discharge under combined 50 Hz AC $V_{ac,rms}$=1 kV_{RMS} and DC V_{dc}=10 kV voltage

P=50 kN/mm

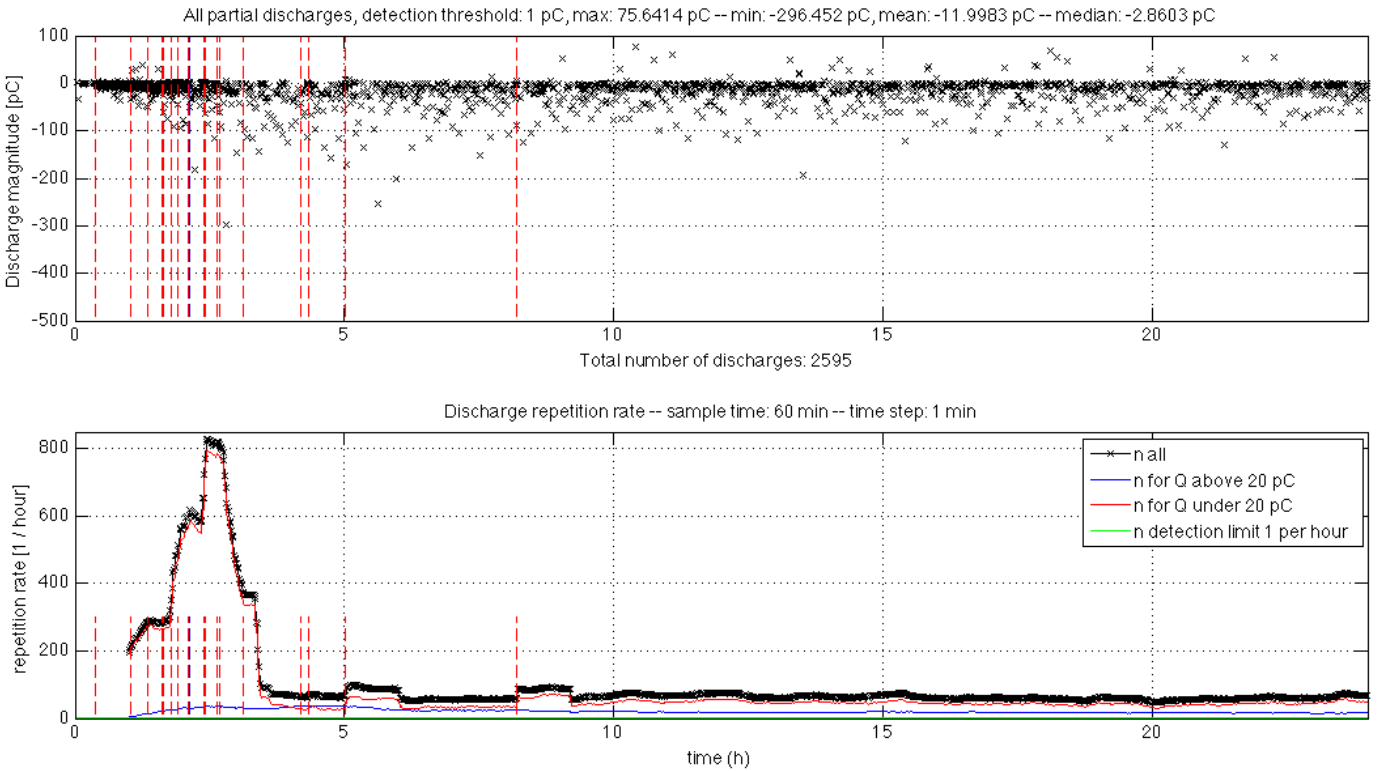

Figure D.1: PET 4, 3×100 μm layered sample without cavity, 10 kV_{DC}, 1 $kV_{AC,RMS}$, f= 50Hz, P=50 kN/mm, t=24 hours, T=60°

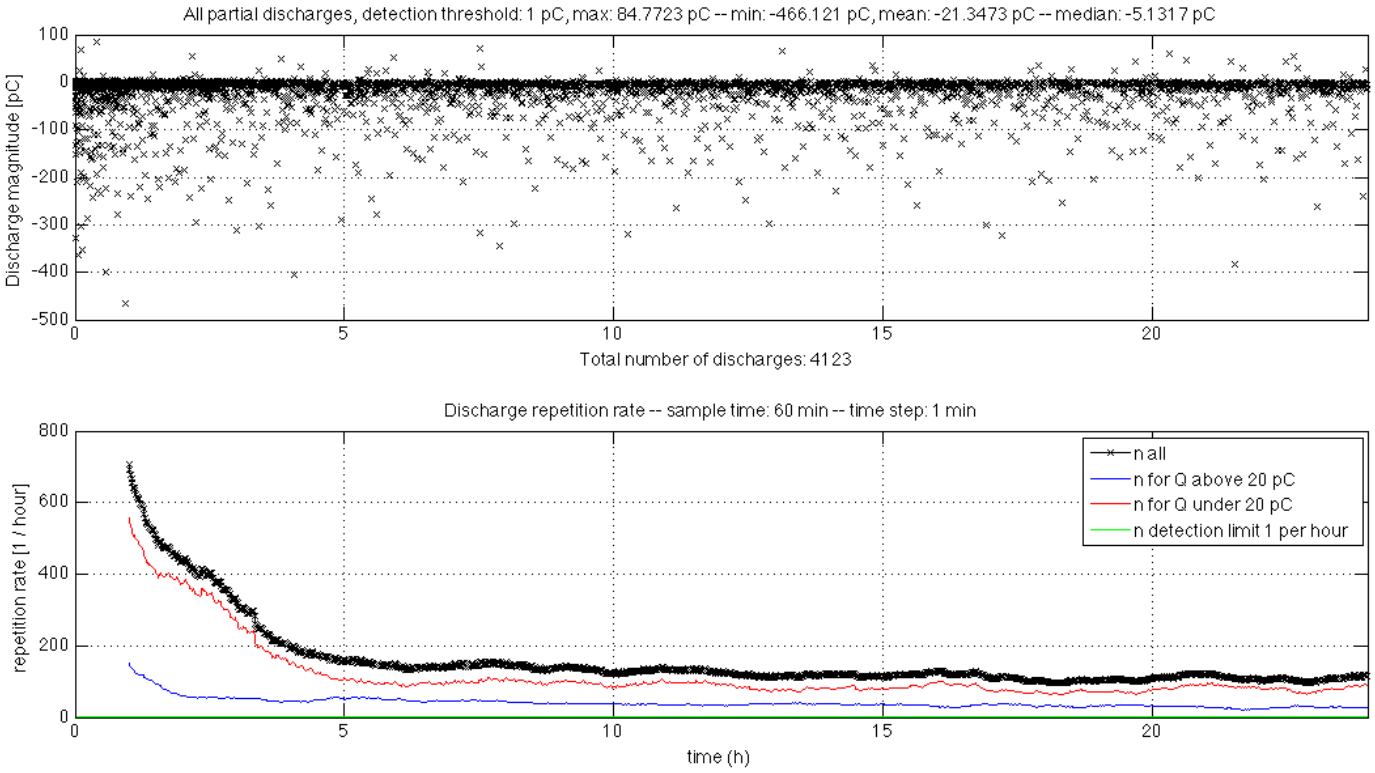

Figure D.2: PET 5, 3×100 μm layered sample without cavity, 10 kV_{DC}, 1 $kV_{AC,RMS}$, f= 50Hz, P=50 kN/mm, t=24 hours, T=60°C

E. Main test

E.1 Partial discharge under DC V_{dc}=10 kV voltage

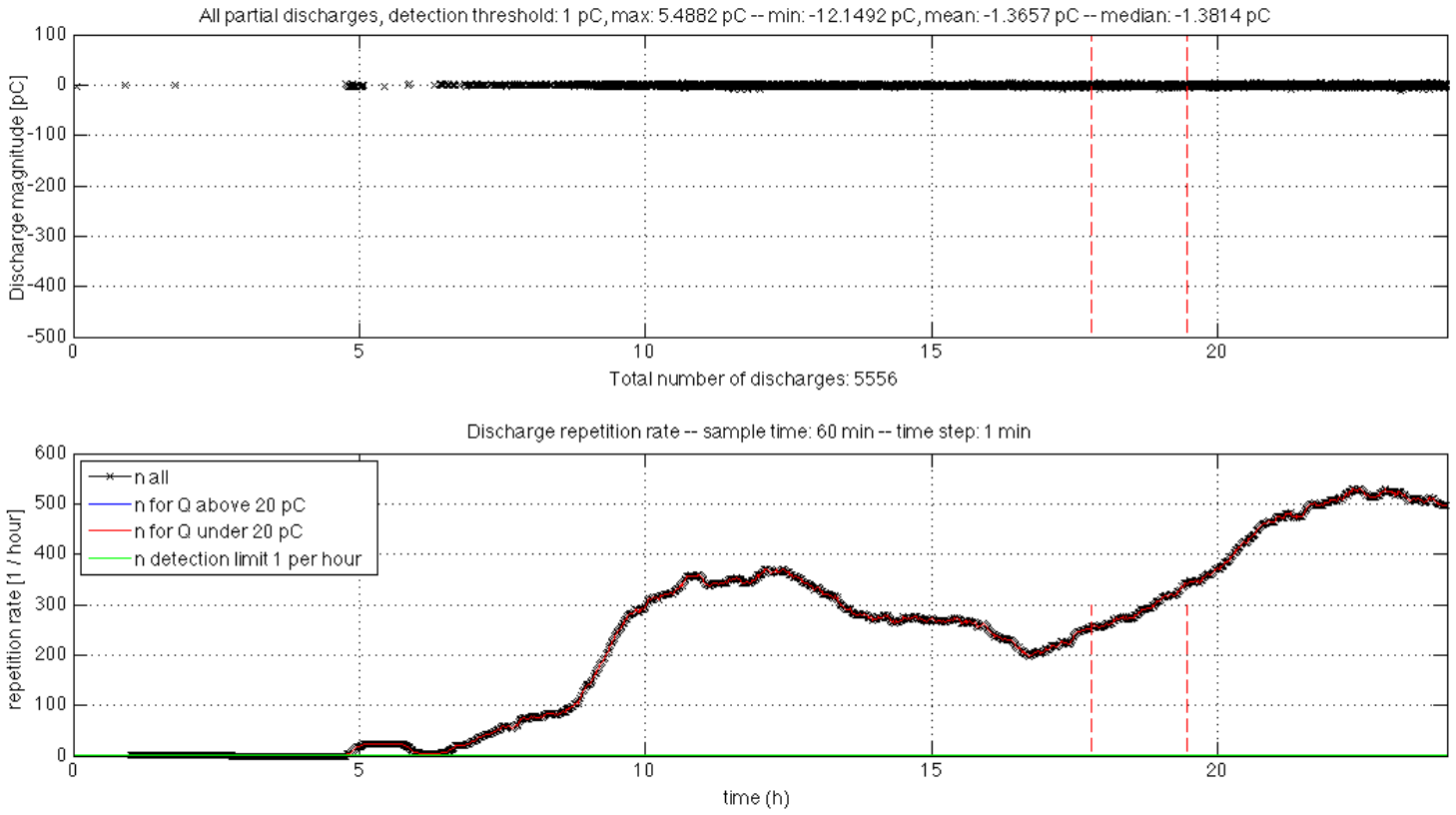

Figure E.1: PET 21.2, 3×100 μm layered sample with cavity r=1 mm, 10 kV_{DC}, P=75 kN/mm, t=24 hours, T=60°C

xxx

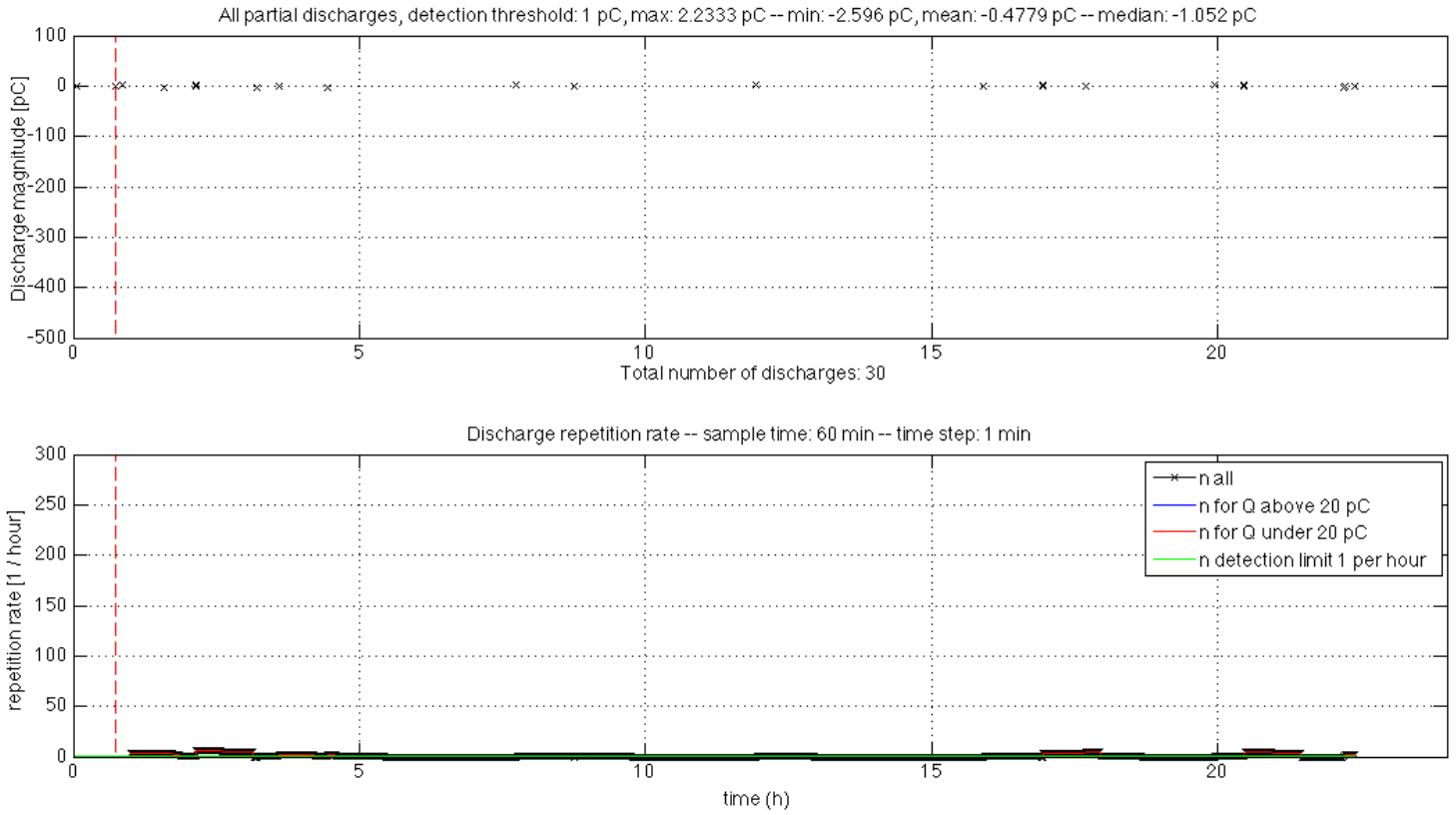

Figure E.2: PET 22, 3×100 μm layered sample with cavity r=1 mm, 10 kV_{DC}, P=75 kN/mm, t=24 hours, T=60°C

E.2 Partial discharge under DC V_{dc}=20 kV voltage

Table E.1: PD data for PET 22.2

Total number of discharges	673
Maximum magnitude	40.6697 pC
Minimum magnitude	-116.622 pC
Mean discharge magnitude	-2.1025 pC
Median discharge magnitude	-1.296 pC

With cavity r=1 mm

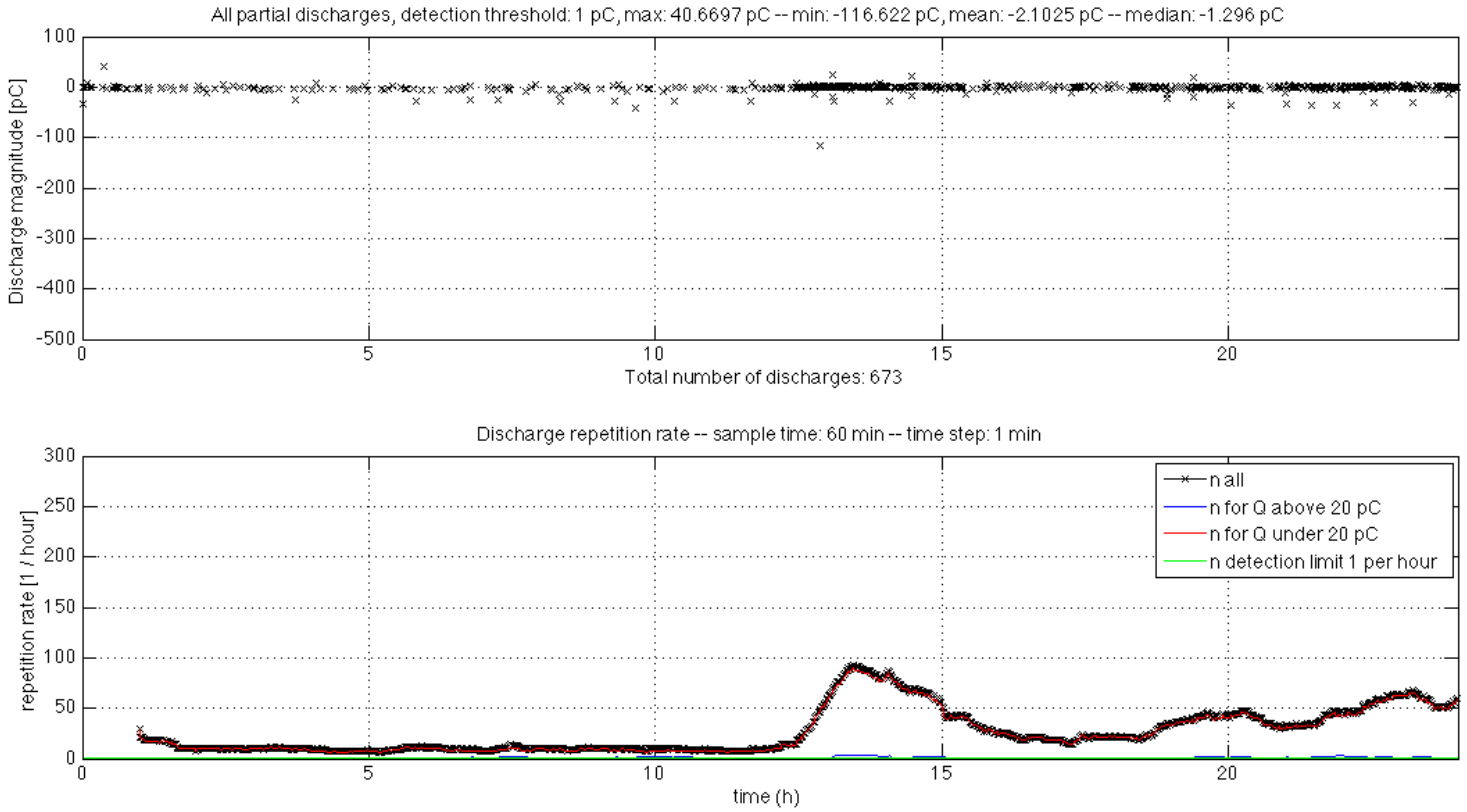

Figure E.3: PET 22.2, 3×100 μm layered sample with cavity r=1 mm, 20 kV_{DC}, P=75 kN/mm, t=24 hours, T=60°C

E.3 Partial discharge under combined DC V_{dc}=10 kV and 50 Hz AC $V_{ac,rms}$=0.5 kV_{RMS}

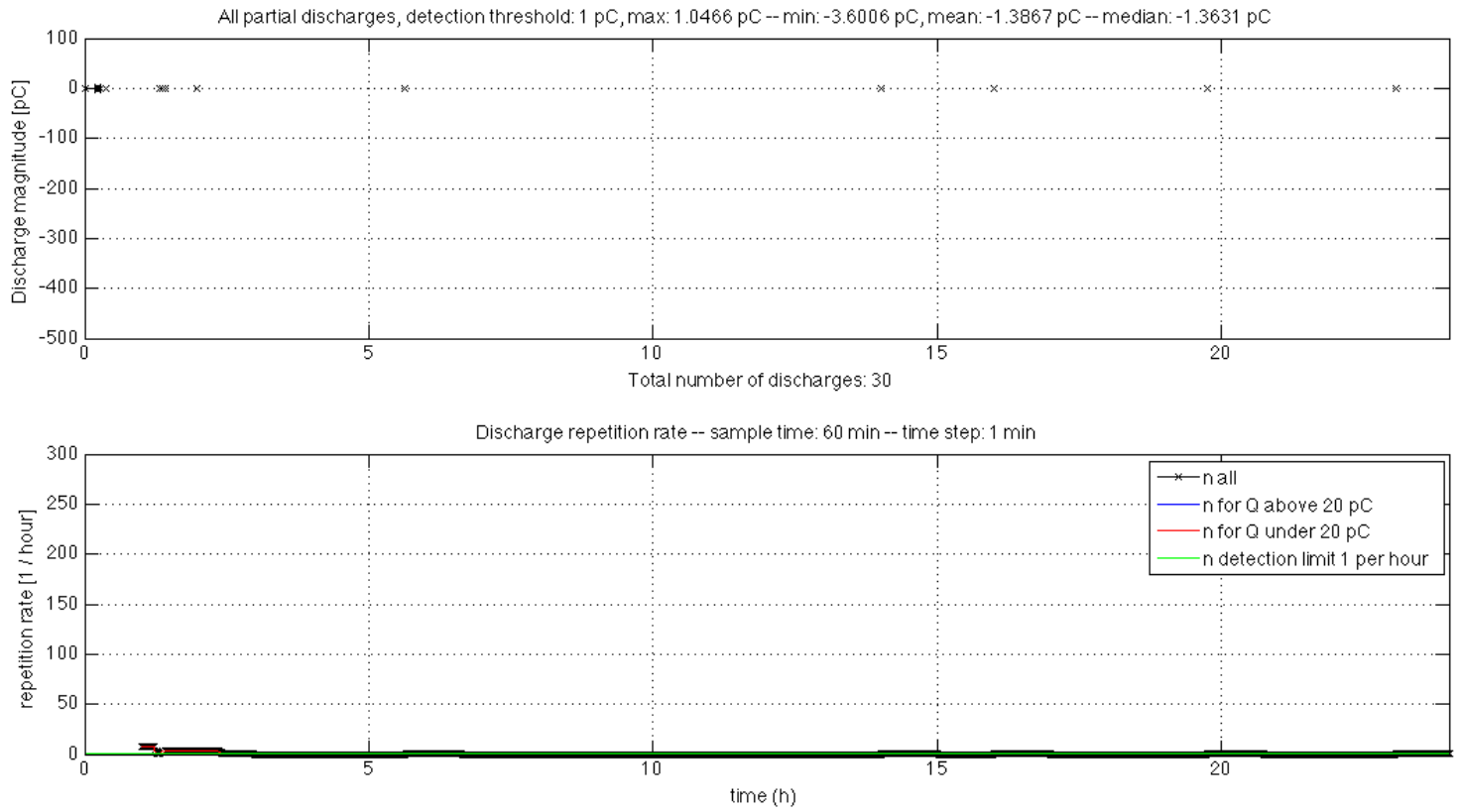

Figure E.4: PET 12, 3×100 μm layered sample without cavity, 10 kV_{DC}, 0.5 $kV_{AC,RMS}$, f= 50 Hz, P=75 kN/mm, t=24 hours, T=60°C

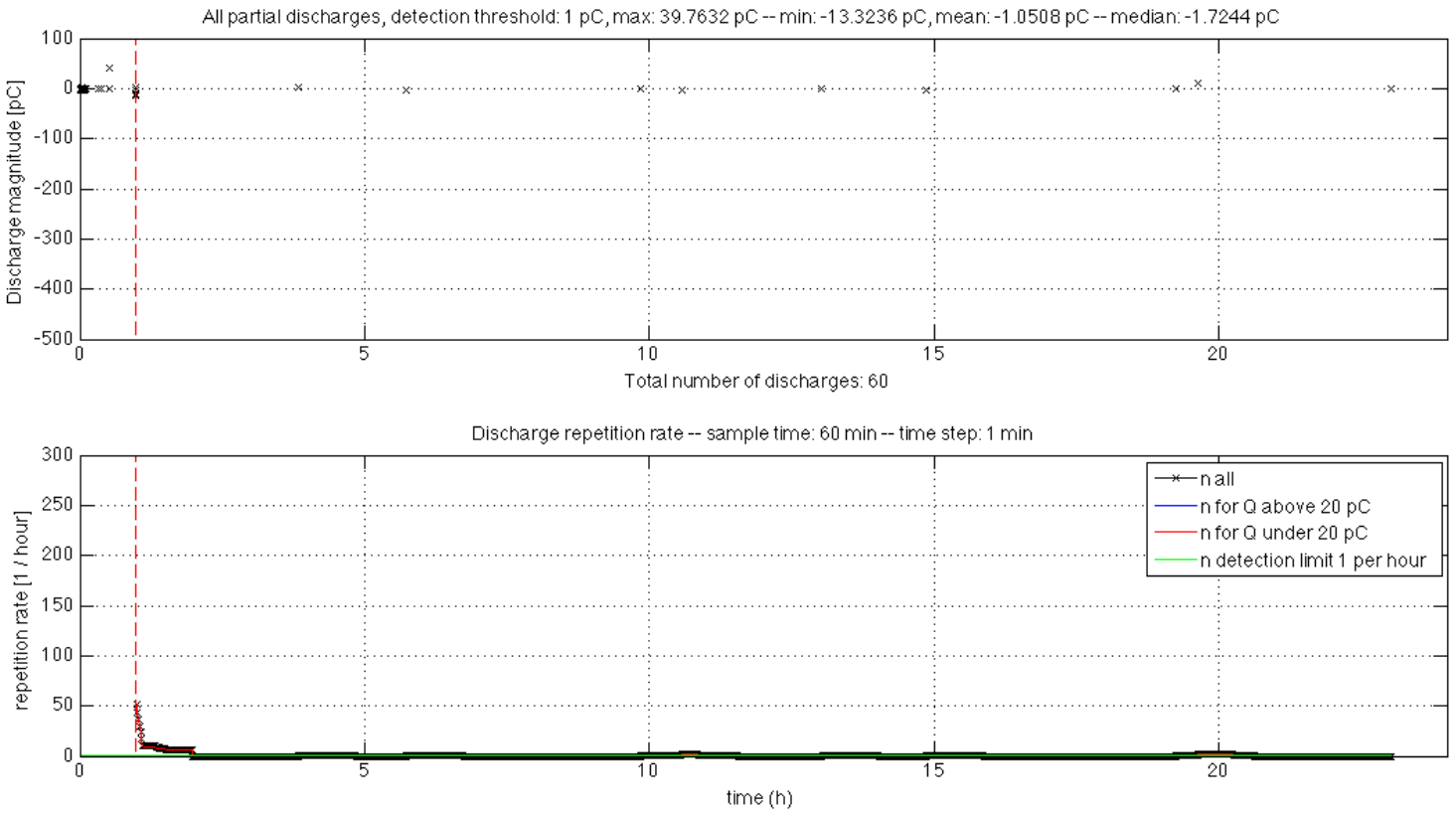

Figure E.5: PET 20, 3×100 μm layered sample without cavity, 10 kV_{DC}, 0.5 $kV_{AC,RMS}$, f=50 Hz, P=75 kN/mm, t=24 hours, T=60°C

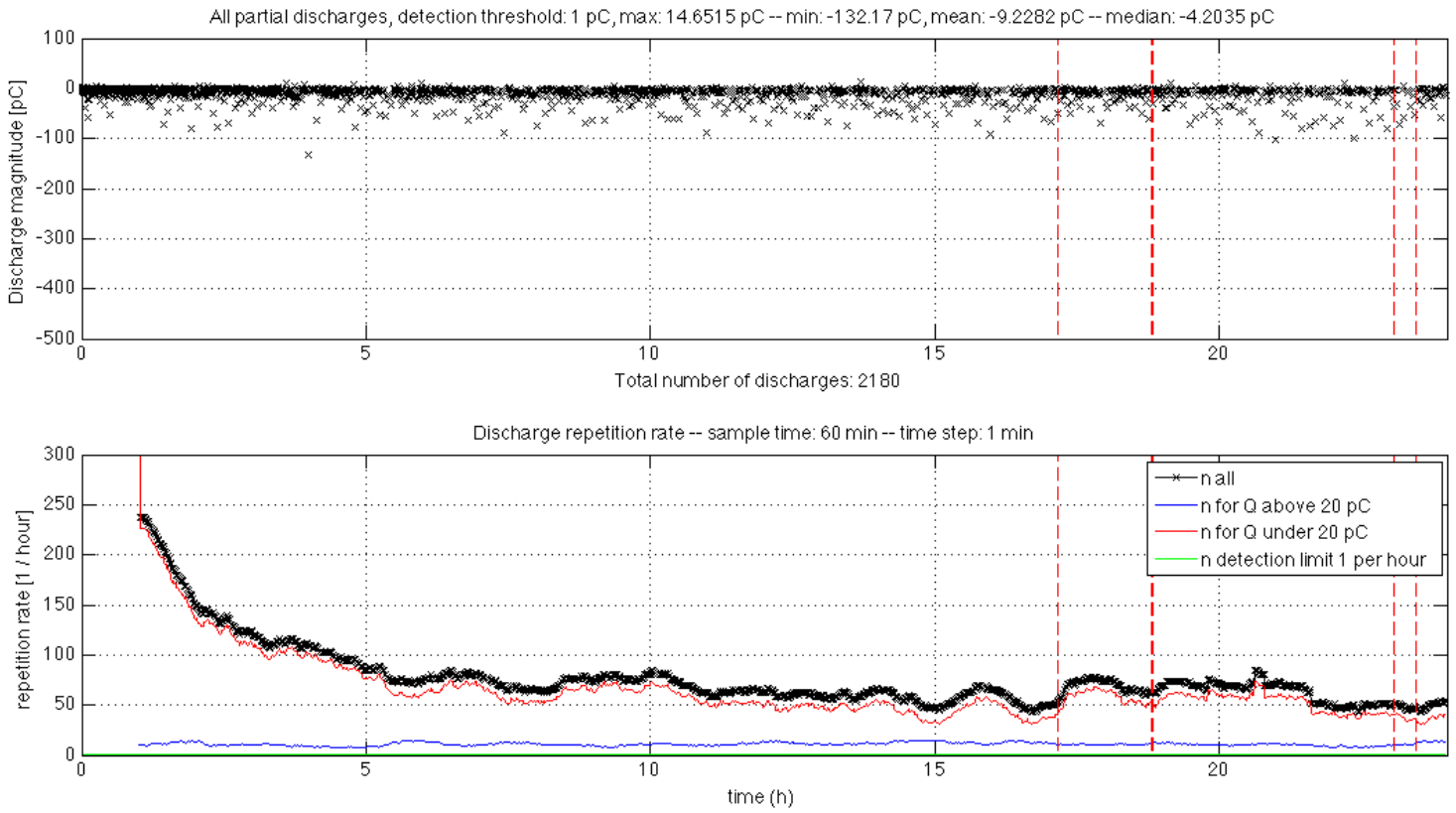

Figure E.6: PET 8, 3×100 μm layered sample with cavity r=1 mm, 10 kV_{DC}, 0.5 $kV_{AC,RMS}$, f=50 Hz, P=75 kN/mm, t=24 hours, T=60°C

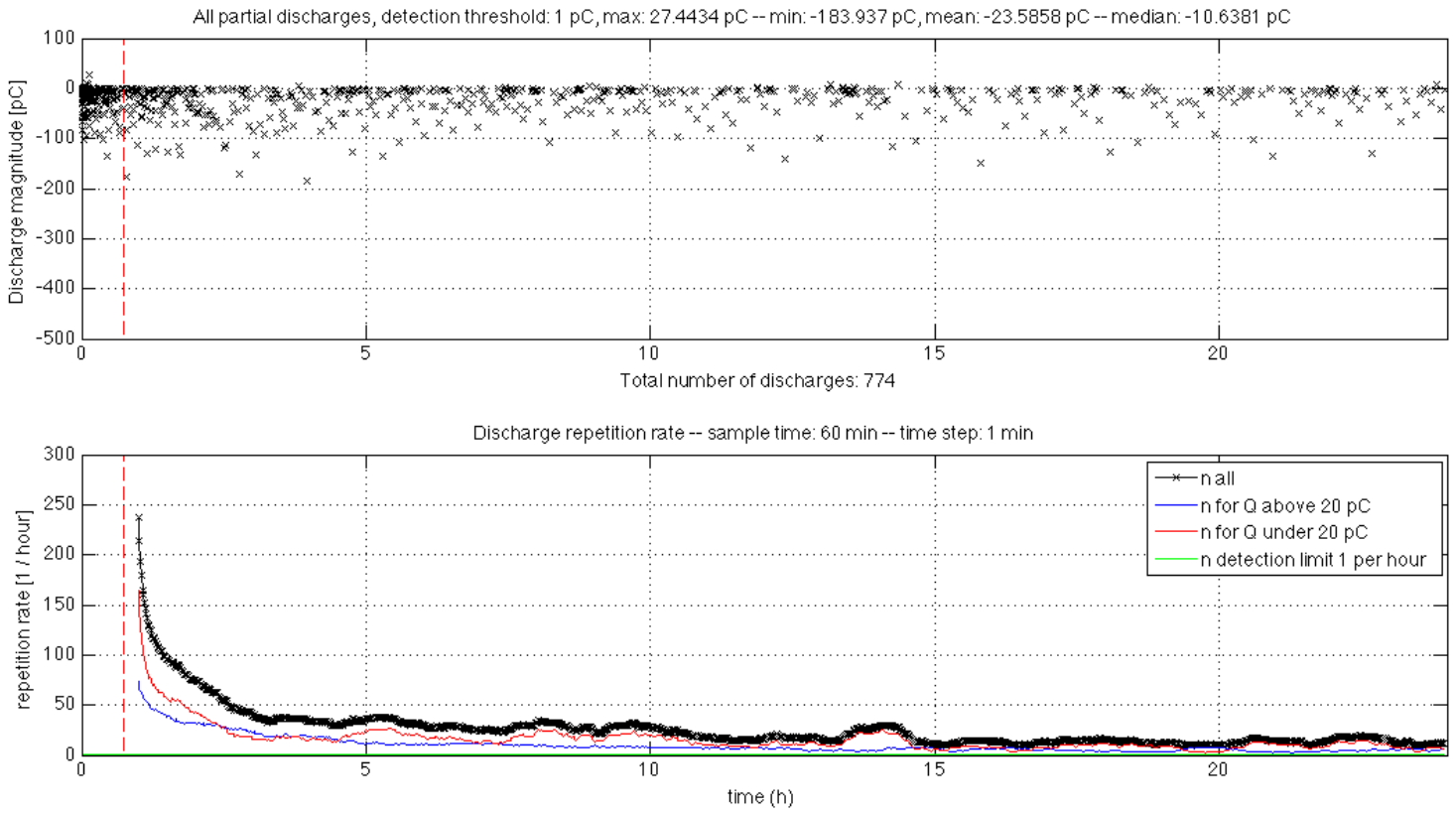

Figure E.7: PET 15, 3×100 μm layered sample with cavity r=1 mm, 10 kV_{DC}, 0.5 $kV_{AC,RMS}$, f=50 Hz, P=75 kN/mm, t=24 hours, T=60°C

E.4 Partial discharge under combined 1000 Hz AC $V_{ac,rms}$=0.5 kV_{RMS} and DC V_{dc}=10 kV voltage

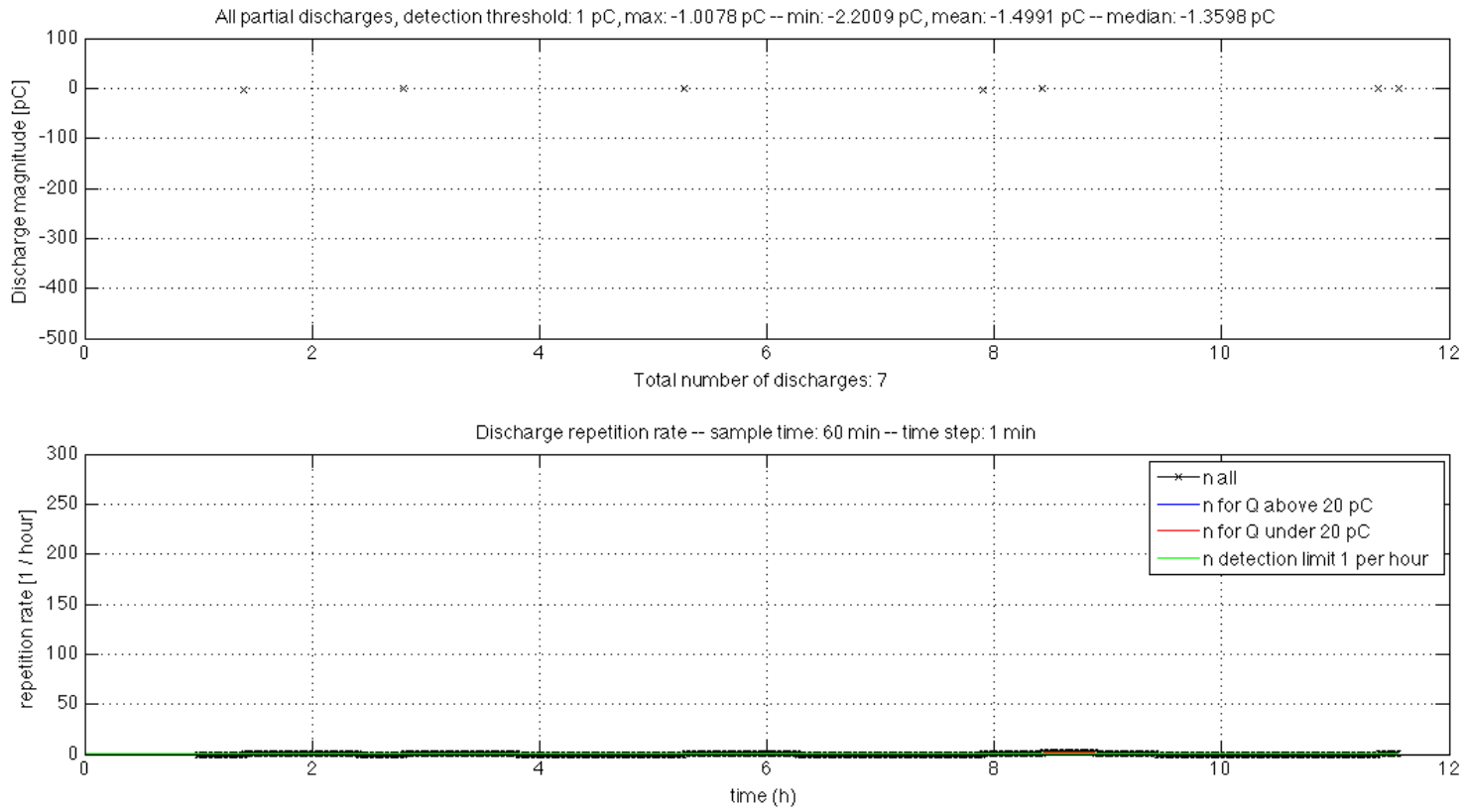

Figure E.8: PET 25, 3×100 μm layered sample with cavity r=1 mm, 10 kV_{DC}, 0.5 $kV_{AC,RMS}$, f=1 kHz, P=75 kN/mm, t=12 hours, T=60°C

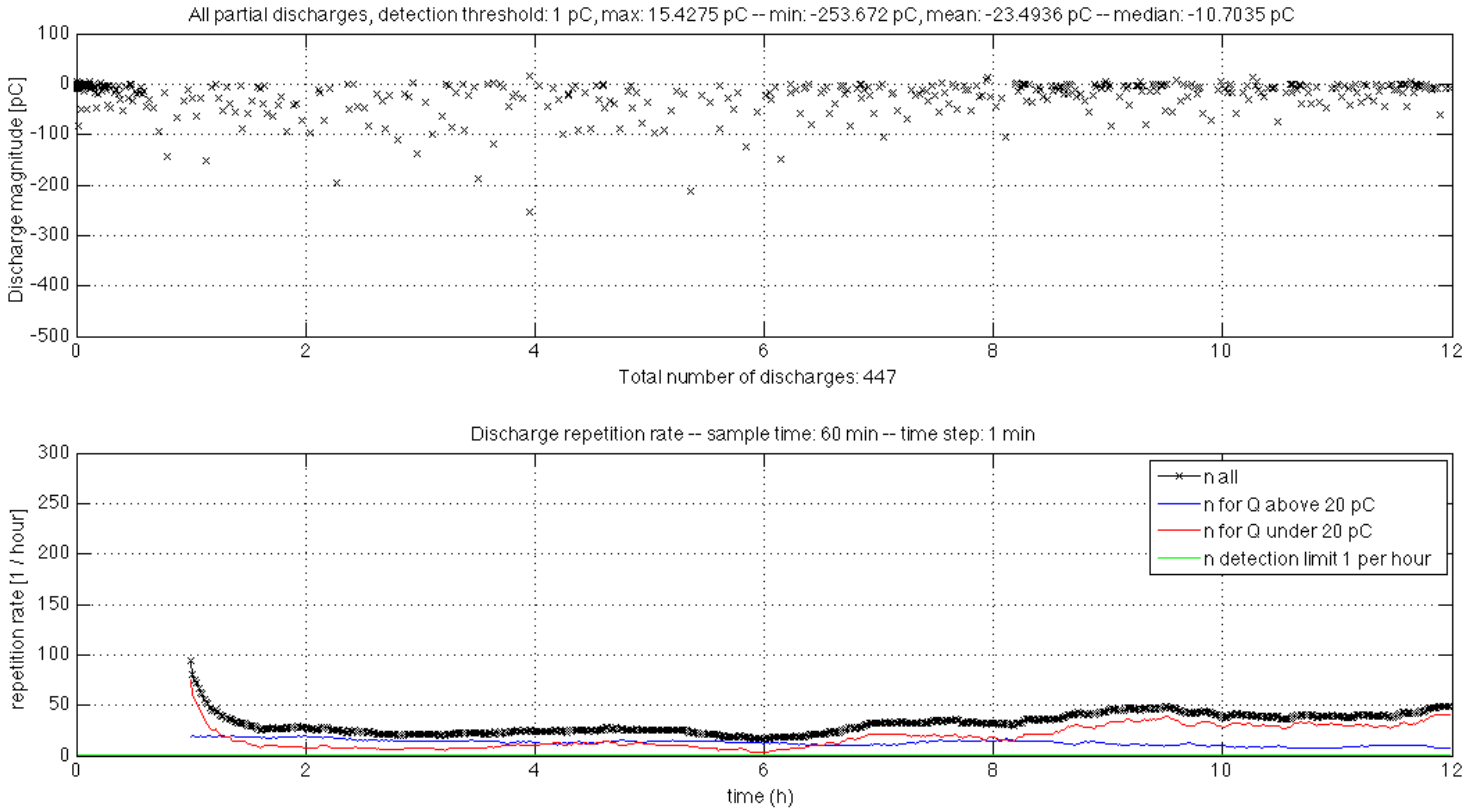

Figure E.9: PET 27, 3×100 μm layered sample with cavity r=1 mm, 10 kV_{DC}, 0.5 $kV_{AC,RMS}$, f=1 kHz, P=75 kN/mm, t=12 hours, T=60°C